AD-A021 996

IDENTIFICATION OF T-2 AERODYNAMIC DERIVATIVES FROM
FLIGHT DATA

D. A. Buenz, et al

Systems Control, Incorporated

Prepared for:

Naval Air Development Center

March 1975

DISTRIBUTED BY:

NTIS

National Technical Information Service
U. S. DEPARTMENT OF COMMERCE

084103

SYSTEMS CONTROL, INC. (VT)
PALO ALTO, CALIFORNIA

MARCH 1976

FINAL REPORT

DETERMINATION OF THE AERODYNAMIC DERIVATIVES FROM FLIGHT DATA

Prepared for

NAVAL AIR DEVELOPMENT CENTER
WASHINGTON, D.C.

DDC

MAR 16 1976

ABSTRACT

This report presents the stability and control derivatives
of a low speed Navy trainer aircraft, the T-2B, as determined
from flight test data. The maximum likelihood method is used
for the estimation of the aerodynamic derivatives, instrument
biases and random errors, and gust effects. The two flight
conditions considered are: (a) low speed, gear down, flaps
deflected, sea level, and (b) high speed, gear and flaps up,
10,000 feet altitude. It is shown that it is necessary to
include control input bias and in some cases gust effects to
get reliable results. Techniques for handling input bias and
random noise in input measurement are given.

The identified models in each case are verified through
several prediction runs.

ACKNOWLEDGEMENT

TABLE OF CONTENTS

LIST OF FIGURES

LIST OF FIGURES (CONTINUED)

LIST OF TABLES

LIST OF SYMBOLS

a_x = fore-aft acceleration, ft/sec^2

a_z = vehicle acceleration, ft/sec^2

g = gust; acceleration due to gravity, ft/sec^2

b = bias, units same as biased quantity

h = altitude, feet

I = pitch moment of inertia, $lb\text{-}ft^2$

K_α = alpha-vane calibration factor, [dimensionless]

ℓ_α = distance of α-vane from aircraft C.G., feet

M = pitch moment, lb-ft

n = random noise, units same as noisy quantity

q = pitch rate, rad/sec^2

Q = power spectral density of random noise, units same as quantity

R = covariance of measurement noise

t = time, sec

u = perturbation in forward speed of ft/sec^1; input in state representation

V = total speed, ft/sec

w = white noise, units depend on disturbance source

x = system state

x,z = forward and downward positive axes (see Figure i)

X = forward force, lb (see Figure i)

y = output or measurements

Z = vertical force, lb (see Figure i)

α =   angle-of-attack, radians, degrees

γ =   flight path angle, radians, degrees

θ =   pitch angle, radians, degrees

δ_e =   elevator input, radians, degrees

ω_c =   break frequency of Dryden model, rad/sec[1]

σ =   standard deviation, units same as quantity
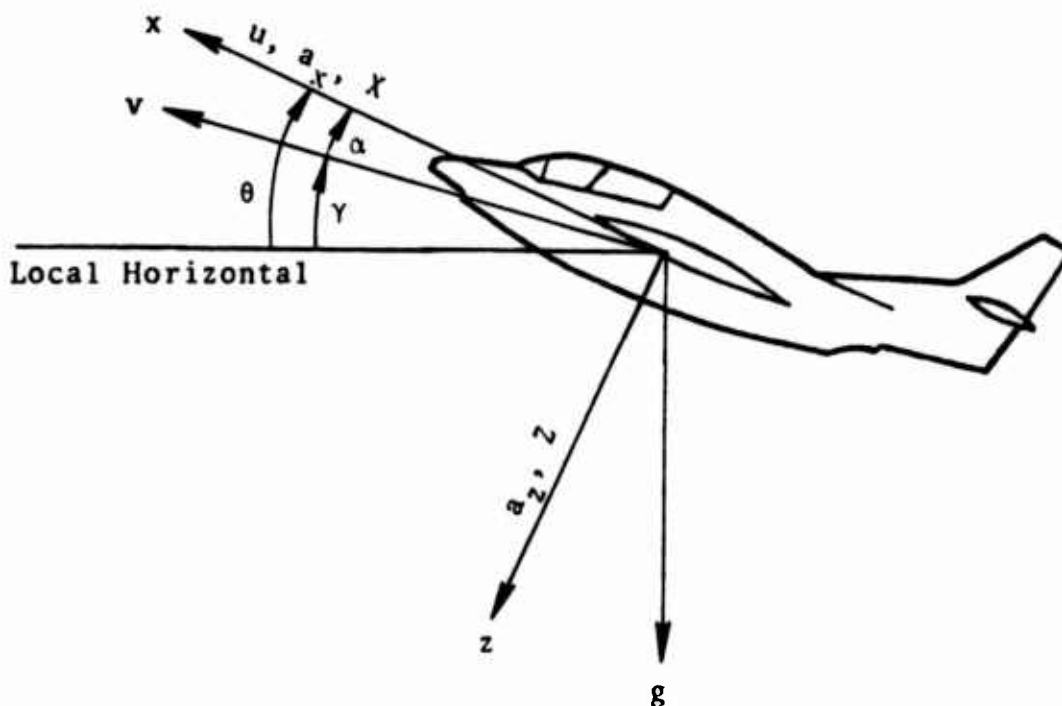
Figure i   Sign and Axes Conventions

I. INTRODUCTION AND BACKGROUND

The Naval Air Development Center (NADC) has conducted extensive flight tests of a T-2B aircraft. The object of these tests is to provide a comprehensive data base of measurements of the aircraft response which could be used to estimate stability and control derivatives. The data has been supplied to Systems Control, Inc. (SCI) for processing with an advanced maximum likelihood parameter identification program. This report details the results of that processing.

The T-2B aircraft used for the flight tests was extensively instrumented, including measurements of all attitude angles, rates, and accelerations. The aircraft responses were excited by several types of inputs at different flight conditions in order to isolate the input effectiveness in allowing accurate derivative estimates. Specifically, the flight data records supplied by NADC are at two flight conditions and have excitation of both short period and phugoid modes in the longitudinal motion. Flight condition 1 is an approach configuration at 236 ft sec^{-1} and sea level with gear down and flaps deflected. Flight condition 2 is at 679 ft sec^{-1} and 10,000 ft altitude in clean configuration [see Table 1]. The wind tunnel values of stability and control derivatives at these flight conditions are given in Table 2.

To process this data, a maximum likelihood algorithm was used which could identify random input noise effects on the aircraft states. The algorithm used to achieve this is highly efficient. Parameters which are not identifiable are isolated automatically during the computation. The measurement bias and random white noise errors are determined. The process noise power spectral density is identified in certain cases. The results are compared to wind tunnel values and to results obtained by using simple output error programs, which do not con-

Table 1
T-2 Flight Conditions and Configurations

	Flight Condition	
	1 (Approach Configuration)	2 (Clean Configuration)
Mach No.	0.212	0.63
True Airspeed (ft/sec)	236	679
Altitude (ft)	sea level	10,000
Gear Position	down	up
Flap Position (deg)	16	0
Speed Brake Position	closed	closed
Weight (lbs)	11,000	11,000
CG Position (% c)	20	20
I_y (slug - ft^2)	14,600	14,600
I_x (slug - ft^2)	9,000	9,000
I_z (slug - ft^2)	19,000	19,000
α Trim (deg)	4.7	1.2

Table 2
T-2 Dimensional Longitudinal Derivative Estimates From Wind Tunnel

	Flight Condition	
	1 (Approach Configuration)	2 (Clean Configuration)
X_u (1/sec)	-0.046	-0.016
X_α (ft/(sec^2 - rad))	-23.2	-36.91
Z_u (1/ft)	-0.00114	-0.00018
Z_α (1/(sec - rad))	-0.974	-2.458
Z_{δ_e} (1/(sec - rad))	-0.102	-0.178
M_u (1/(ft - sec))	0.006	0.0017
M_α (1/(sec^2 - rad))	-4.59	-22.50
$M_{\dot\alpha}$ (1/(sec - rad))	-0.53	-1.57
M_q (1/(sec - rad))	-1.42	-3.39
M_{δ_e} (1/(sec^2 - rad))	-9.63	-52.12

sider identifiability problems, and with results ignoring process
noise (e.g., wind gust effects and noise in the measurement of
input).

The comparison of various inputs shows clearly that certain
inputs are more efficient than others in that they provide better
estimates of parameters. In general, the inputs of larger ampli-
tude and lasting for longer periods of time are desirable. Also,
for a fixed length of the flight test and input amplitude, the
specially designed inputs are better than conventional inputs
such as pulses and doublets. It is shown that it is important
to estimate the bias in the inputs to get accurate parameter
estimates.

The parameter estimates from different runs at the same
flight condition show comparable mean values of the estimates over
various inputs. A prediction test (predicting one response from
the parameters estimates of a previous ran) is also shown to be
successful.

II.   EQUATIONS OF MOTION AND MEASUREMENTS

In the linear uncoupled aircraft model, the longitudinal equations of motion of an aircraft can be described by four states. They are angle-of-attack α, change in forward speed u, pitch rate q and pitch angle θ. The input is the elevator deflection δ_e. The equations of motion governing these states are [1]

$$
\frac{d}{dt}
\begin{bmatrix} \alpha \\ u \\ q \\ \theta \end{bmatrix}
=
\begin{bmatrix}
Z_\alpha & Z_u & Z_q & 0 \\
X_\alpha & X_u & X_q & -g \\
M_\alpha & M_u & M_q & 0 \\
0 & 0 & 1 & 0
\end{bmatrix}
\begin{bmatrix} \alpha \\ u \\ q \\ \theta \end{bmatrix}
+
\begin{bmatrix} Z_{\delta e} \\ X_{\delta e} \\ M_{\delta e} \\ 0 \end{bmatrix}
\delta_e
+
\begin{bmatrix} Z_\alpha \\ X_\alpha \\ M_\alpha \\ 0 \end{bmatrix}
\alpha_g
\tag{1}
$$

where α_g is the change in effective angle-of-attack due to wind gusts. The wind disturbance is modeled as a first order exponentially correlated process (Dryden Model).

$$
\dot{\alpha}_g = -\omega \alpha_g + w
\tag{2}
$$

ω is break frequency and w is a white noise process. We can combine Eqs. (1) and (2) to get a five state model driven by white noise

$$
\frac{d}{dt}
\begin{bmatrix} \alpha \\ u \\ q \\ \theta \\ \alpha_g \end{bmatrix}
=
\begin{bmatrix}
Z_\alpha & Z_u & Z_q & 0 & Z_\alpha \\
X_\alpha & X_u & X_q & -g & X_\alpha \\
M_\alpha & M_u & M_q & 0 & M_\alpha \\
0 & 0 & 1 & 0 & 0 \\
0 & 0 & 0 & 0 & -\omega
\end{bmatrix}
\begin{bmatrix} \alpha \\ u \\ q \\ \theta \\ \alpha_g \end{bmatrix}
+
\begin{bmatrix} Z_{\delta e} \\ X_{\delta e} \\ M_{\delta e} \\ 0 \\ 0 \end{bmatrix}
\delta e
+
\begin{bmatrix} 0 \\ 0 \\ 0 \\ 0 \\ 1 \end{bmatrix}
w
\tag{3}
$$

There are 12 parameters in the longitudinal equations of motion.
They are Z_α, Z_u, Z_q, X_α, X_u, X_q, M_α, M_u, M_q, Z_{δ_e}, X_{δ_e}, and M_{δ_e}.
There are two additional unknown parameters associated with the wind
model-power spectral density of w and break frequency ω. This fifth
order system has five poles. There is a slow, lightly damped com-
plex pole pair for the phugoid motion and another fast, highly
damped, complex pair for the short period motion. The fifth pole
(e.g., pole associated with the wind model) is at ω. If there is
only short period excitation, the velocity is almost constant and
we can use the following four state model

$$\frac{d}{dt}\begin{bmatrix} \alpha \\ q \\ \theta \\ \alpha_g \end{bmatrix} = \begin{bmatrix} Z_\alpha & Z_q & 0 & Z_\alpha \\ M_\alpha & M_q & 0 & M_\alpha \\ 0 & 1 & 0 & 0 \\ 0 & 0 & 0 & -\omega \end{bmatrix}\begin{bmatrix} \alpha \\ q \\ \theta \\ \alpha_g \end{bmatrix} + \begin{bmatrix} Z_{\delta_e} \\ M_{\delta_e} \\ 0 \\ 0 \end{bmatrix}\delta_e + \begin{bmatrix} 0 \\ 0 \\ 0 \\ 1 \end{bmatrix} w \quad (4)$$

When there is no measurement of pitch angle θ and the gust can
be assumed a white noise process, the usual two state approximation
to the short period motions can be applied.

$$\frac{d}{dt}\begin{bmatrix} \alpha \\ q \end{bmatrix} = \begin{bmatrix} Z_\alpha & Z_q \\ M_\alpha & M_q \end{bmatrix}\begin{bmatrix} \alpha \\ q \end{bmatrix} + \begin{bmatrix} Z_{\delta_e} \\ M_{\delta_e} \end{bmatrix}\delta_e + \begin{bmatrix} Z_\alpha \\ M_\alpha \end{bmatrix}\alpha_g$$

Measurements

There are ten measurements of inputs, angles, rates and
accelerations (excluding speed brake, which is kept fixed) at a
sampling interval of 0.05 sec. Table 3 shows the measurements and
the functional relations to inputs and states. Five longitudinal
measurements were chosen for identification of the aircraft deriva-
tives, unless otherwise mentioned. They are angle-of-attack, pitch

Table 3

Measurements During T-2 Flight Tests

	MEASUREMENT	FUNCTIONAL RELATIONSHIP	REMARKS
INPUT	Elevator Deflection	δ_e	Measured on Aerodynamic Surface, Very Noisy
ANGLES	Angle-of-Attack	$K_\alpha [\alpha + \alpha_g + \dfrac{\ell_\alpha}{V} q]$	α-Vane, Good
	Pitch Angle	θ	Gyro Measurements, Fairly Good
RATES	Pitch Rate	q	Rate Gyro, Good
	Airspeed	u	Very Noisy
ACCELERATIONS	Pitch Acceleration	$\dot{q}$	Computed from Linear Accelerometers, Very Noisy
	Pitch Acceleration	$\dot{q}$	Measured Directly, Very Noisy
	Normal Acceleration	$-V[Z_\alpha (\alpha + \alpha_g) + Z_u u + Z_{\delta_e} \delta_e]$	Noisy
	Fore-Aft Acceleration	$[X_\alpha (\alpha + \alpha_g) + X_u u + X_q q - g\theta]$	Noisy
OTHER	Altitude	h	

angle, pitch rate, airspeed and normal acceleration in addition to the elevator deflection input. The angle-of-attack is measured using an α-vane. Since the α-vane is not located at the C.G. of the aircraft, it also detects a component of pitch rate. The equations governing the five measurments are

$$
\begin{bmatrix} \alpha_m \\ u_m \\ q_m \\ \theta_m \\ a_z \end{bmatrix} = \begin{bmatrix} K_\alpha & 0 & K_\alpha \ell_\alpha/V & 0 & K_\alpha \\ 0 & 1 & 0 & 0 & 0 \\ 0 & 0 & 1 & 0 & 0 \\ 0 & 0 & 0 & 1 & 0 \\ -VZ_\alpha & -VZ_u & 0 & 0 & -VZ_\alpha \end{bmatrix} \begin{bmatrix} \alpha \\ u \\ q \\ \theta \\ \alpha_g \end{bmatrix} + \begin{bmatrix} 0 \\ 0 \\ 0 \\ 0 \\ -VZ_{\delta_e} \end{bmatrix} \delta_e
$$

$$
+ \begin{bmatrix} b_\alpha \\ b_u \\ b_q \\ b_\theta \\ b_{a_z} \end{bmatrix} + \begin{bmatrix} n_\alpha \\ n_u \\ n_q \\ n_\theta \\ n_{a_z} \end{bmatrix} \tag{6}
$$

Where b_α, etc., are the bias and n_α, etc., are the random white noise in the measurements of α, u, q, θ and a_z. The unknowns in the measurement equations are K_α, ℓ_α, b_α, b_u, b_q, b_θ, b_{a_z} and five white noise covariances. These parameters are included in the set to be identified.

7

III. THE IDENTIFICATION PROCEDURE

3.1 INTRODUCTION

Aircraft identification is the process of determining aircraft
stability and control derivatives from flight test data. The
integrated identification procedure is shown in Figure 1. The
control inputs are chosen to excite the desired modes of the air-
craft. The flight test is performed and the measured output vari-
ables are recorded. Then the identification algorithm is used to
process the data and provide estimates of the desired stability
and control derivatives and other unknown parameters in the instru-
ment models or gust models.

Figure 2 indicates the various steps in the data processing
stage. The input-output data, together with the physical know-
ledge of the system, are used to formulate a model and the set of
parameters to be identified. Then, the response data is used
again to estimate the parameters in the selected model. Here,
one of various techniques can be used. The parameter estimation
error covariances are also determined in this stage. Next, the
formulated model with the identified parameters is verified. This
is the most important stage in the identification and is often
overlooked. If the model verification test fails, the model may
have to be reformulated or the flight test repeated.

3.2 CHOICE OF PARAMETER IDENTIFICATION TECHNIQUE

Two identification techniques have been used to identify
the stability and control derivatives as well as bias and noise
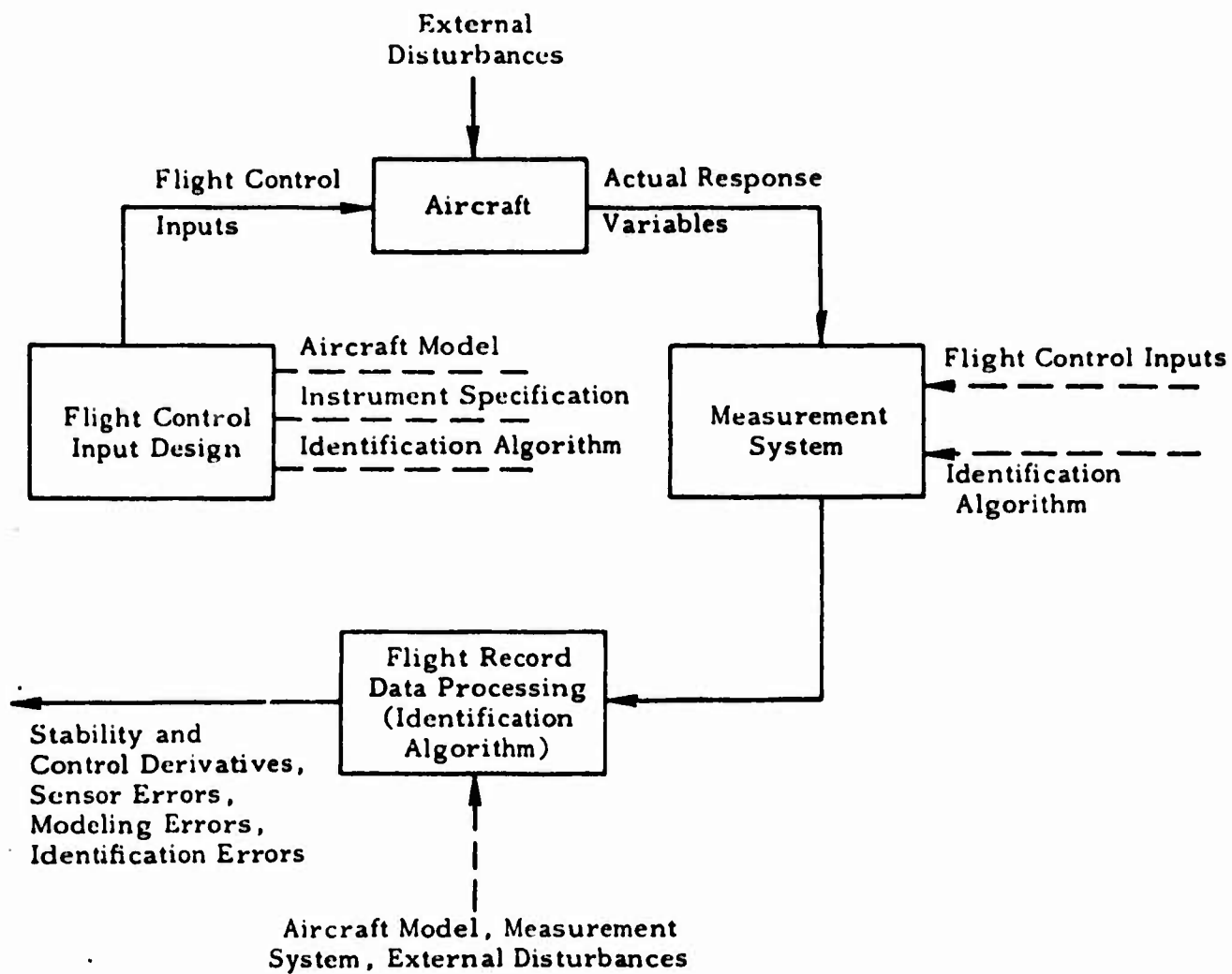covariances in instruments from flight test data.

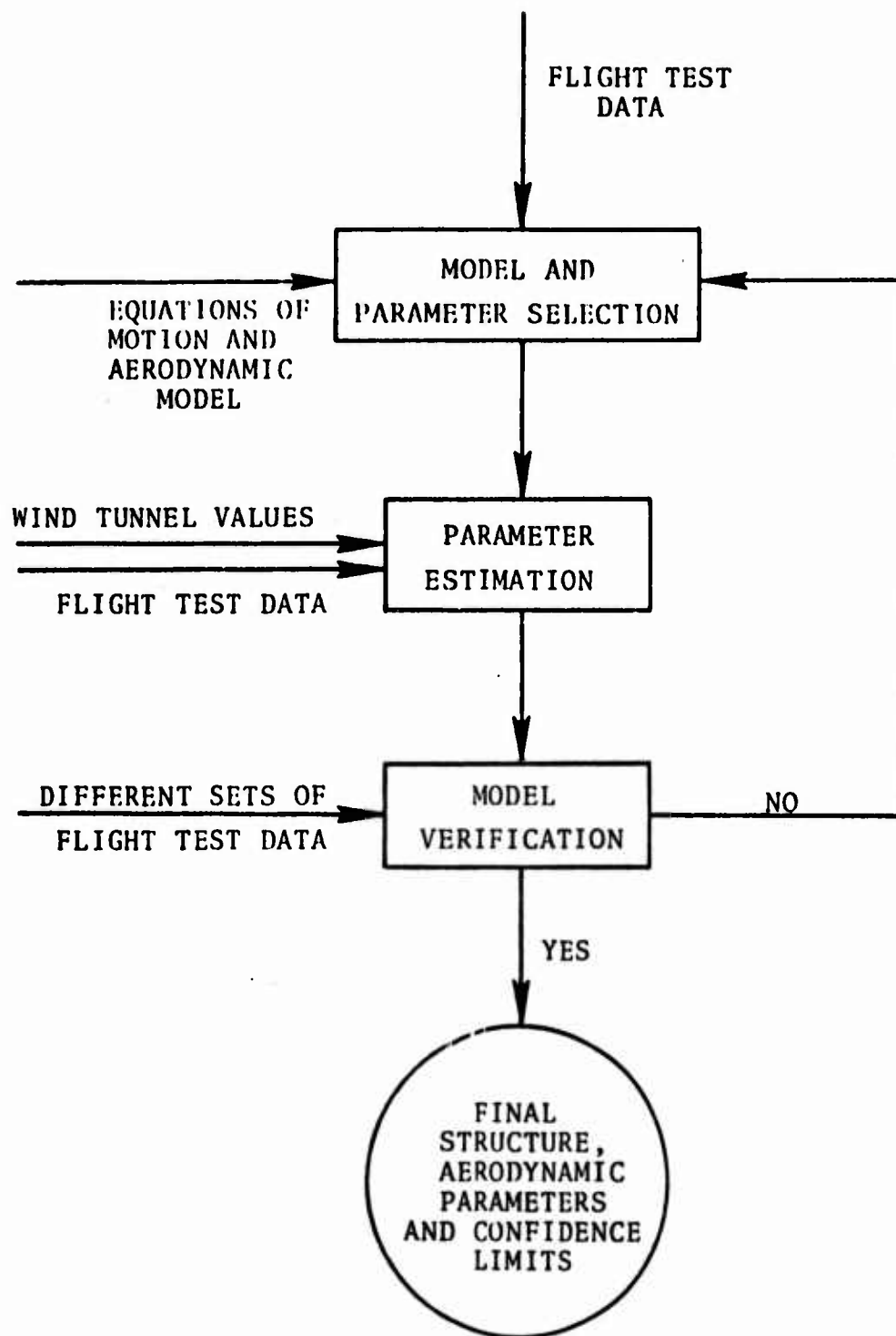Figure 1   The Integrated Aircraft Parameter
Identification Process

Figure 2 Three-Step Procedure for Flight Data Analysis

3.2.1 Instrumental Variables Approach

This is an approach in which the parameters are determined from a single pass through the data. This is a least squares type approach except that the bias of the least squares estimates (because of noise in the measurements of response variables) is eliminated by suitably chosen data transformations. The technique is very fast, does not require good parameter estimates to ensure convergence, and gives reasonable parameter estimates. In this application, the instrumental variables approach is used together with the wind tunnel values for start up for the more advanced and more accurate maximum likelihood method. The technique is described in Reference 2.

3.2.2 Maximum Likelihood Identification

In the maximum likelihood approach, the likelihood of the parameters given the measurements is maximized. Conceptually, this technique can be summarized as follows:

Find the probability density functions of the observations for all possible combinations of unknown parameter values. Select the density function whose value is highest among all density functions at the measured values of the observations. The corresponding parameter values are the maximum likelihood estimates.

The likelihood is a complicated nonlinear function of the mesaurements and the parameters. Several techniques have been used to maximize this function. There are some advantages to using the Gauss-Newton gradient approach in this case [3]. A Kalman filter is used for state estimation when process noise is present.

One procedure to implement the Gauss-Newton optimization technique to maximize the likelihood function for a system governed by linear equations of motion is shown in Figure 3. The important thing to note is that the first and second gradients of the likelihood function can be determined in terms of the first gradient of the innovation process. As has been shown by Gupta-Mehra [3], the innovations and their gradients with respect to parameters can be computed very efficiently through sensitivity function reductions technique.

If there is no process noise, the likelihood function reduces to the output error criterion. The details of this method are given in Appendix A.

3.3 MODEL VERIFICATION

In the model verification stage, we perform one or more tests to verify the formulated model and the identified parameters.

Several checks are used when the parameters are being identified. The time history of the aircraft responses computed from the identified model should be close to the measured responses. The difference (i.e., the innovations) should be a white noise process and the root-mean-square value of this process should be close to the noise in the instruments (slightly higher if there is process noise). Also, the estimates of stability and control derivatives obtained from different runs at the same flight condition should be close to each other. It is important to note the estimated covariance of the parameter identification errors. If the standard deviations of estimation errors is of the same order as parameter values, then the identified parameters are not useful.

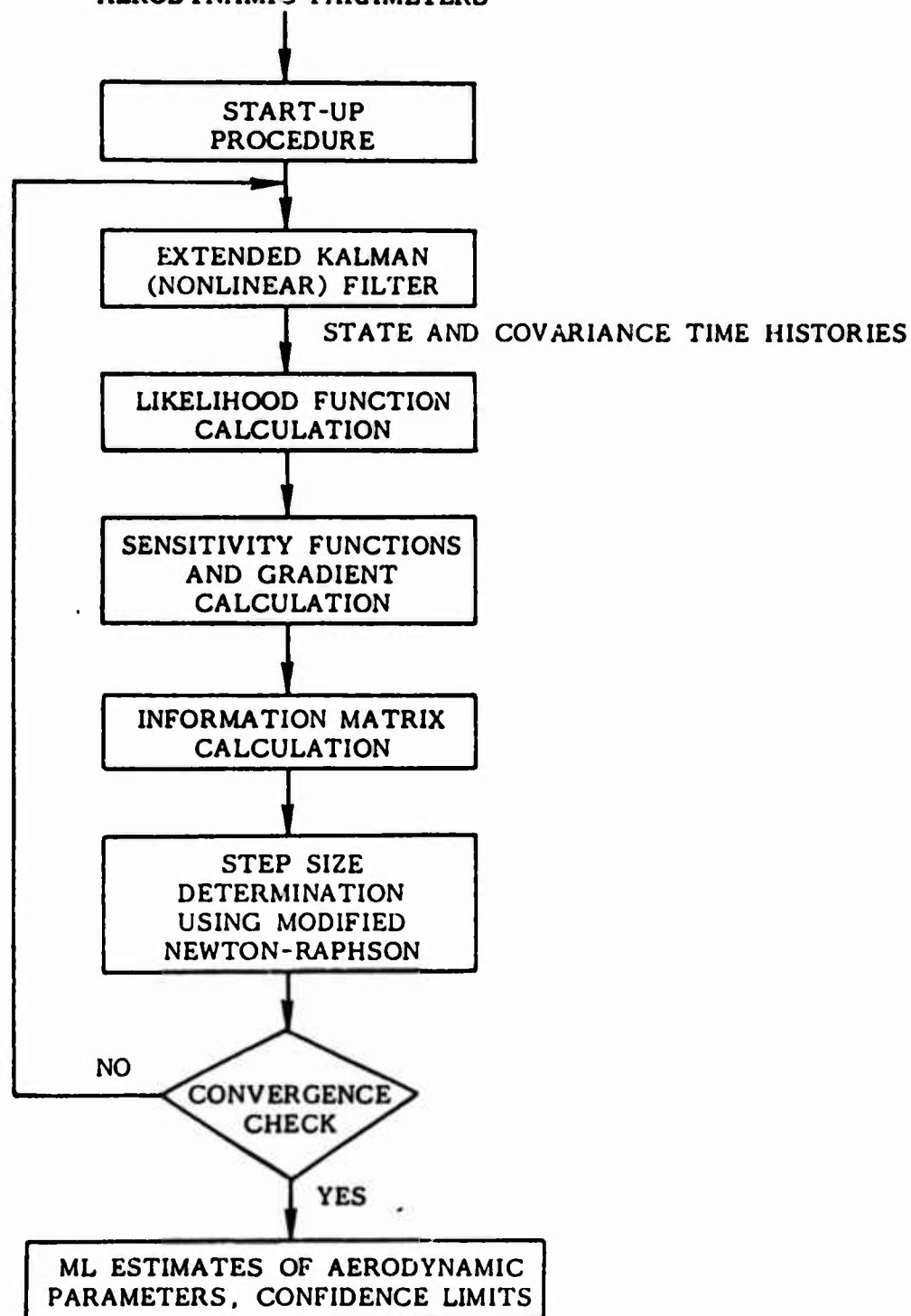FLIGHT TEST DATA, WIND TUNNEL VALUES OF
AERODYNAMIC PARAMETERS

```
                    │
                    ▼
           ┌─────────────────┐
           │    START-UP     │
           │    PROCEDURE    │
           └─────────────────┘
                    │
   ┌────────────────┤
   │                ▼
   │       ┌─────────────────┐
   │       │ EXTENDED KALMAN │
   │       │ (NONLINEAR) FILTER │
   │       └─────────────────┘
   │                │    STATE AND COVARIANCE TIME HISTORIES
   │                ▼
   │       ┌─────────────────┐
   │       │ LIKELIHOOD FUNCTION │
   │       │   CALCULATION   │
   │       └─────────────────┘
   │                │
   │                ▼
   │       ┌─────────────────┐
   │       │ SENSITIVITY FUNCTIONS │
   │       │   AND GRADIENT  │
   │       │   CALCULATION   │
   │       └─────────────────┘
   │                │
   │                ▼
   │       ┌─────────────────┐
   │       │ INFORMATION MATRIX │
   │       │   CALCULATION   │
   │       └─────────────────┘
   │                │
   │                ▼
   │       ┌─────────────────┐
   │       │    STEP SIZE    │
   │       │  DETERMINATION  │
   │       │  USING MODIFIED │
   │       │ NEWTON-RAPHSON  │
   │       └─────────────────┘
   │                │
   │                ▼
   │  NO         ◇ CONVERGENCE ◇
   └────────────   CHECK
                    │
                   YES
                    ▼
           ┌─────────────────────────┐
           │ ML ESTIMATES OF AERODYNAMIC │
           │ PARAMETERS, CONFIDENCE LIMITS │
           └─────────────────────────┘
```

Figure 3   Flow Chart of Maximum Likelihood Identification Program

All these are, of course, only the necessary conditions for a realistic model. It has been suggested by several researchers (e.g., Akaike [4] and Taylor [5]), that one of the useful tests is the prediction capability of the identified model. A schematic chart of how this is done to verify the identified model of the T-2 aircraft is shown in Figure 4. The measured control input and aircraft response is used to identify the parameter of the model. Then the aircraft response to another flight control input, at the identical flight condition, is measured. At the same time, the identified model is driven by the same control input. The measured response of the aircraft will be close to the predicted response if the identified model is correct.

3.4 CONSIDERATIONS IN THE USE OF THE MAXIMUM LIKELIHOOD TECHNIQUE

The maximum likelihood formulation of Appendix A holds strictly for the case when the "true" model is linear and the measurement and process noise sources are white.* In actual engineering applications, this is never the case. Therefore, the use of the maximum likelihood technique in parameter estimation problems requires considerable engineering judgment. Many failures of the maximum likelihood method are directly attributed to a lack of proper implementation. Several considerations are important in the identification of aircraft stability and control coefficients using the maximum likelihood approach:

1. Wind Gust Effects

In many implementations, the wind gusts are not included in the model. This produces biased parameter estimates. In simpler terms, there is a consistent error in the estimated value of parameters. This effect is included as

---

*The model we refer to here is the aircraft plus wind model. The gusts acting on the aircraft usually cannot be approximated as white noise. A good approximation of the gusts is white noise passed through a linear filter.
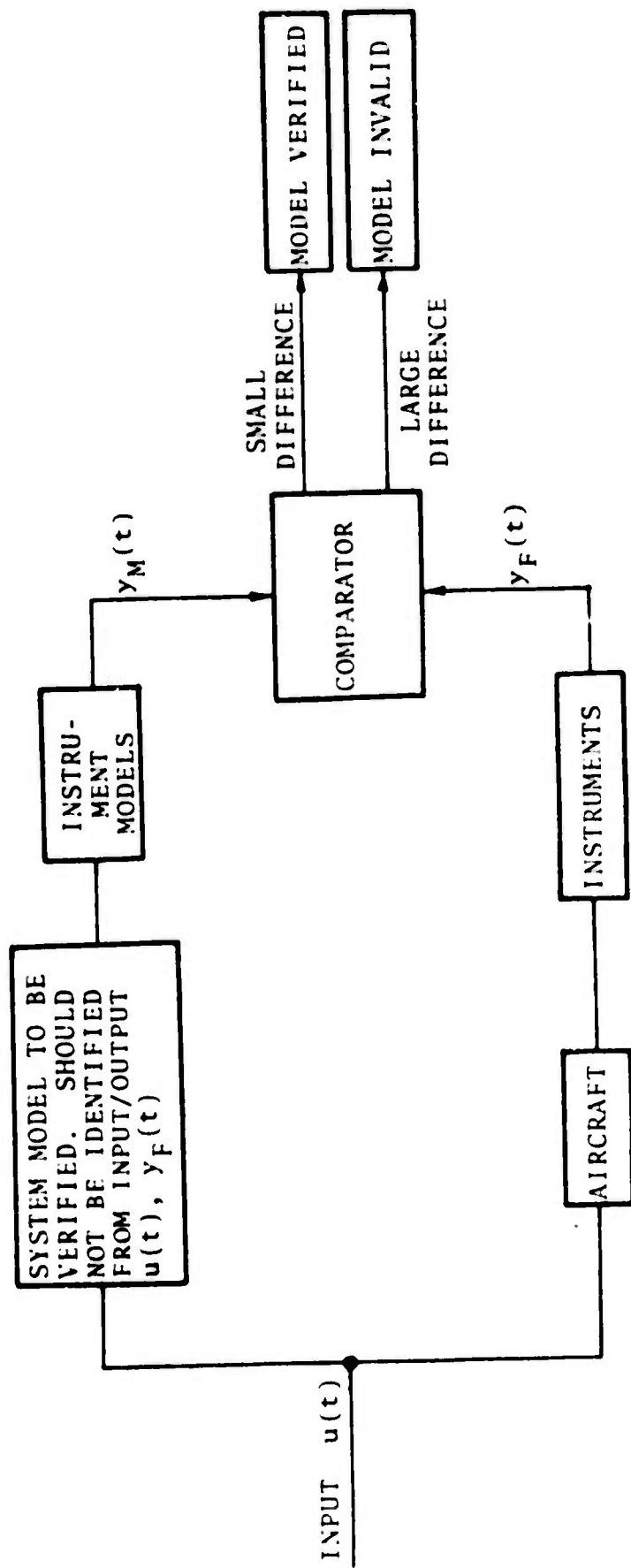
Figure 4 Model Verification Via Independent Prediction

detailed in Chapter II of this report. By including and
identifying the gust statistical model, the bias in the
parameters is reduced.

2. Bias and Noise in Control Input

The elevator deflection input is usually measured at
the aerodynamic surface using a potentiometer. Therefore, the
measurement of the input is contaminated by calibration biases
and random noise in the potentiometer. There are additional
bias effects because of uncertainty in the trim condition of
the elevator deflection. Notice that this is an important
effect because we take deviations from the trim condition to
identify parameters in the aircraft model. The modification to
the maximum likelihood method when the inputs have bias and
random noise is given in Appendix B.

3. Identifiability Problems

The maximum likelihood method gives the parameter esti-
mates as well as the predicted error covariance of the esti-
mation error. As discussed earlier, these error covariances
play an important role in the integrated parameter identifi-
cation process. Special attention should be given to these
covariances because a large covariance implies an
inaccurate estimate. Parameter estimates can be improved
by using a proper control input in a subsequent flight test.

4. Choice of Inputs and Instrumentation

Considerable work has been done on the choice of con-
trol inputs to improve identification accuracy of parameter
estimates (see Gupta-Hall [6] and Mehra-Gupta [7]). Differ-
ent inputs provide different estimation errors for the para-

meters of interest. Equally important is the choice of
instruments and the location of the chosen instruments. In
many instances, however, the set of instruments available
is fixed and it is not practical to relocate the instruments,
as in the present case. Then the choice of the control
input is the only design element to improve the accuracy of
the parameters.

IV. RESULTS

4.1 SUMMARY OF RESULTS

The instrumental variables and the maximum likelihood estimation methods are used to identify the stability and control coefficients of the T-2 aircraft. In addition, the biases and noise covariances in the instruments are also determined. One important feature of the computer program used to process the data is that it gives the covariance of the parameter estimation errors during the identification.

Flight test runs for the low speed approach configuration (flight condition 1) and higher speed clean configuration (flight condition 2) (see Table 1) are processed. State noise is identified in certain cases. The results from different flight tests at the same flight condition are compared. Finally, two prediction runs are made, as explained in Section 4.3, to verify the identified models.

4.2 LOW SPEED APPROACH CONFIGURATION (FLIGHT CONDITION 1)

The stability and control coefficients are determined at flight condition 1 (Table 1) using response data from runs 2, 3, 5, and 6. These maneuvers are the responses to a two cycle sine waves (runs 2 and 5), a low amplitude pulse (run 3), and a high amplitude pulse (run 6).

4.2.1 Two Cycle Sine Wave Elevator Input (Run 2)

The elevator input used to excite the aircraft modes is shown in Figure 5. Based on the duration of the run and the input, there
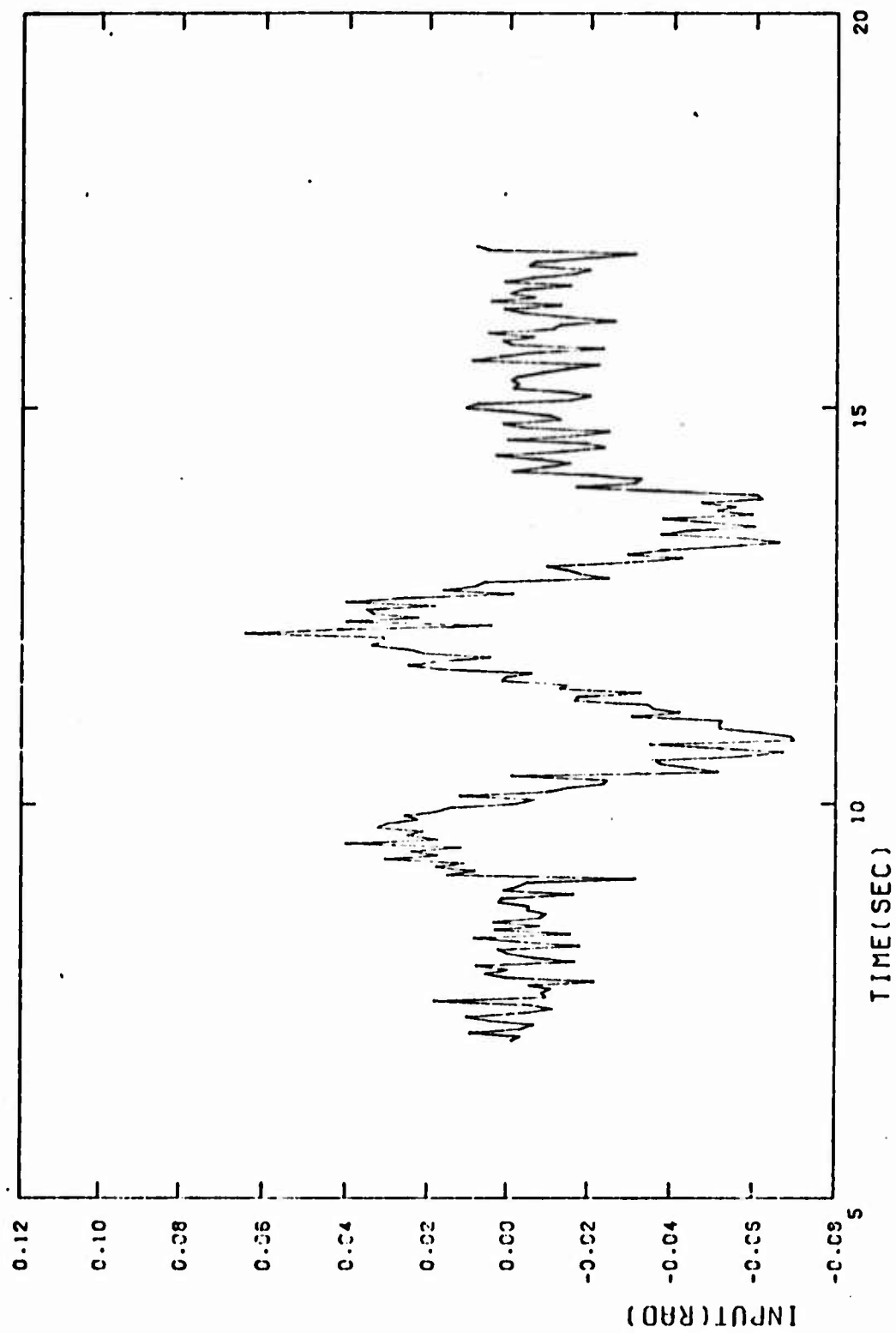
Figure 5   Two Cycle Sine Wave Elevator Input for Run 2

is only short period excitation. Since this maneuver is considered
a base line case, extensive processing was performed to isolate
various error sources in the data. The following paragraphs detail
the effects on identified parameters for: (1) erroneous acceleration
measurements, (2) non-uniqueness of estimates due to identifiability
problems, (3) gust disturbances, (4) noise in the control measure-
ment, and (5) bias errors due to out-of-trim.

Effect of Erroneous Acceleration Measurement

The aerodynamic derivatives are evaluated using an output
error program in which all parameters are assumed identifiable. In
this run, measurements of normal acceleration , pitch acceleration,
and fore-aft acceleration are also used. The estimated parameters are
shown in Table 4. The actual response time histories and computed
response time histories for the estimated parameters are shown in
Figure 6. It is clear that the sign of fore-aft acceleration is
incorrect in the data. Another run was made with changed sign of
the fore-aft acceleration. The parameter estimates are shown in
Table 4 and corresponding time history matches in Figure 7. The
sign problem is solved. Notice that the short period parameters are
not very different even when an incorrect sign is taken for fore-aft
acceleration. Table 5 shows the bias and white noise errors in the
instruments.

Rank Deficient Solution to Avoid Identifiability Problems

A rank deficient solution is used in which all but the short
period parameters are discarded since there is insignificant phu-
goid excitation. Measurements of angle-of-attack, pitch rate,
pitch angle and normal acceleration are used for identification.
Table 6 shows the wind tunnel values, the start up values for maxi-
mum likelihood and the final identified values assuming no process
noise. The corresponding plots of actual and predicted time

Table 4

T-2 Parameters Using Output Error and Assuming
All Parameters Identifiable

PARAMETER	INCORRECT SIGN FOR FORE-AFT ACCELERATION		CORRECTED SIGN FOR FORE-AFT ACCELERATION	
	ESTIMATE	STANDARD DEVIATION	ESTIMATE	STANDARD DEVIATION
Z_α	-0.994	0.048	-0.965	0.043
Z_u	-0.00135	0.0013	-0.0012	0.0001
Z_q	1.388	0.39	1.23	0.03
X_α	8.76	3.62	-15.82	2.52
X_u	-0.0168	0.00689	0.0329	0.00427
M_α	-4.42	0.134	-4.52	0.13
M_u	0.00373	0.00344	0.00434	0.00027
M_q	-1.81	0.068	-1.863	0.059
$Z_{\delta e}$	-0.03	0.1	-0.07	0.085
$X_{\delta e}$	0.3	3.46	-0.3	1.99
$M_{\delta e}$	-8.42	0.131	-8.562	0.121
K_α	1.0 (fixed)		1.0 (fixed)	
$\dfrac{K_\alpha \ell_\alpha}{V}$	0 (fixed)		0 (fixed)	

(All values in units of ft, rad, sec)

Table 5

Measurement Noise Statistics

MEASUREMENT	UNITS	BIAS	RMS OF WHITE NOISE
α	rad	-0.00301	0.00642
u	ft sec^{-1}	-2.41	3.68
q	rad sec^{-1}	-0.00113	0.00535
θ	rad	0.00933	0.0117
a_x	ft sec^{-2}	-1.19	0.748
$\dot{q}$	rad sec^{-2}	-0.00102	0.0636
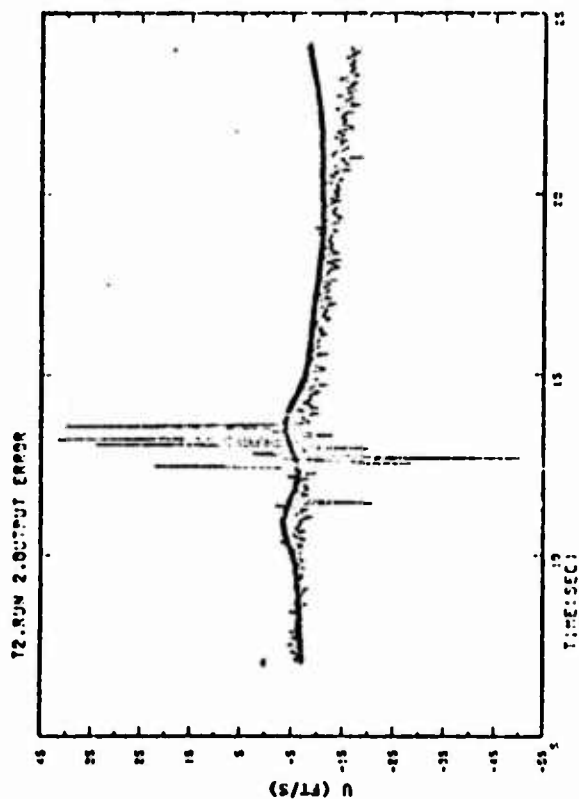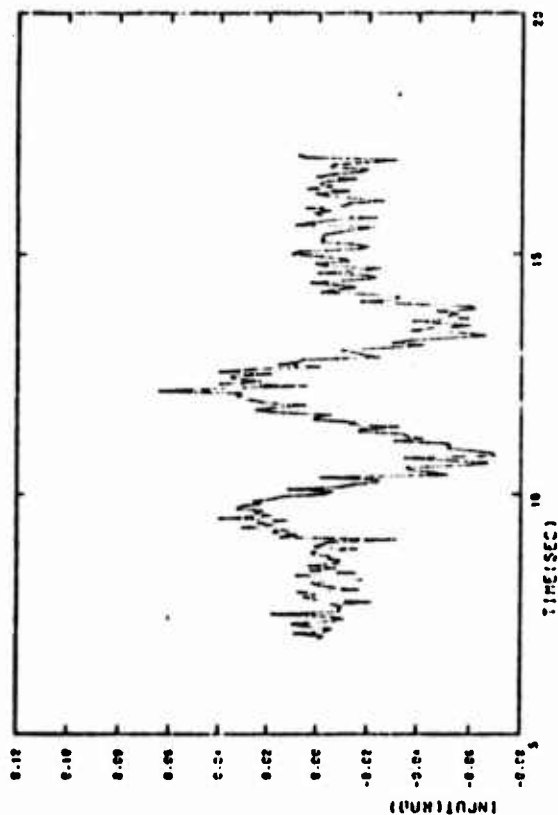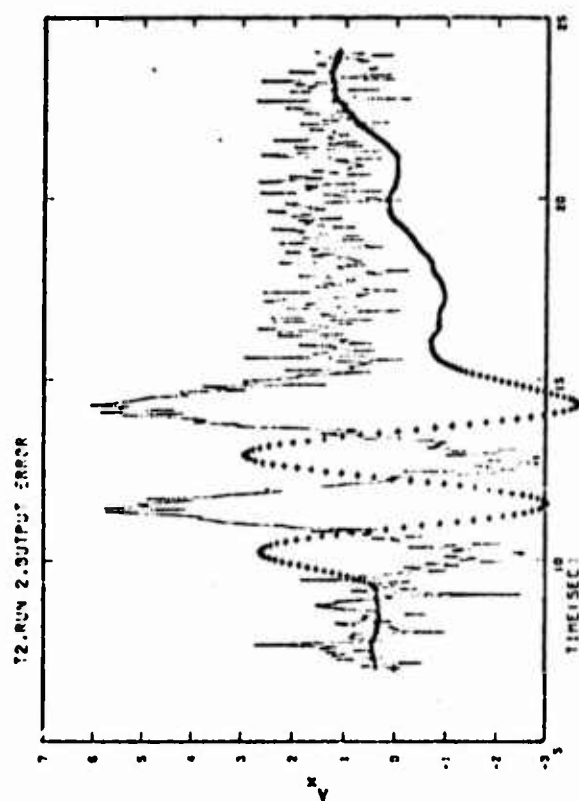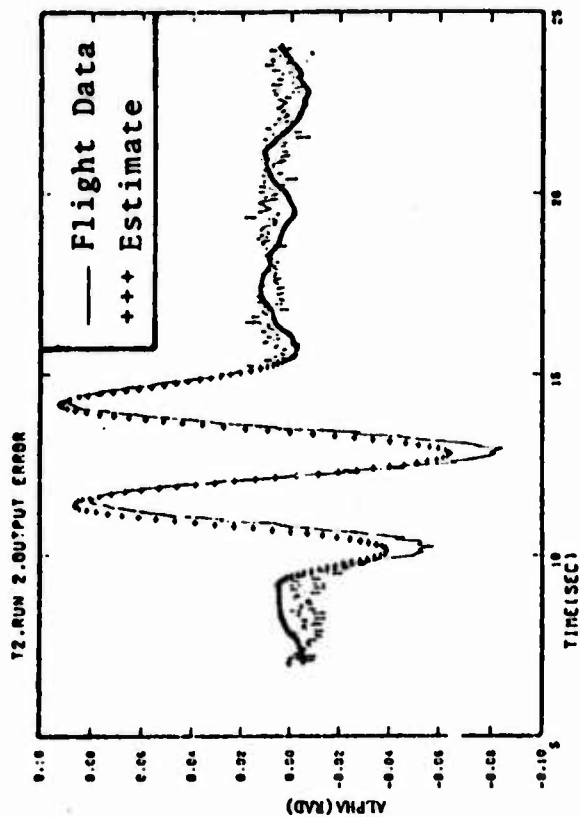
Figure 6   Time History Plots for Run 2 with <u>Incorrect</u> Sign for a_x
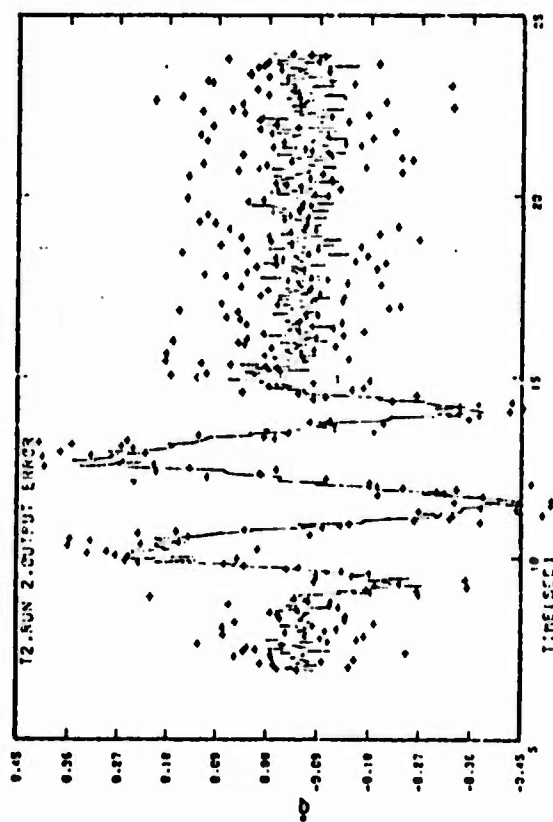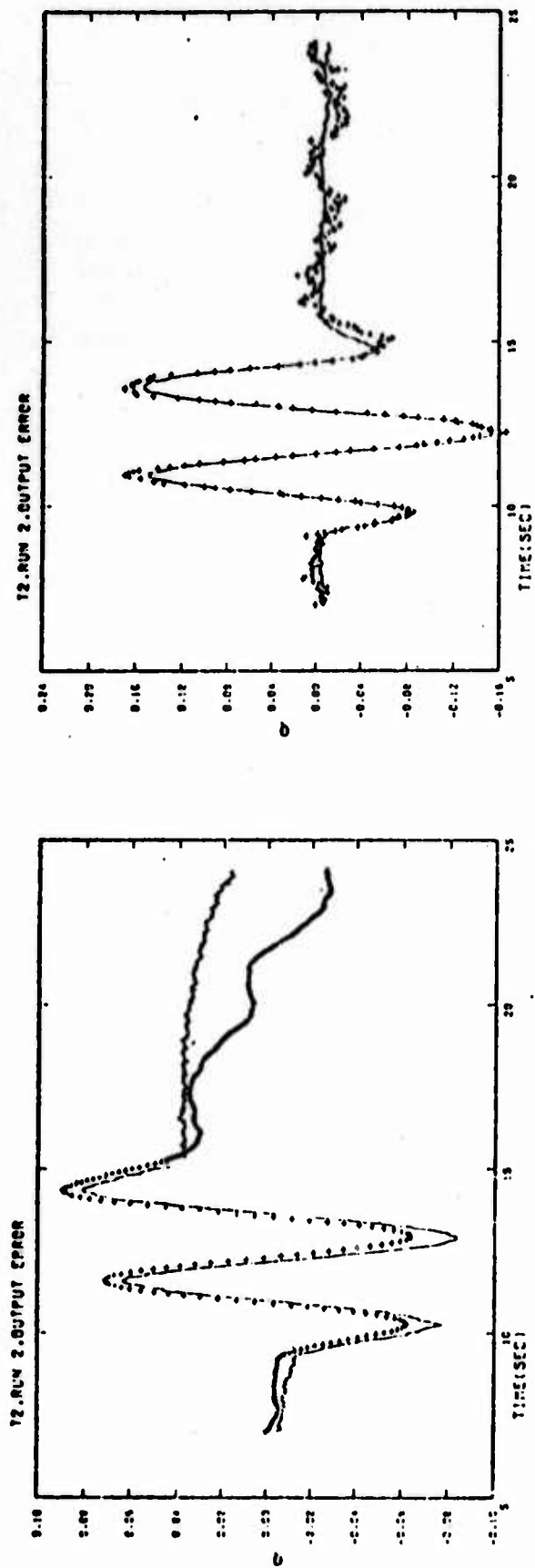
Figure 6 (Concluded) Time History Plots for Run 2 With <u>Incorrect Sign</u> for a_x
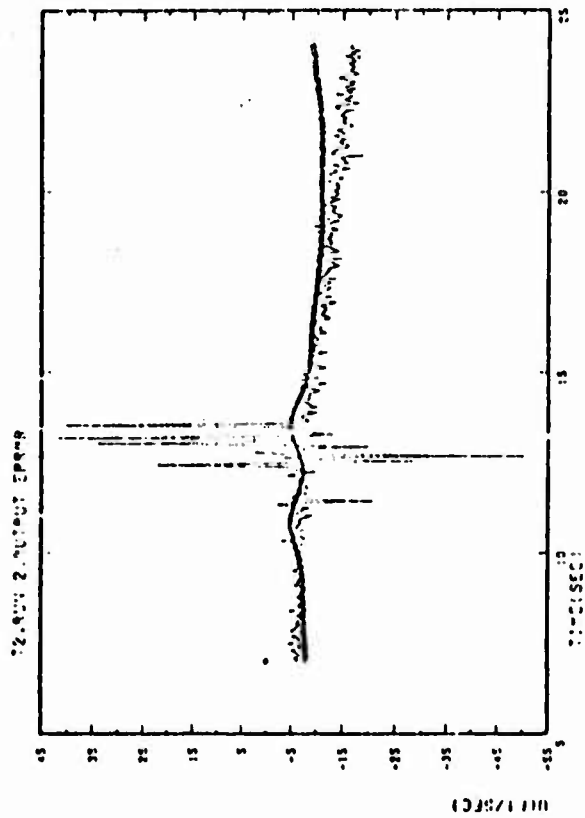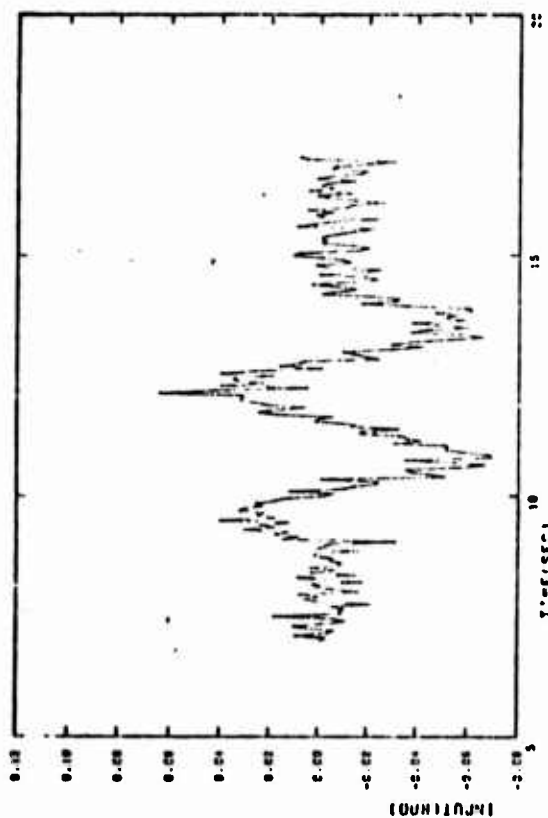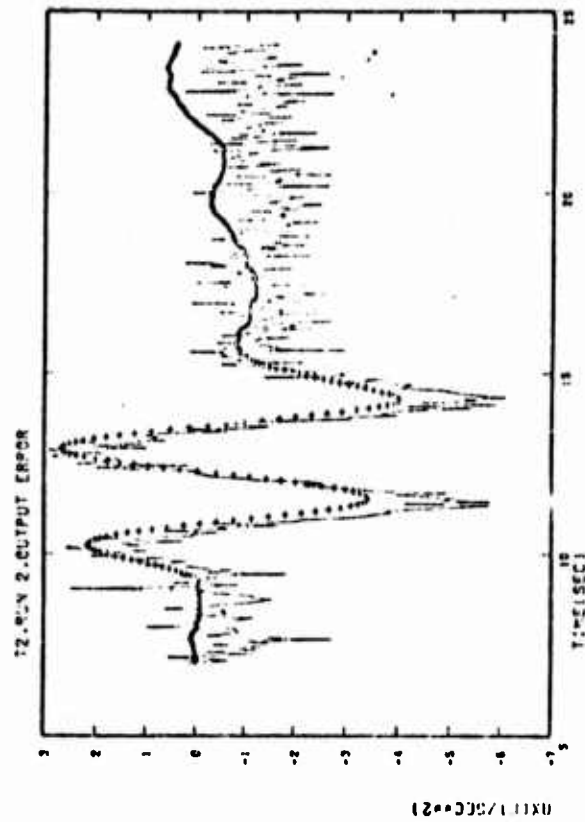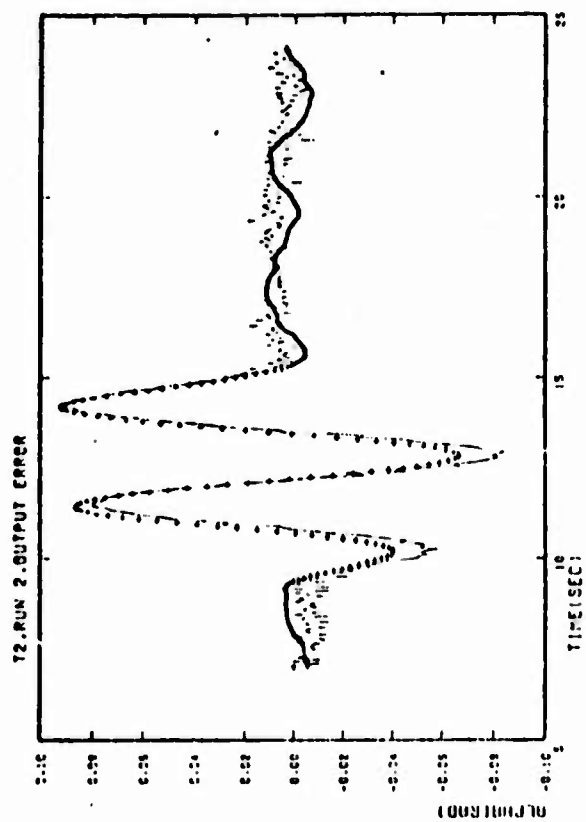
Figure 7 Time History Plots for Run 2 with Correct Sign for a_x
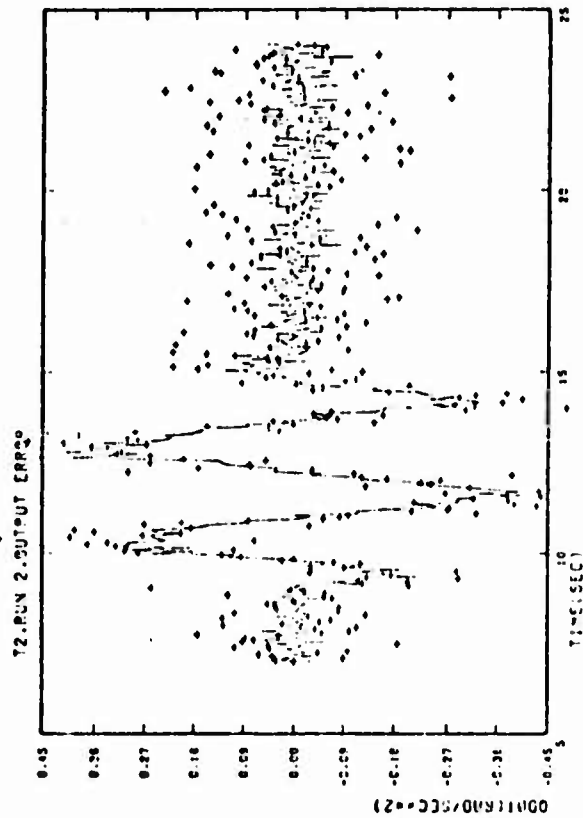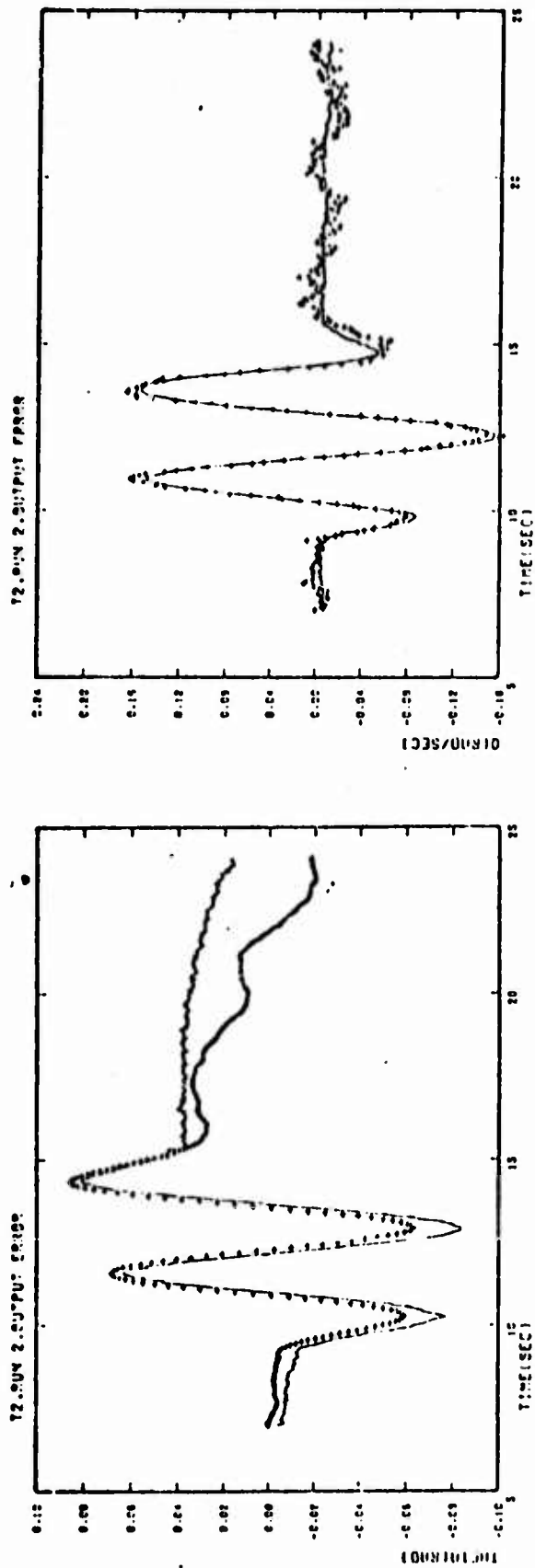
Figure 7 (Concluded) Time History Plots for Run 2 with Correct Sign for a_x

Table 6
Identified Derivatives Using Rank Deficient Solution - Run 2
(Approach Configuration)

PARAMETER	WIND TUNNEL	START-UP VALUES FOR MAXIMUM LIKELIHOOD	OUTPUT ERROR	PROCESS NOISE
Z_α	-0.974	-1.046	-0.903 ± 0.032	-0.873 ± 0.0266
Z_u	-0.011	0.0		
Z_q	1.0	1.0	1.0	1.0
γ	0.0	0.0		
X_α	-23.2	0.0		
X_u	-0.046	0.0		
X_q	0.0	0.0		
M_α	-4.59	-6.0	-4.323 ± 0.0588	-4.26 ± 0.0922
M_u	0.006	0.0		
M_q	-1.42	-0.48	-1.658 ± 0.103	-1.543 ± 0.114
ω_c		0.5		0.5
$Z_{\delta e}$	-0.102	0.912	-0.5724 ± 0.787	0.215 ± 0.039
$X_{\delta e}$	0.0	0.0		
$M_{\delta e}$	-9.63	-8.3978	-7.445 ± 0.196	-7.32 ± 0.33
K_α		1.0		✦
$K_\alpha \ell_\alpha/V$		0.0		✦
Q		0.0		0.000175 ± 0.0000288
σ_α		0.0063	0.0091	0.0125
σ_q		0.0055	0.0125	0.0153
σ_θ		0.0118	0.0137	0.0170
σ_{a_z}		0.71	4.26	4.85

(All values in units of ft, rad, sec)

Flight Conditions: Altitude = Sea Level; V_{trim} = 266.5 ft/sec; α_{trim} = 5.8°
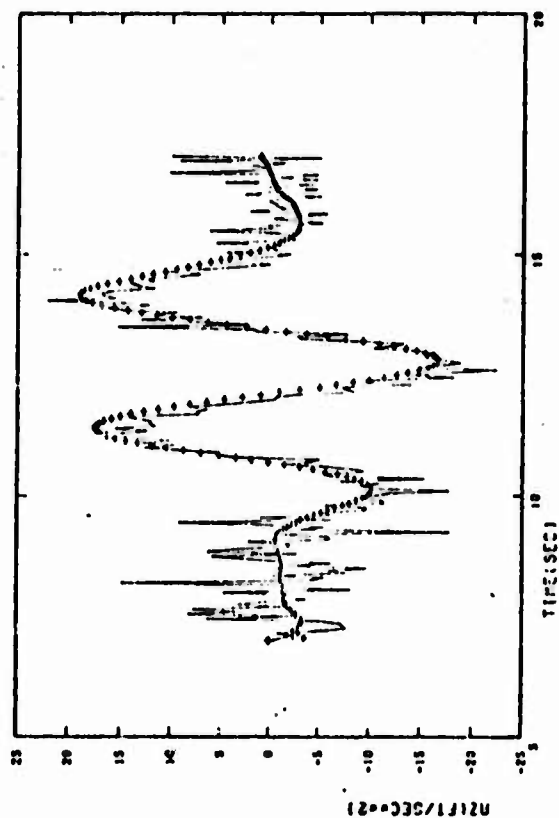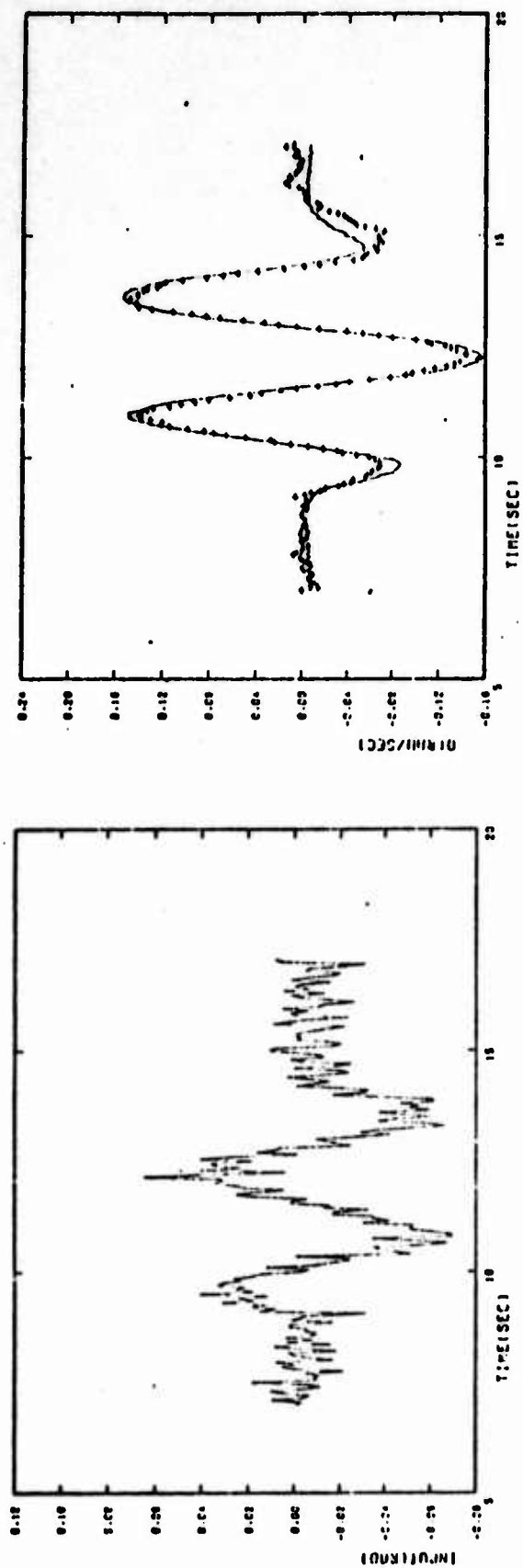
Figure 8   Time History Plots for Run 2 with Rank Deficient Solution
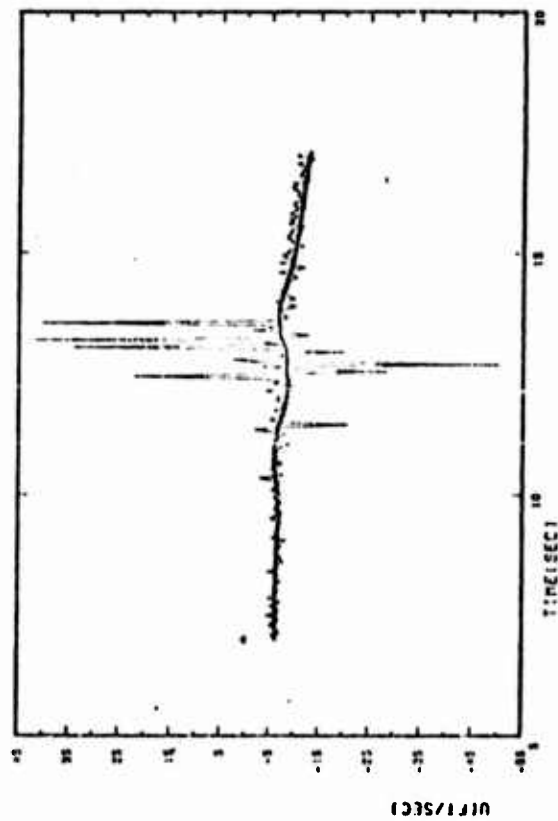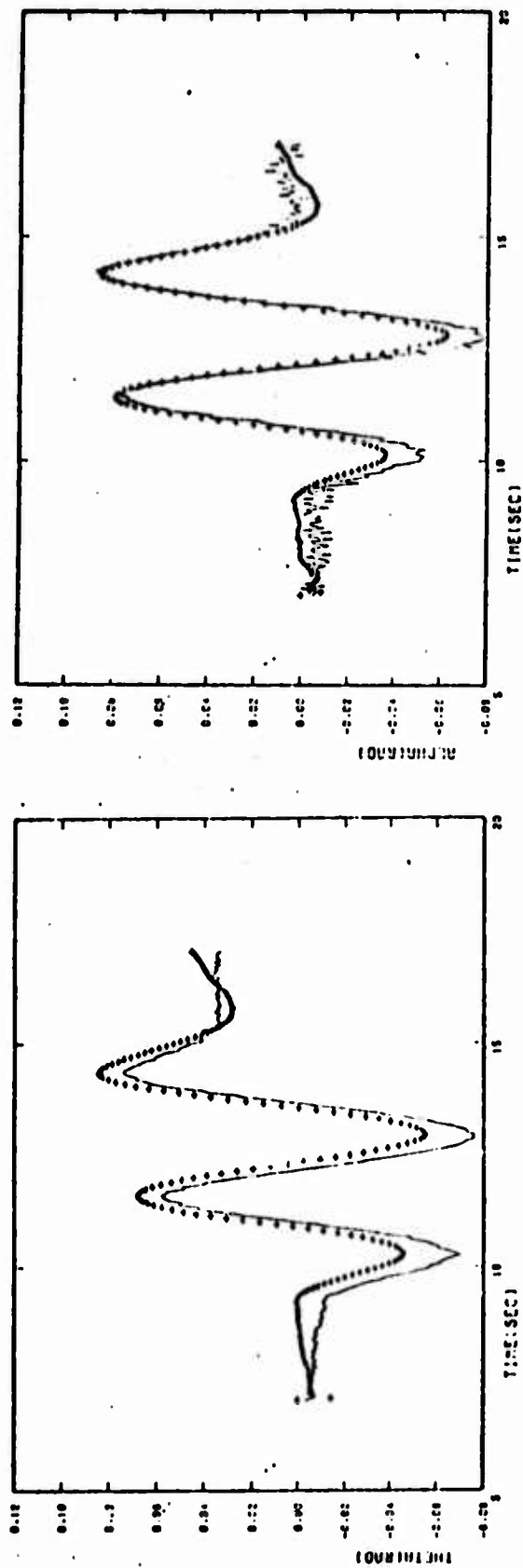
Figure 8 (Concluded)   Time History Plots for Run 2 with Rank Deficient Solution

histories are in Figure 8. Only five parameters are enough to obtain a good fit to the measurements and, therefore, are the only significant parameters.

Process Noise Estimation to Remove Gust Effects

Next, the process noise effects are included in the rank deficient solution. Table 6 compares the parameter estimates obtained from run 2 response with and without the inclusion of the process noise in the aircraft model. Figure 9 shows the time history plots. There are two major effects of including the process noise. The parameter estimates are slightly different from those obtained by the output error techniques removing, partly, the bias in the output error estimates. Secondly, the one σ on parameter estimation error is increased, providing a more realistic confidence bound on the errors. Notice that the random noise in the elevator deflection measurement enters the system as process noise, though at a different point than the gust effects. However, since these two points are not orthogonal, part of the input noise is reflected in the gust root-mean-square value.

Since the identified power spectral density is 0.000175 and the break frequency in the Dryden model is 0.5 rad sec^{-1}, the root-mean-square gust is

$$(\alpha_g)_{rms} = \sqrt{\frac{0.000175}{2 \times 0.5}} = 0.0132 \text{ rad}$$

$$= 0.75 \text{ deg} \tag{7}$$

Random Noise in Input

It is clear from Figure 5 that the measurement of the elevator input is very noisy. A major part of the error is because of noise in the telemetry link and is essentially white. The input
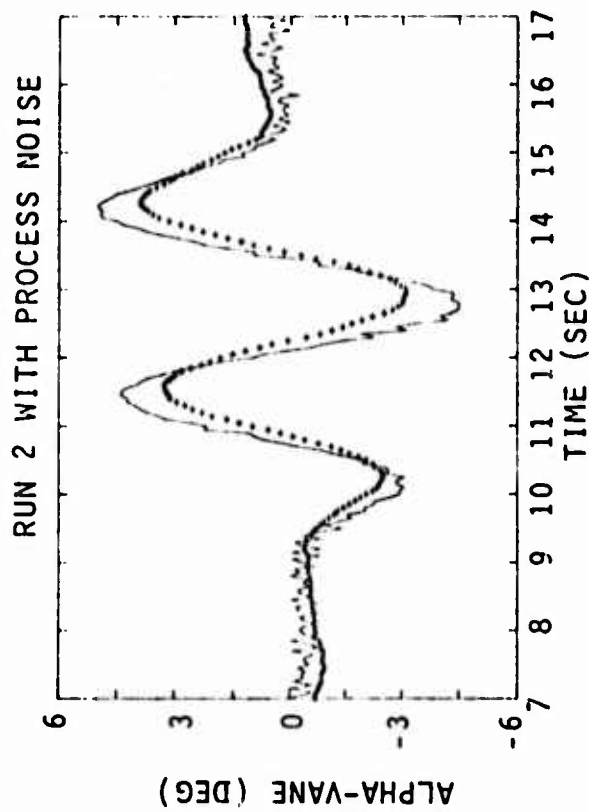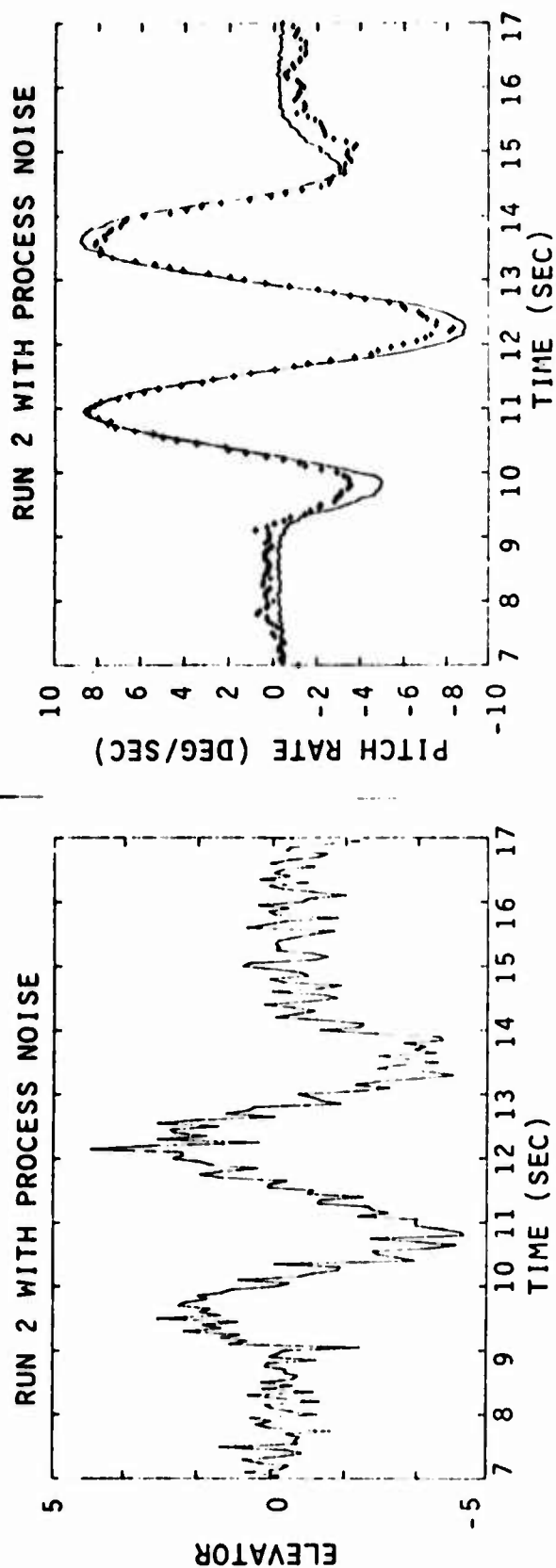
Figure 9 Time History Plots for Run 2 with Process Noise
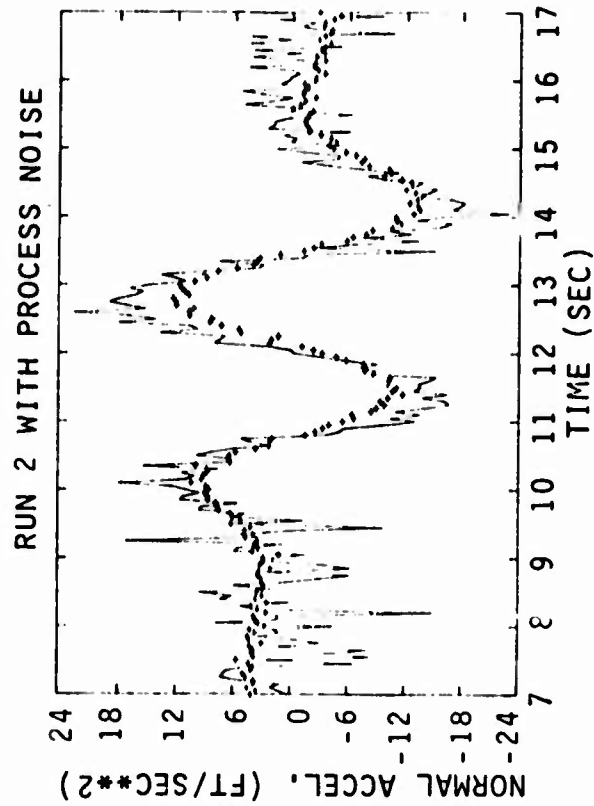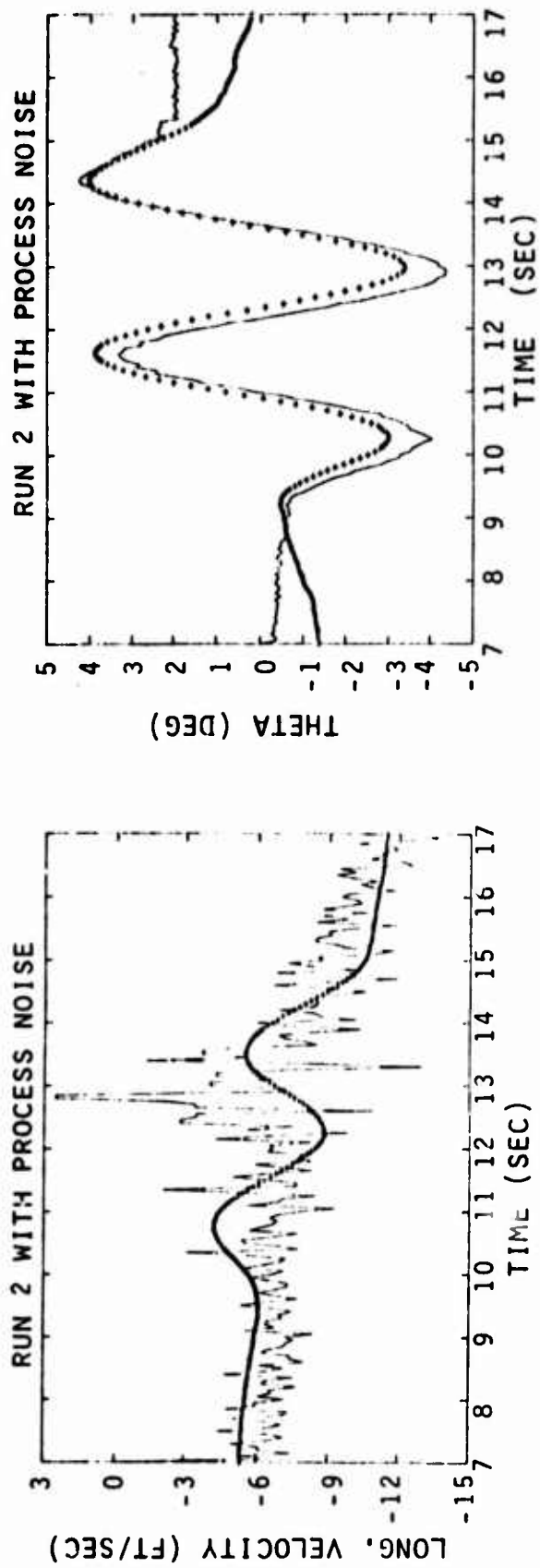
Figure 9 (Concluded)   Time History Plots for Run 2 with Process Noise

was, therefore, smoothed as shown in Figure 10. The SCIDNT is run using Figure 10 as the elevator deflection input and the same measurements as before. Table 7 shows the identified derivatives with and without the inclusion of process noise. Time history plots of the true and predicted measurements are given in Figures 11 and 12 (output error and process noise cases, respectively). The results are not as good as the output error and the process noise case when the input is not smoothed. It shows that an optimal smoothing as outlined in Appendix B is required.

Trim Bias

As explained before, there is a bias in the input because the trim value is not exactly known. In this run, the input bias is included in the model and is identified by the maximum likelihood approach of Appendix A. The identified stability and control derivatives are given in Table 9 and the time history plots are shown in Figure 13, for the output error case. The identified bias in the input is about 0.7 deg. These parameter estimates are more accurate because such a bias in the input is quite important. The importance of this bias is quite evident in the fit to the θ measurement (compare with Figure 8).

4.2.2 Two Cycle Sine Wave Input (Run 5)

Run 5 is at the same flight condition as run 2, and the input is the same, but the data length is shorter. An 8 sec long record is used for identification of aircraft stability and control derivatives. Again, a rank deficient solution in the output error mode is used. Only the short period parameters are identifiable. The parameter values are shown in Table 10, together with measurement noise standard deviation. The time histories are given in Figure 14.
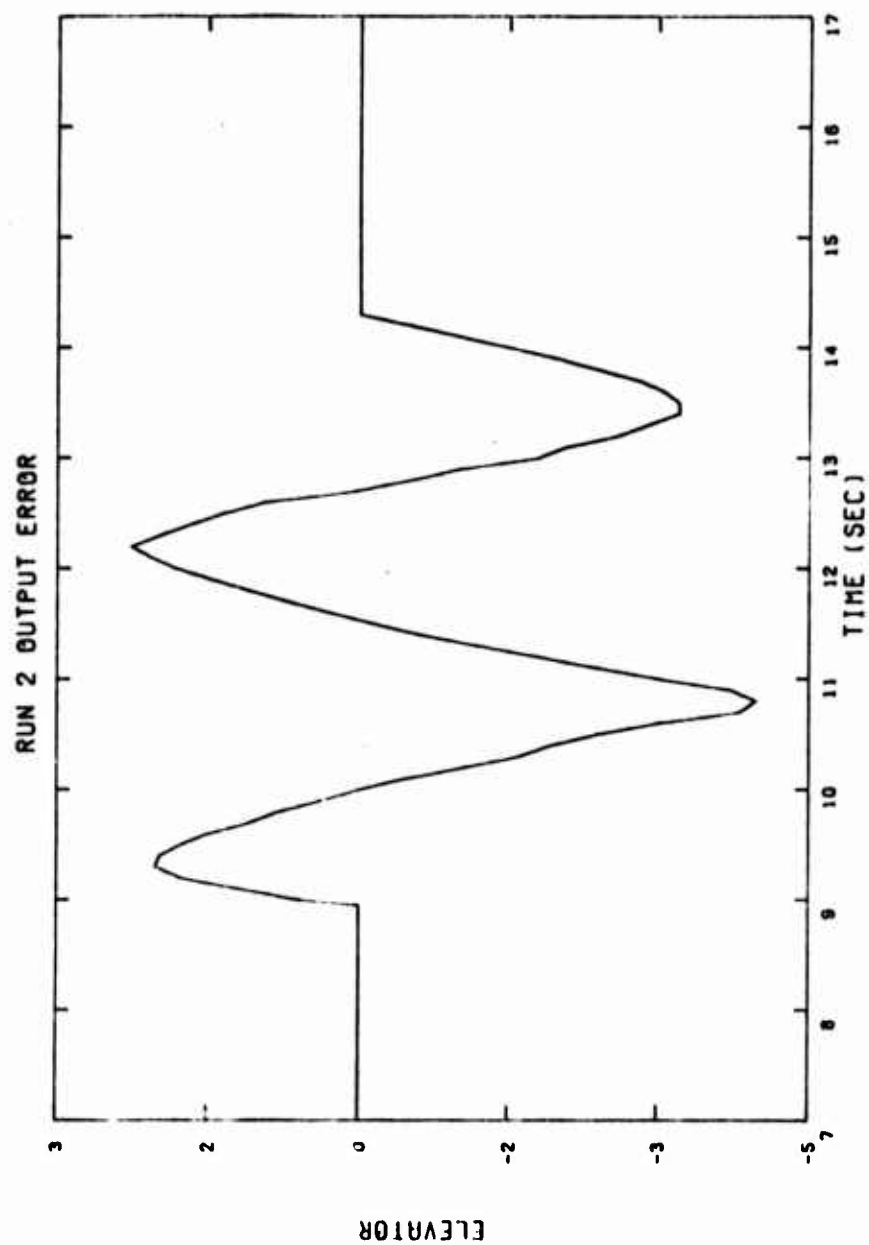
Figure 10 Smoothed Elevator Input for Run 2

Table 7
Identified Derivatives Using Smoothed Input - Run 2
10 Sec Data Length

PARAMETER	WIND TUNNEL	STARTING VALUES	OUTPUT ERROR	PROCESS NOISE
Z_α	-0.974	-0.978	-0.899	-0.819 ± 0.012
Z_u	-0.011	-0.011	*	*
Z_q	1.0	1.0	1.0	1.0
γ	0.0	0.0	*	*
X_α	-23.2	-25.8	*	*
X_u	-0.046	-0.46	*	*
X_q	0.0	0.0	*	*
M_α	-4.59	-4.59	-5.85	-3.57 ± 0.0695
M_u	0.006	0.006	*	*
M_q	-1.42	-1.95	-1.102	-2.19 ± 0.0935
ω_c	----	0.5	----	*
$Z_{\delta e}$	-0.102	-0.102	0.0221	0.0987 ± 0.0162
$X_{\delta e}$	0.0	0.0	0.0	0.0
$M_{\delta c}$	-9.63	-9.63	-5.59	-8.19 ± 0.296
K_α	1.0	1.0	1.0	1.0
$K_\alpha \ell_\alpha/V$	0.0	0.0	0.0	0.0
Q	----	0.0001	----	0.0000240 + 0.00000140
σ_α		0.007	0.0155	0.0077
σ_q		0.015	0.0264	0.0211
σ_θ		0.015	0.045	0.0275
σ_{a_z}		0.9	4.49	4.12

(All values in units of ft, sec, rad)

Table 8
Bias and Initial Conditions - Run 2
Smoothed Input, 10 Sec

	OUTPUT ERROR	PROCESS NOISE
BIASES		
b_α	-0.00326	-0.00230
b_u	-5.99	-6.29
b_q	0.00853	-0.0148
b_θ	0.00334	-0.0391
b_{a_z}	1.77	1.52
INITIAL CONDITIONS		
α	0.0	0.0
u	0.0	0.0
q	0.0	0.0
θ	0.0	0.0
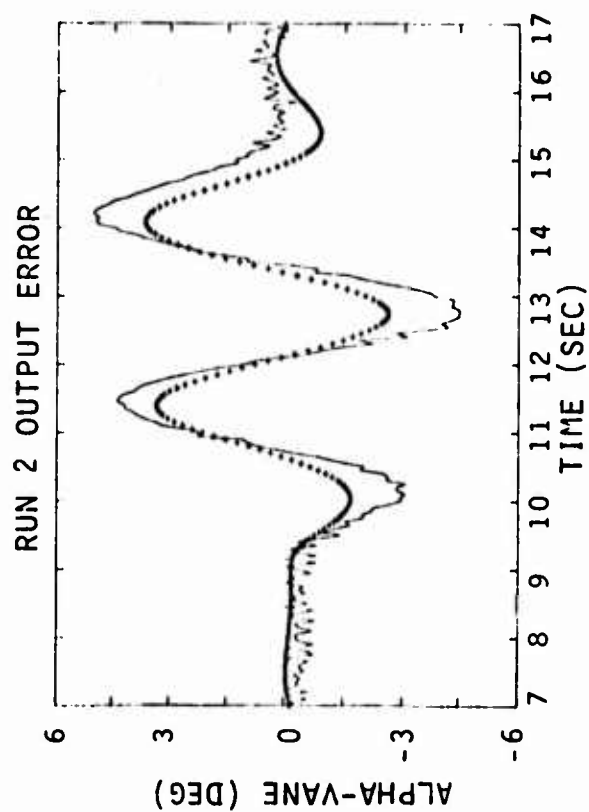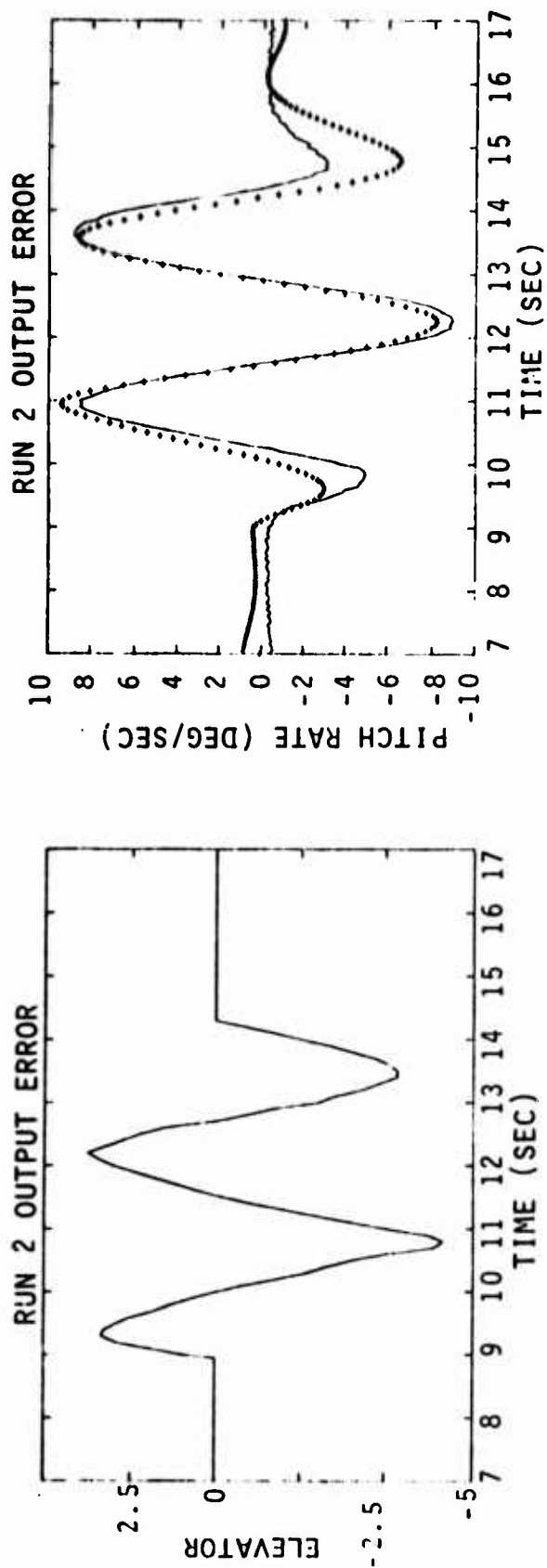
Figure 11   Time History Plots for Run 2 with Output Error
(Smoothed Input)
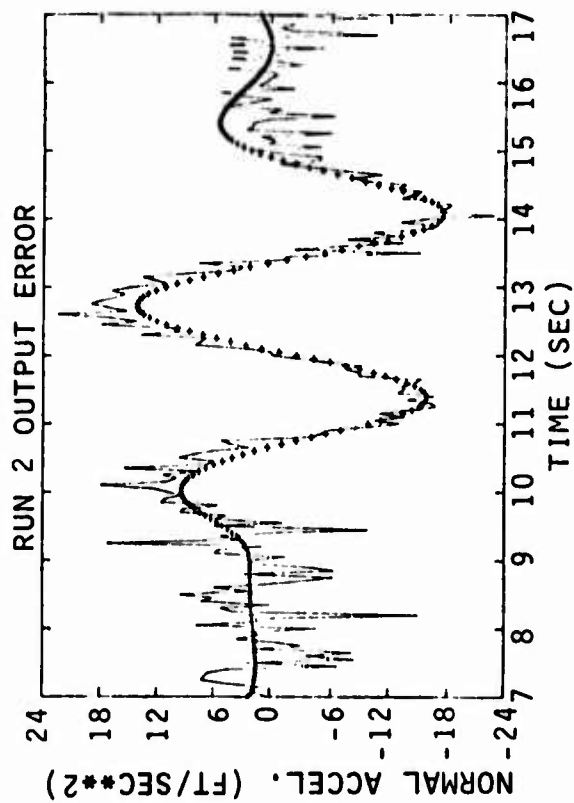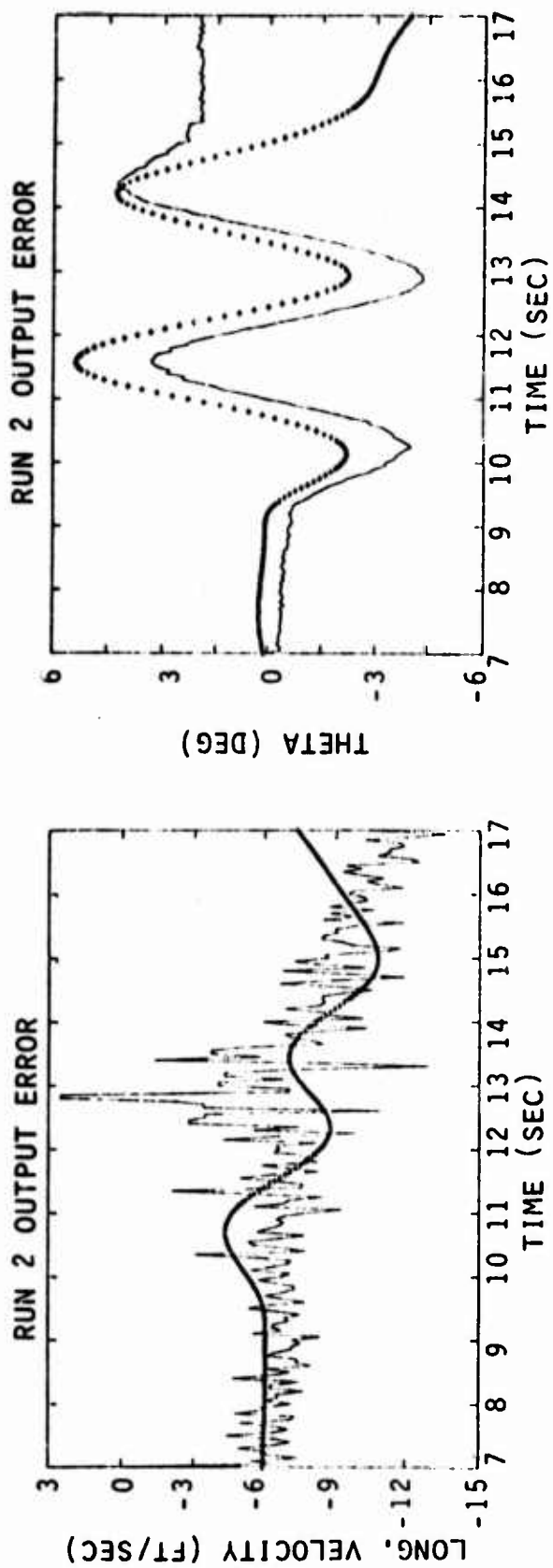
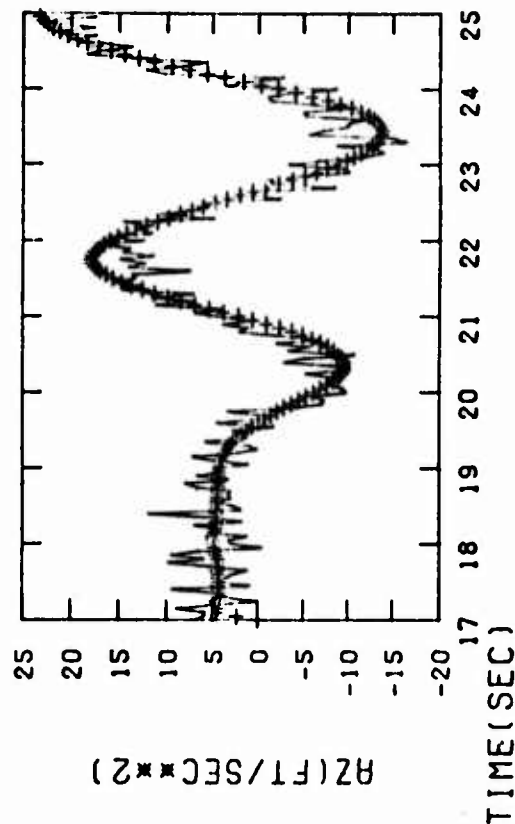Figure 11 (Concluded) Time History Plots for Run 2 with Output Error (Smoothed Input)

RUN 2 WITH NOISE

RUN 2 WITH NOISE
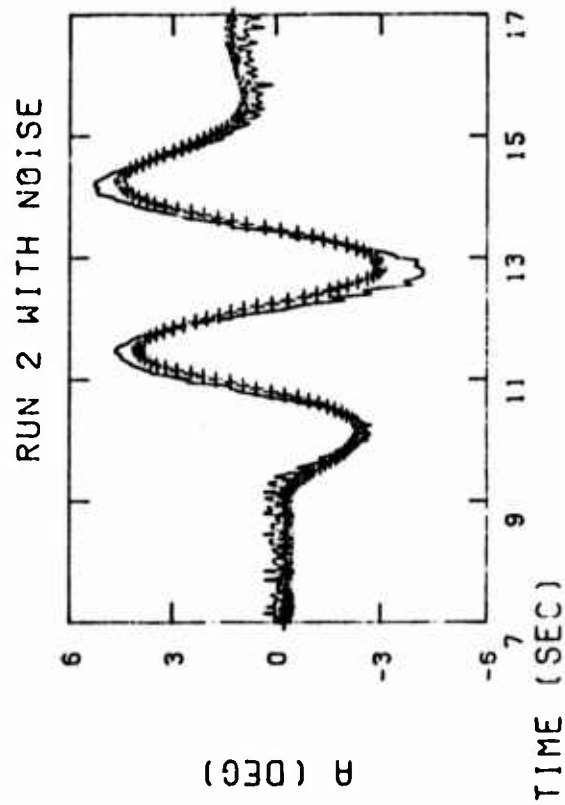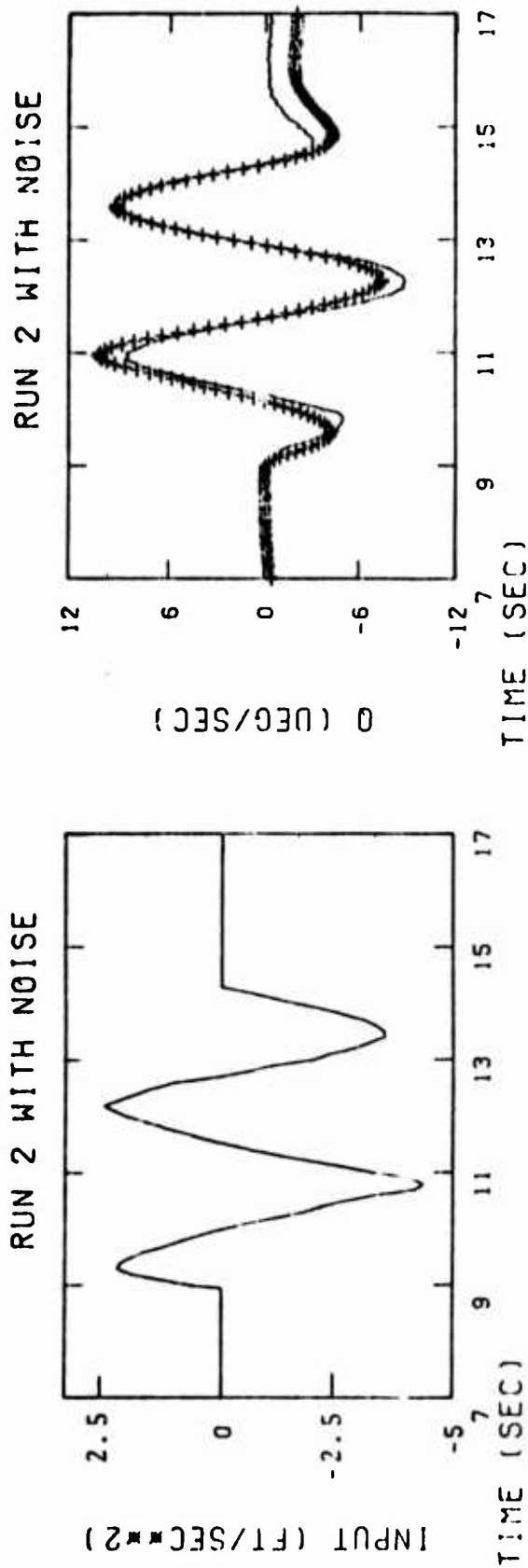
RUN 2 WITH NOISE

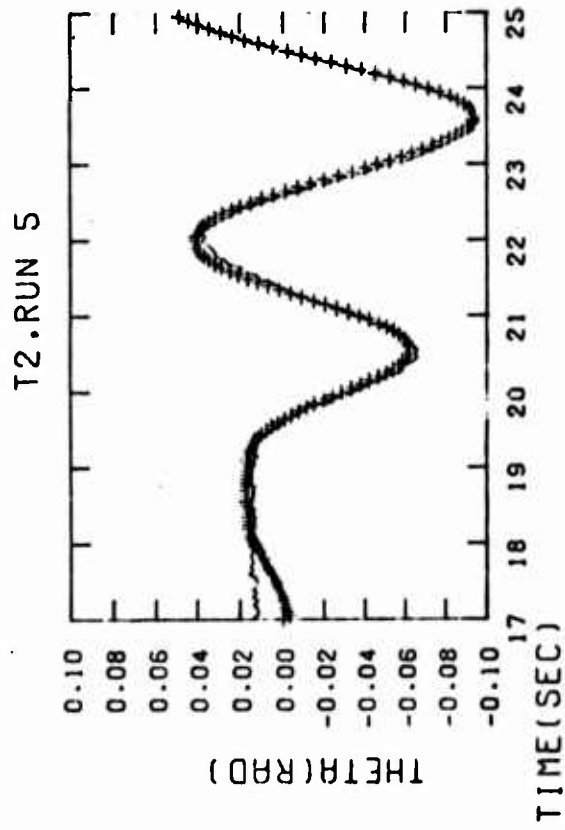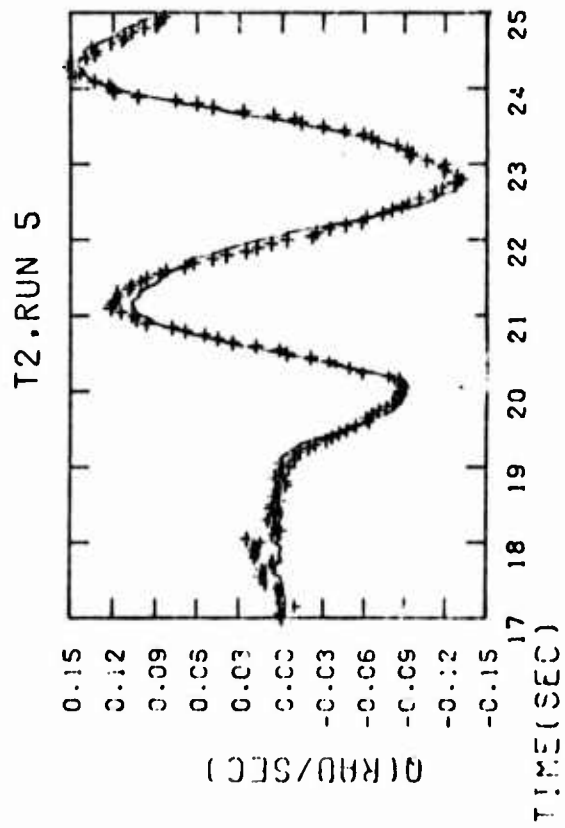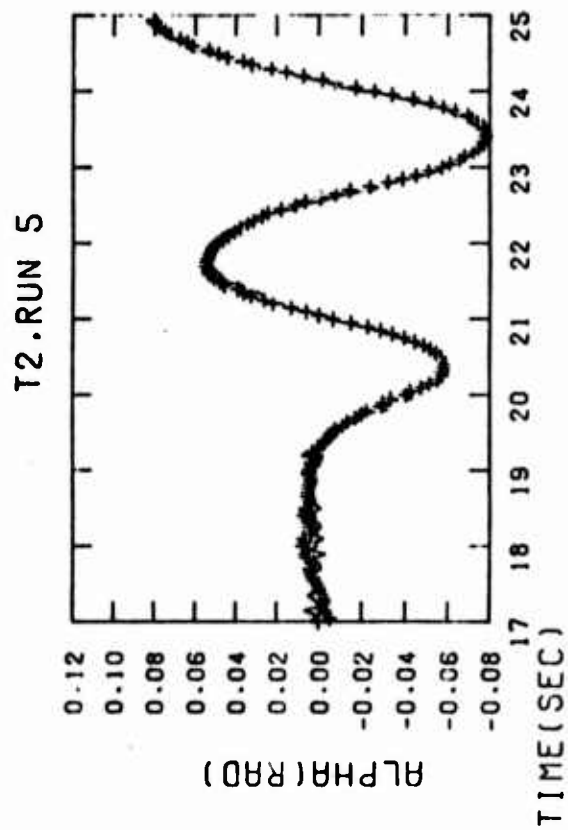Figure 12   Time History Plots for Run 2 with Noise
(Smoothed Input)
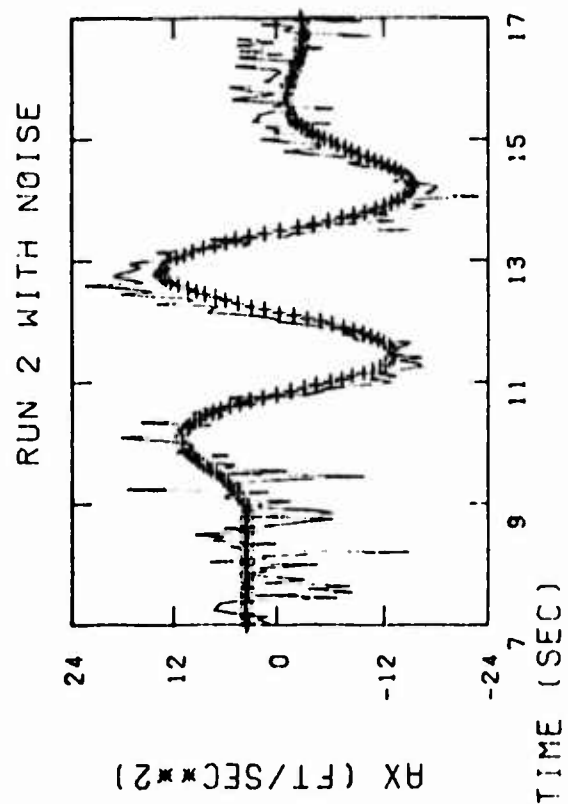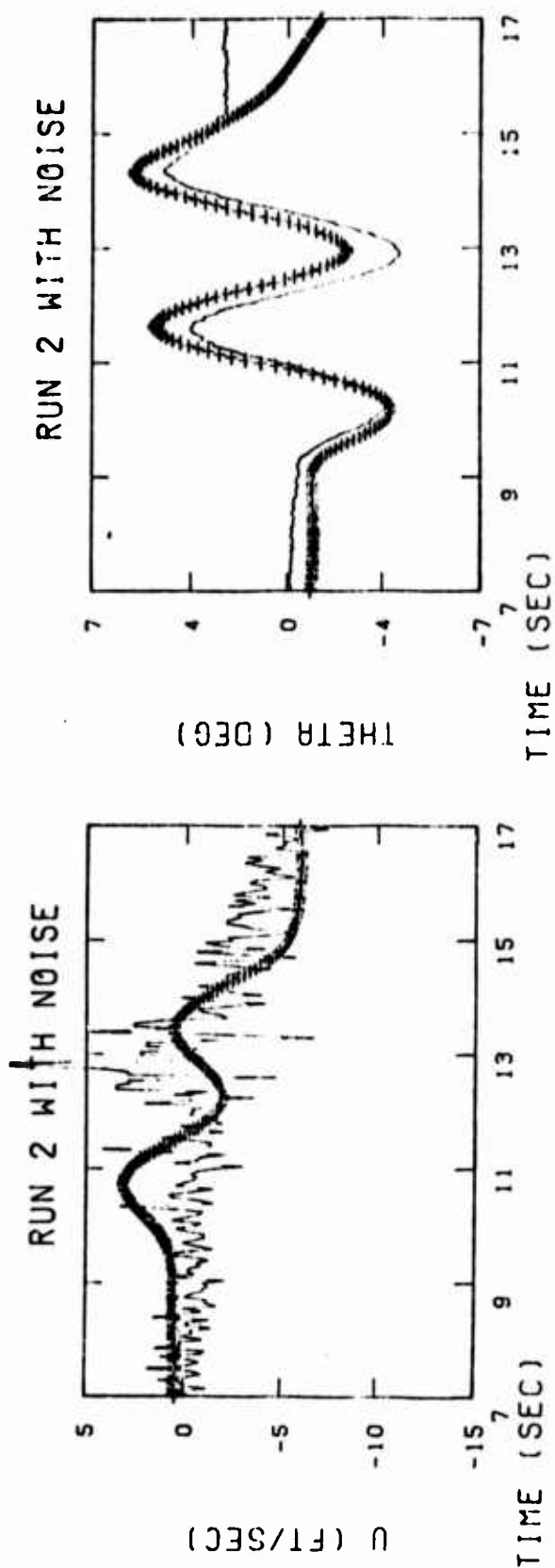
Figure 12 (Concluded)   Time History Plots for Run 2 with Noise
(Smoothed Input)

Table 9
Identified Parameters for Run 2 with Trim Bias Removed

PARAMETER	WIND TUNNEL	OUTPUT ERROR
Z_α	-0.974	-0.985
Z_u	-0.011	*
Z_q	1.0	1.0
γ	0.0	*
X_α	-23.2	*
X_u	-0.046	*
X_q	0.0	*
M_α	-4.59	-5.81
M_u	0.006	*
M_q	-1.42	-1.52
ω_c		*
Z_{δ_e}	-0.102	-0.17
X_{δ_e}	0.0	*
M_{δ_e}	-9.63	-7.95
K_α		1.0
$K_\alpha \ell_\alpha/V$		0.0
Q		*
σ_α		0.0097
σ_q		0.021
σ_θ		0.040
σ_{a_z}		4.5

(All values in units of ft, sec, rad)

Figure 13 Time History Plots for Run 2 with Output Error
(Trim Bias Removed)
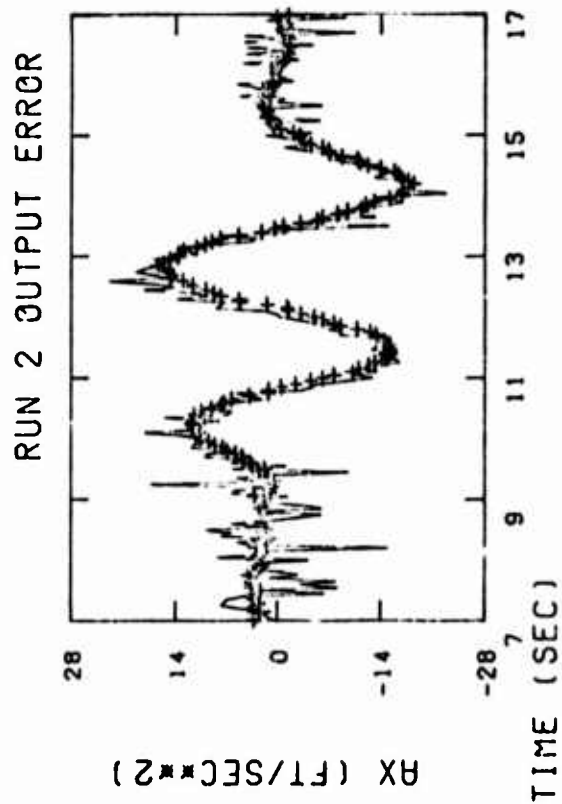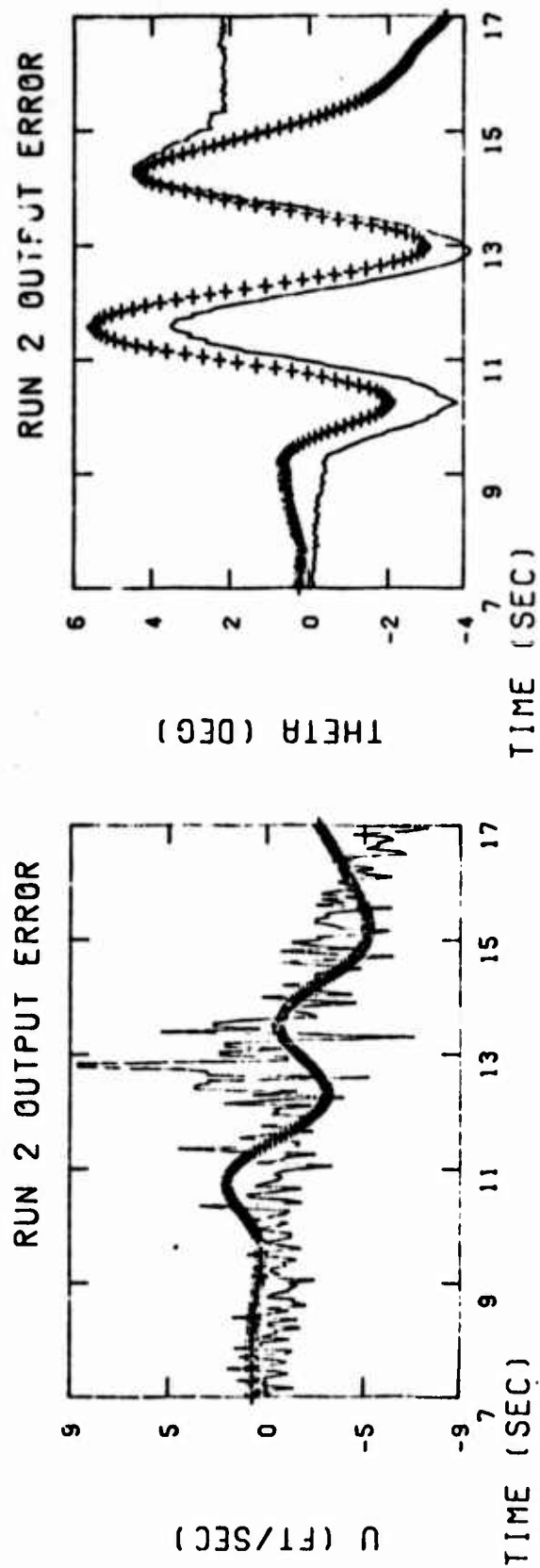
Figure 13 (Concluded) Time History Plots for Run 2 with Output Error
(Trim Bias Removed)

Table 10
Aerodynamic Derivatives With and Without Gust Effects
Doublet Input - (Run 5)
Flight Condition 1
V trim = 255.7 ft sec^{-1}, α trim = 5.2°

PARAMETER	WIND TUNNEL	STARTING VALUES	OUTPUT ERROR	PROCESS NOISE
Z_α	-0.974	-0.903	-0.9928 $\pm$ 0.076	-0.743 $\pm$ 0.123
Z_u	-0.011	0.0		
Z_q	1.0	1.0		
γ	0.0	0.0		
X_α	-23.2	0.0		
X_u	-0.046	0.0		
X_q	0.0	0.0		
M_α	-4.59	-4.32	-4.706 $\pm$ 0.0559	-4.309 $\pm$ 0.1075
M_u	0.006	0.0		
M_q	-1.42	-1.658	-1.565 $\pm$ 0.102	-1.435 $\pm$ 0.0604
ω_c		0.5		
Z_{δ_e}	-0.102	-0.572	-0.354 $\pm$ 0.121	-0.407 $\pm$ 0.1204
X_{δ_e}	0.0	0.0		
M_{δ_e}	-9.63	-7.445	-7.976 $\pm$ 0.347	-7.25 $\pm$ 0.353
K_α		1.0		
$K_\alpha \ell_\alpha/V$		0.0		
Q		0.0		$1.9 \times 10^{-4} \pm 2.2 \times 10^{-5}$
σ_α		0.00911	0.00468	0.00412
σ_q		0.0125	0.0112	0.0093
σ_θ		0.0137	0.00742	0.005
σ_{a_z}		4.35	3.34	3.23

(All values in units of ft, sec, rad)
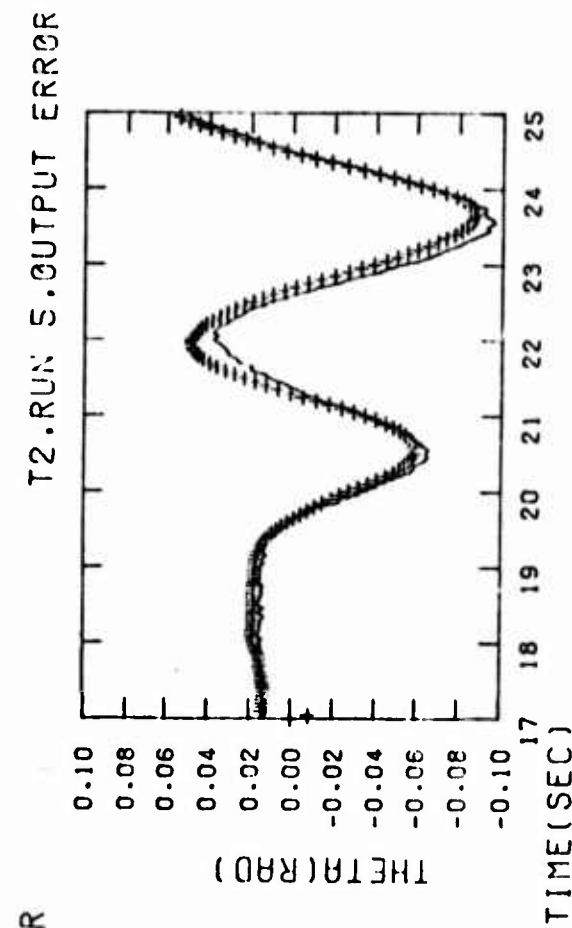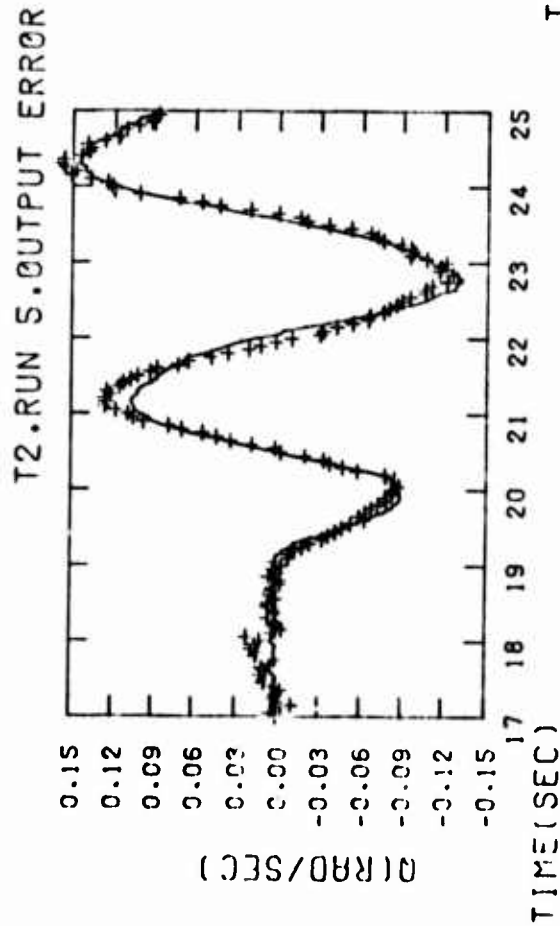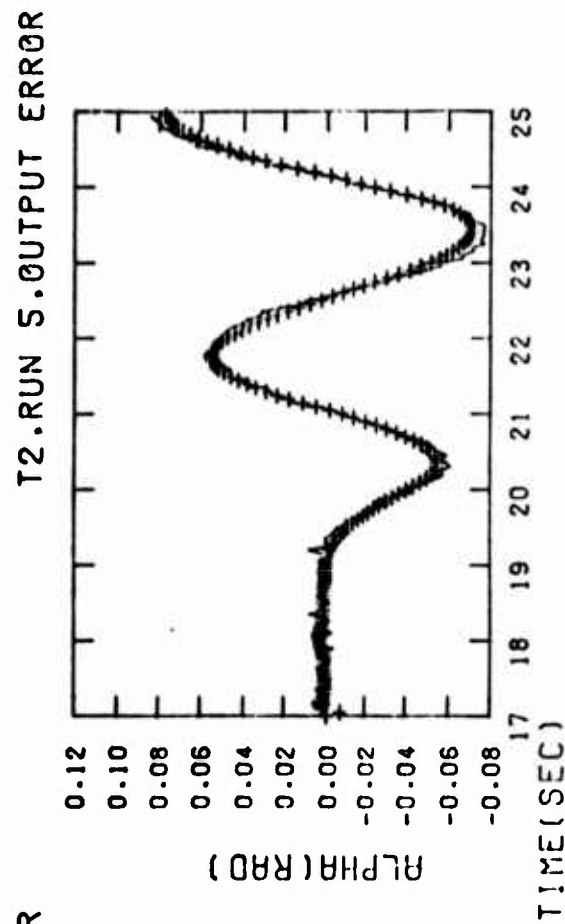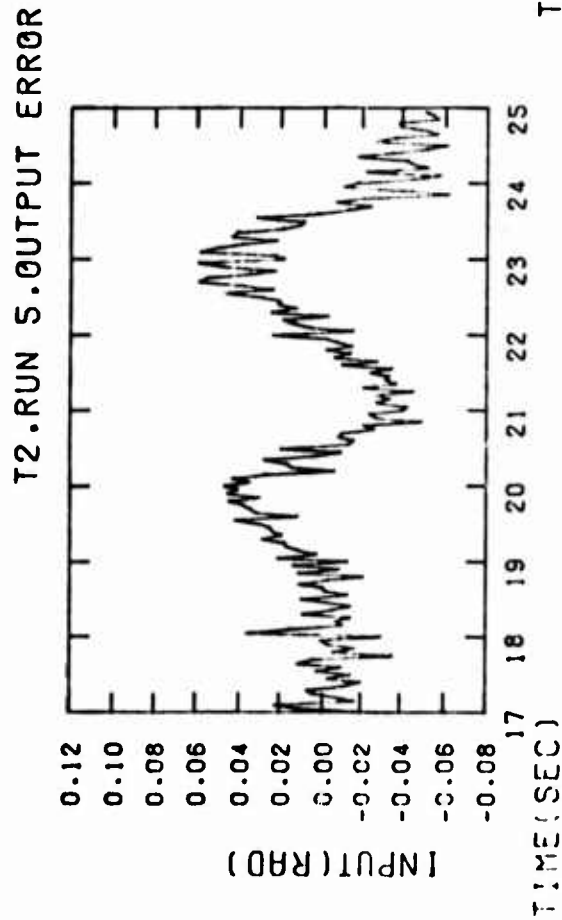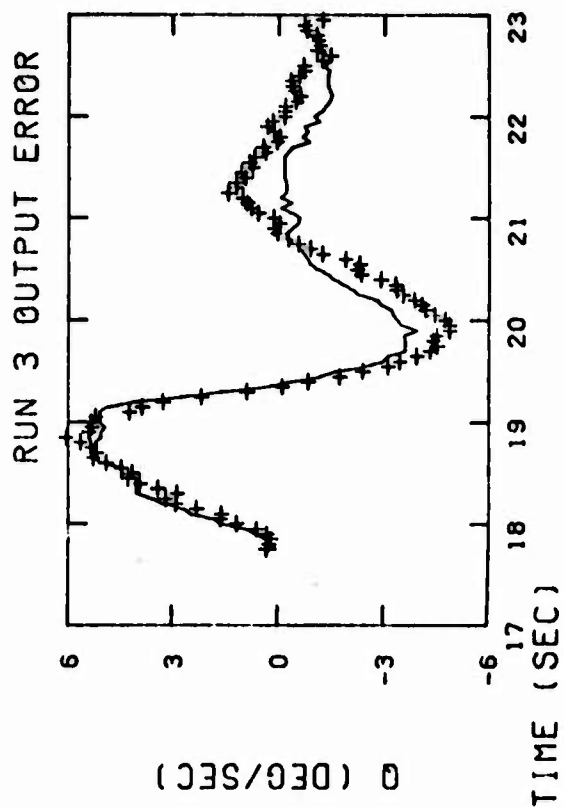
Figure 14 Time History Plots for Run 5 Using Output Error
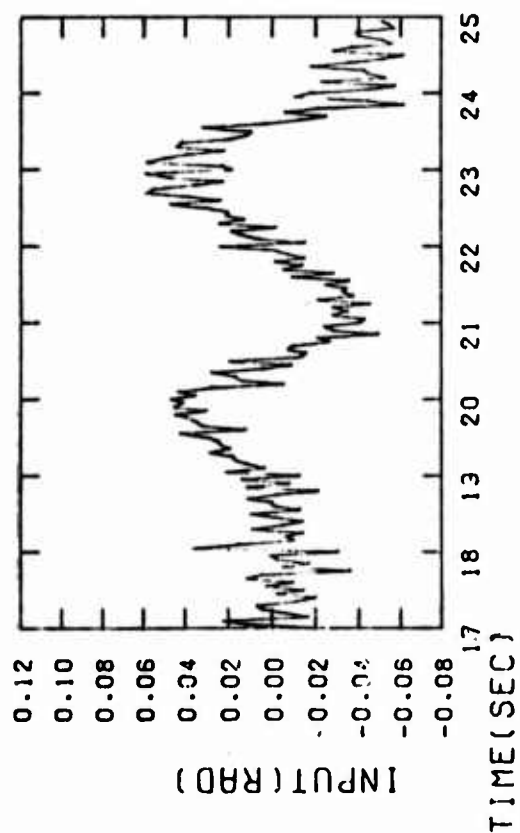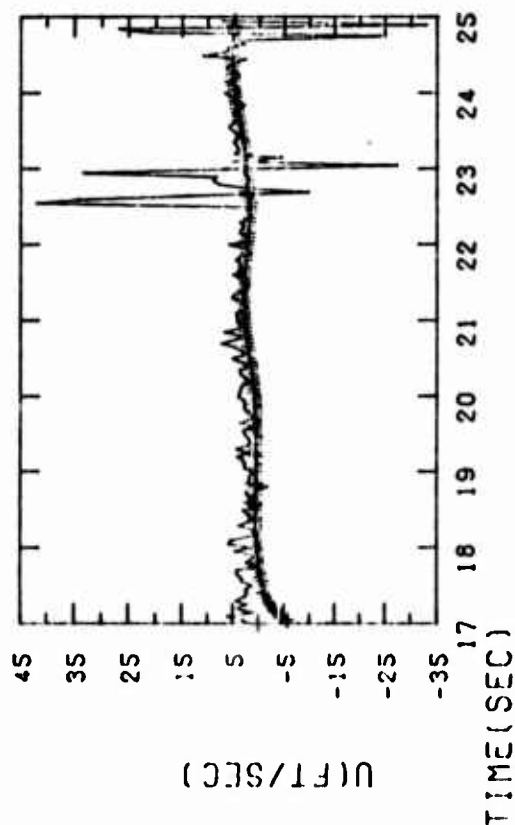
Figure 14 (Concluded) Time History Plots for Run 5 Using Output Error
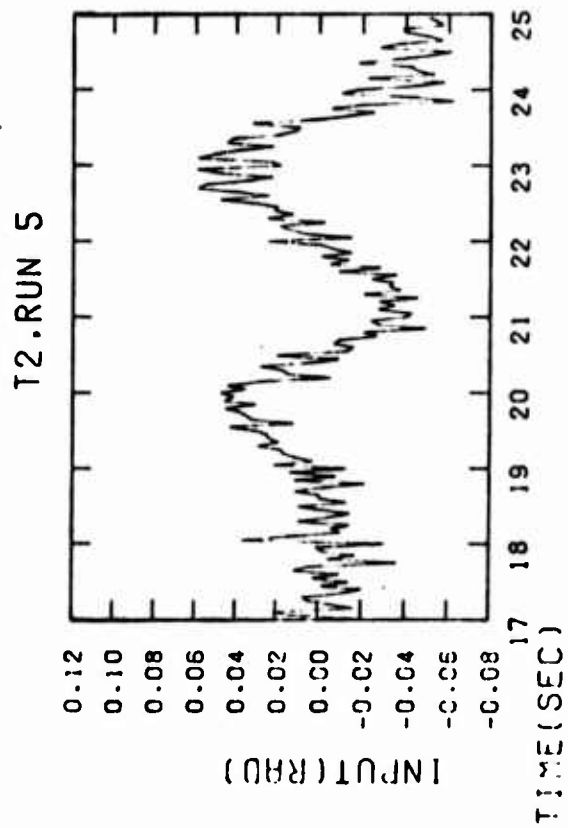
Figure 15 Time History Plots for Run 5 with Process Noise

16
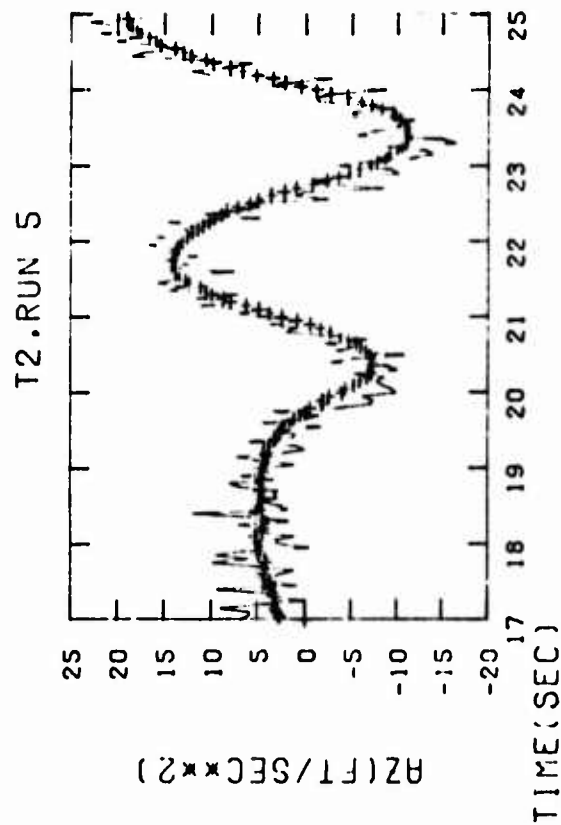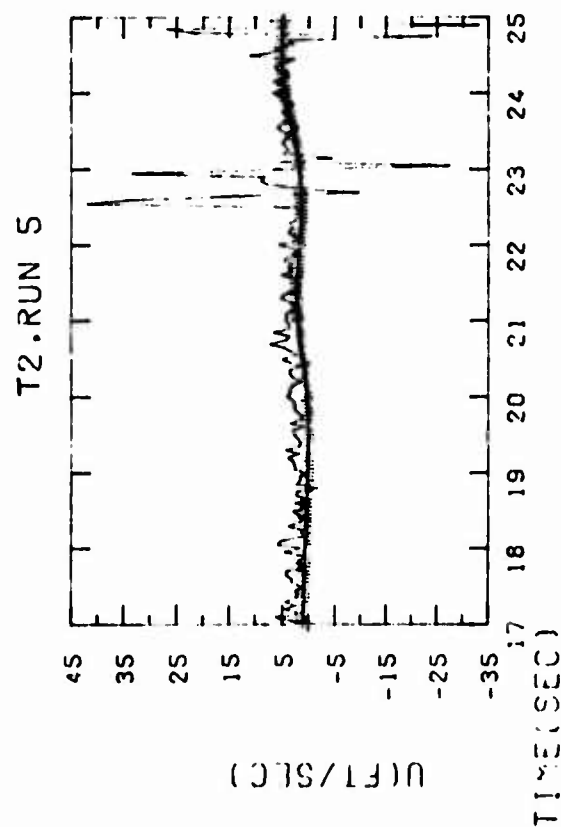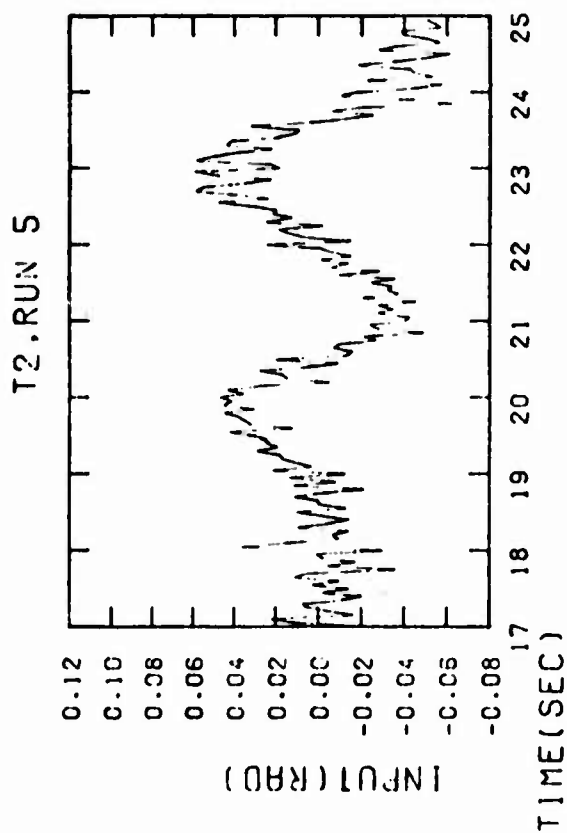
Figure 15 (Concluded) Time History Plots for Run 5 with Process Noise

The maximum likelihood method is repeated with process noise. The time histories shown in Figure 15 have better fit. The aprameter estimates are given in Table 10. The computed one σ values are higher than with output error approach. This shows that the output error method tends to underestimate the parameter estimation errors. This is an important feature from the point of evaluation of accuracy of estimated parameter values. The break frequency is kept fixed at 0.5 rad/sec. Since,

$$\dot{\alpha}_g = -0.5 \; \alpha_g + \omega \tag{8}$$

in the steady state

$$(\alpha_g)_{rms} = \sqrt{Q/(2 \times 0.5)} = \sqrt{Q} \tag{9}$$

where q is the power spectral density of the process noise. Since q = 1.9×10^{-4},

$$(\alpha_g)_{rms} = 0.0138 \; rad = 0.78° \tag{10}$$

4.2.3 Pulse Inputs (Runs 3 and 6)

The measurements of elevator deflection input and the resulting aircraft response for run 3 are plotted in Figure 16. The input is a short duration pulse and there is little excitation of the aircraft. It was suspected that this data record is not going to provide accurate parameter estimates. The data is run through SCIDNT in the output error mode. The parameter values are given in Table 11 and the time history plots in Figure 16. The standard deviation on these parameter estimates is higher than for run 2 or run 5, signifying that these parameter estimates are of poorer quality. Nevertheless, the response time history determined using the parameters is close to the measurements.
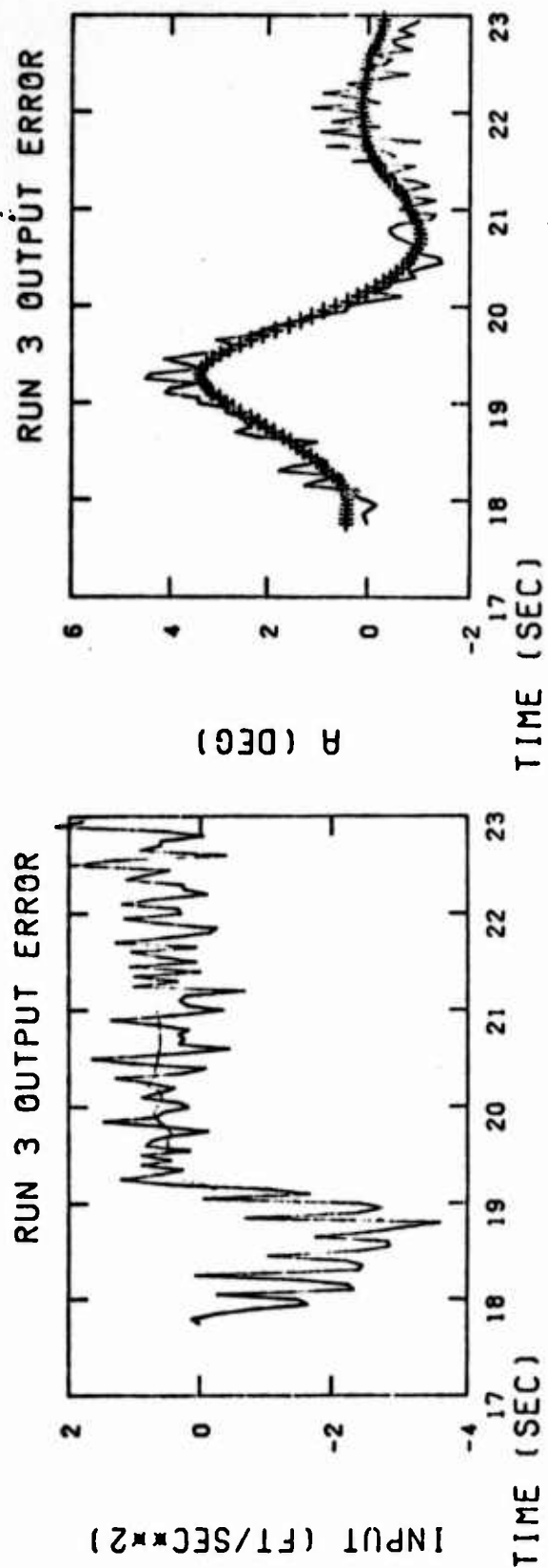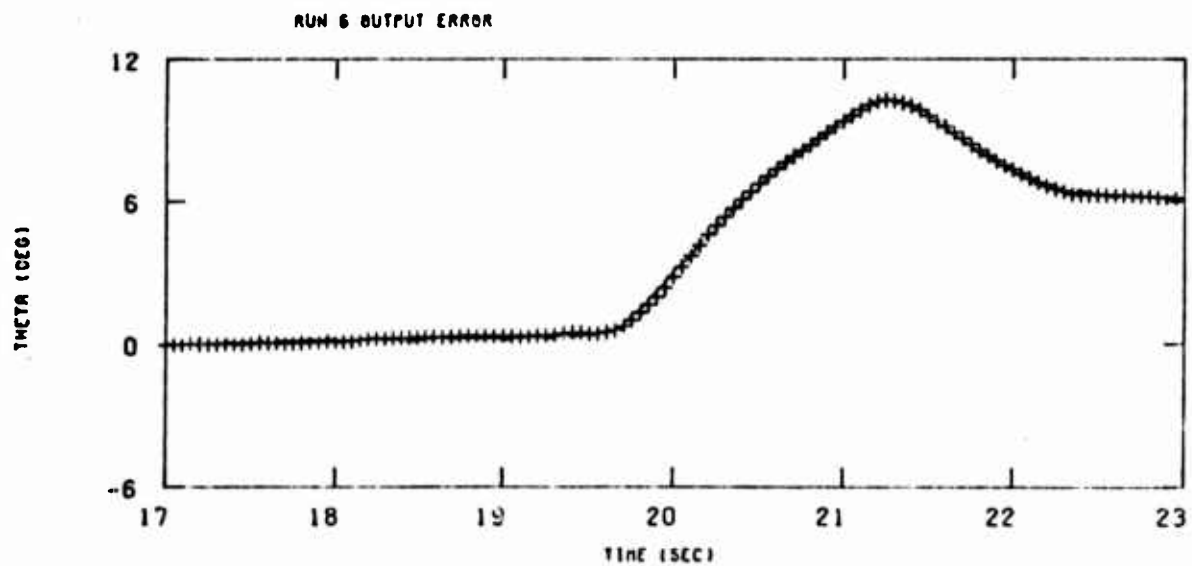
Figure 16   Time History Plots for Pulse Input (Run 3) With Output Error
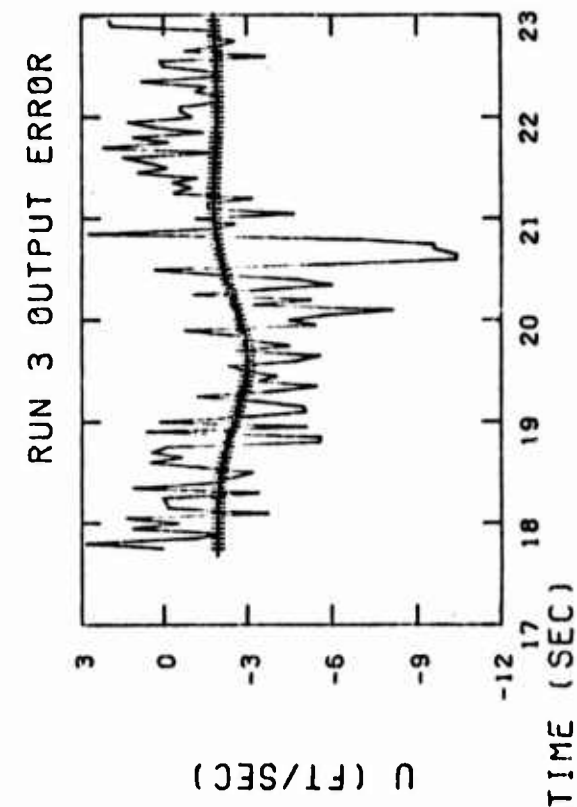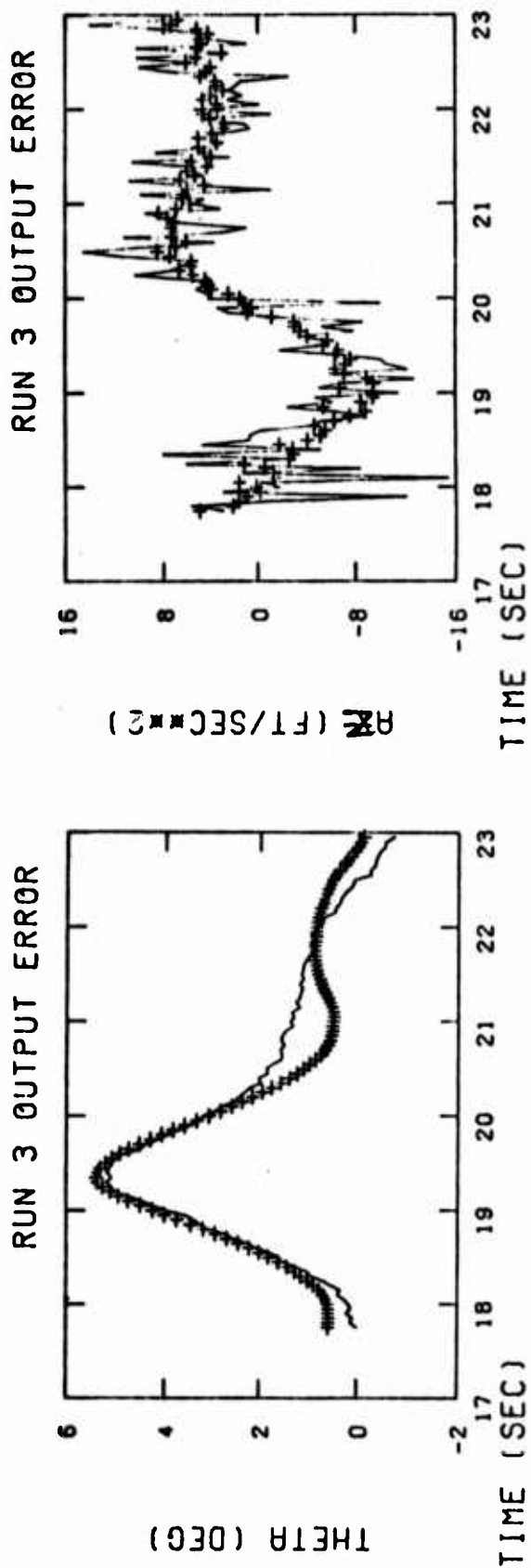
Figure 16 (Concluded) Time History Plots for (Run 3) With Output Error

Table 11
Flight Condition 1 - Pulse Input (Run 3)
17.75-23.00 Sec Data Length

PARAMETER	WIND TUNNEL	STARTING VALUES	OUTPUT ERROR
Z_α	-0.974	-0.974	-0.788 ± 0.1245
Z_u	-0.011	-0.011	*
Z_q	1.0	1.0	1.0
γ	0.0	0.0	*
X_α	-23.2	-25.8	*
X_u	-0.046	-0.046	*
X_q	0.0	0.0	*
M_α	-4.59	-4.59	-4.594 ± 0.1838
M_u	0.0006	0.0006	*
M_q	-1.42	-1.95	-1.649 ± 0.1738
ω_c	- - - -	- - - -	- - - -
Z_{δ_c}	-0.102	-0.102	0.308 ± 0.0197
X_{δ_c}	0.0	0.0	*
M_{δ_e}	-9.63	-9.63	-7.084 ± 0.330
K_α	1.0	1.0	*
$K_\alpha \ell_\alpha / V$	0.0	0.0	*
Q	- - - -	- - - -	- - - -
σ_α	- - - -	0.007	0.0086
σ_q	- - - -	0.015	0.0142
σ_θ	- - - -	0.015	0.0078
σ_{a_z}	- - - -	0.9	3.9
b_α	-0.00753		-0.00753
b_u	- - - -	- - - -	-1.92
b_q	- - - -	- - - -	0.00487
b_θ	- - - -	- - - -	0.01
b_{a_z}	- - - -	- - - -	2.0

(All values in units of ft, sec, rad)

.1

This procedure is repeated for run 6. The parameter values are shown in Table 12 and the comparison of the time history of the measured response and the estimated response is given in Figure 17.

4.2.4 Summary of Results and Model Verification

Identification results for flight condition 1 are summarized in Table 13. Also shown are the aggregate parameter values by combining the estimates from runs 2, 3, 5 and 6 in the inverse ratio of their covariances. The results from different runs are close to each other.

Next, the model is verified by an independent prediction. The parameter estimates obtained from run 2 with noise input and process noise consideration are using to construct a linear aircraft model at the specified flight condition. This model is used with the elevator inputs for runs 3 and 5 to predict the response of the aircraft to these inputs. These predicted responses are compared to the actual responses measured by instruments onboard the aircraft. Figure 18 shows the comparison for run 3 and Figure 19 for run 5. There is a faily good match indicating that the model is valid. Notice that the match would be better if process noise is assumed in the prediction of response for runs 3 and 5.

4.3 HIGH SPEED, CLEAN CONFIGURATION (FLIGHT CONDITION 2)

The flight condition 2 is at 10,000 ft altitude and the speed is 679 ft sec^{-1}. The gear and flaps are retracted. Ten runs were made at this flight condition. Out of these, runs 10, 11, 12, 13, 18 and 19 are processed using SCIDNT.

Table 12
Identified Parameter for Pulse Input (Run 6)

PARAMETER	WIND TUNNEL	STARTING VALUES	OUTPUT ERROR
Z_α	-0.974	-0.974	-0.921 ± 0.0454
Z_u	-0.011	-0.011	*
Z_q	1.0	1.0	*
γ	0.0	0.0	*
X_α	-25.8	-25.8	*
X_u	-0.046	-0.046	*
X_q	0.0	0.0	*
M_α	-4.59	-4.59	-4.81 ± 0.119
M_u	0.006	0.006	*
M_q	-1.95	-1.95	-2.56 ± 0.112
ω_c	- - - -	- - - -	- - - -
$Z_{\delta e}$	-0.102	-0.102	0.183 ± 0.0616
$X_{\delta e}$	0.0	0.0	*
$M_{\delta e}$	-9.63	-9.63	-9.38 ± 0.239
K_α	- - - -	1.0	*
$K_\alpha \ell_\alpha /V$	- - - -	0.0	*
Q	- - - -	0.0	*
σ_α	- - - -	0.0063	0.0103
σ_q	- - - -	0.0055	0.0095
σ_θ	- - - -	0.0118	0.0018
σ_{a_z}	- - - -	0.71	6.2
Z_o	- - - -	0.0	-0.022
M_o	- - - -	0.0	0.0711
b_α	- - - -	0.0	0.0143
b_q	- - - -	0.0	-0.00164
b_0	- - - -	0.0	-0.000567
b_{a_z}	- - - -	0.0	-0.000354

(All values in units of ft, sec, rad)
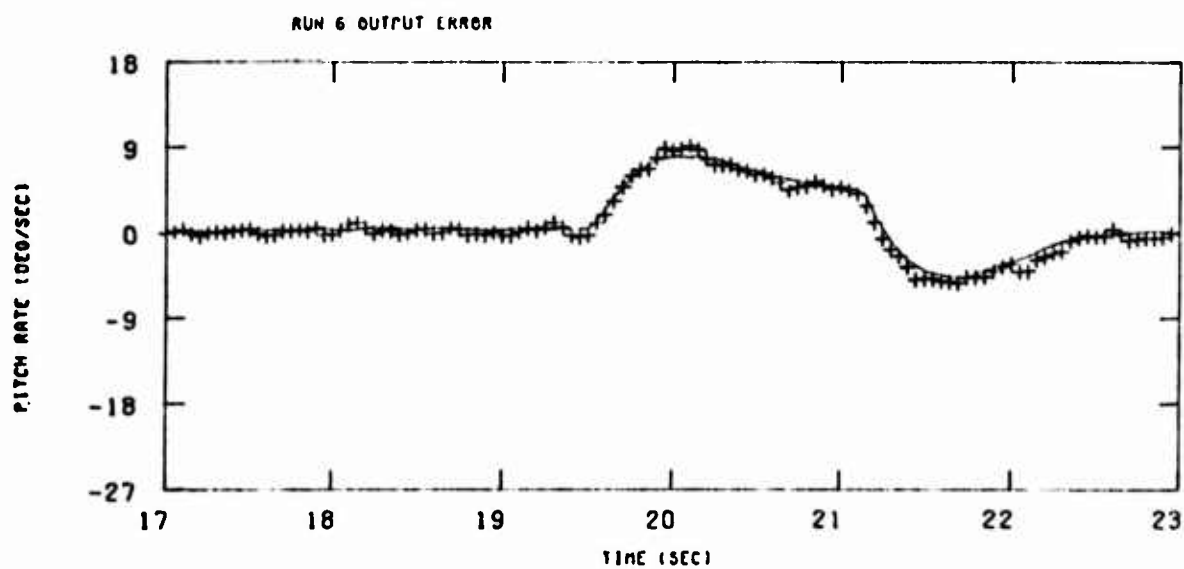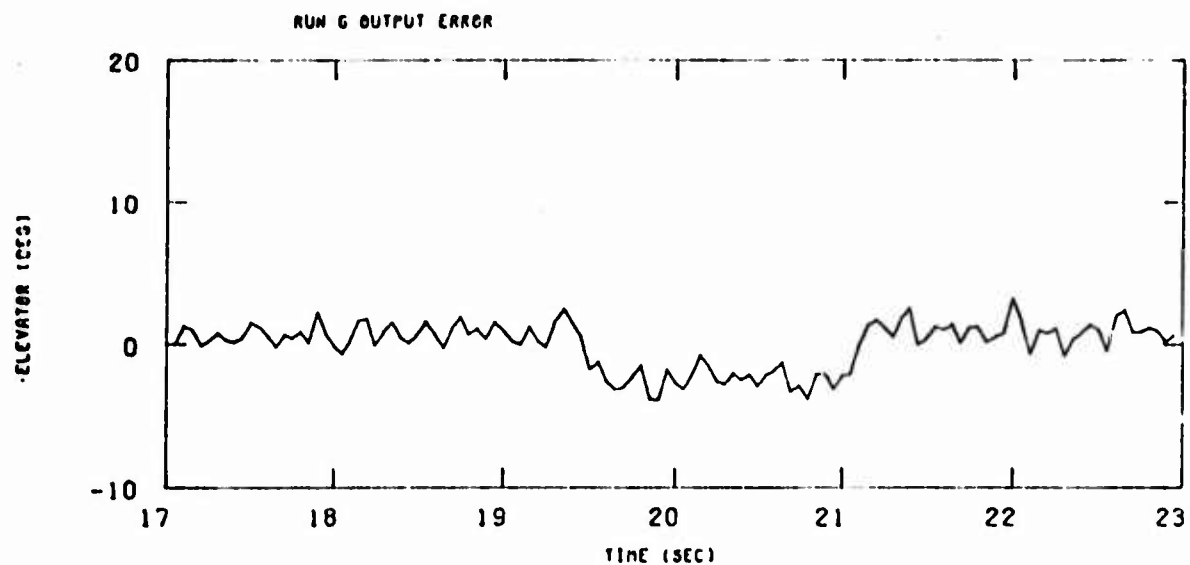
Figure 17 Time History Plots for Pulse Input (Run 6)
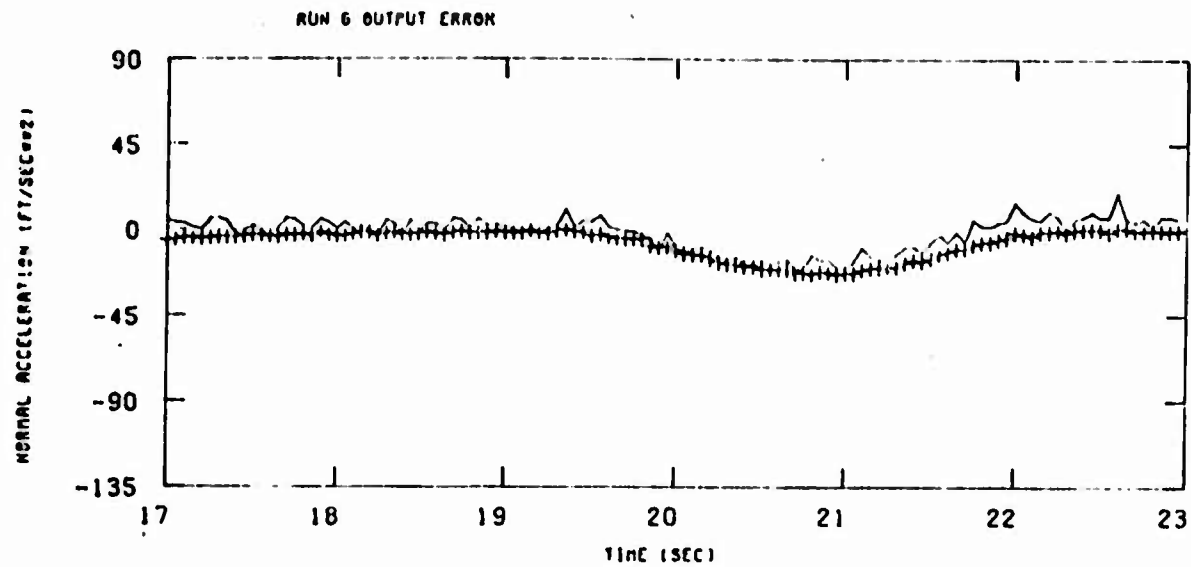
Figure 17 (Continued)   Time History Plots for Pulse Input (Run 6)
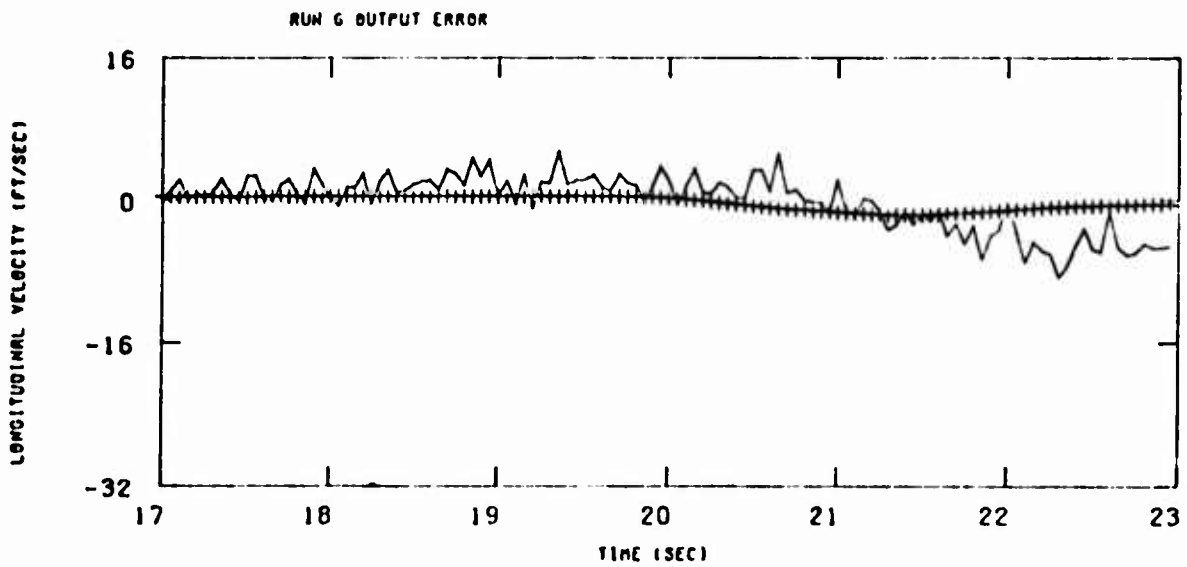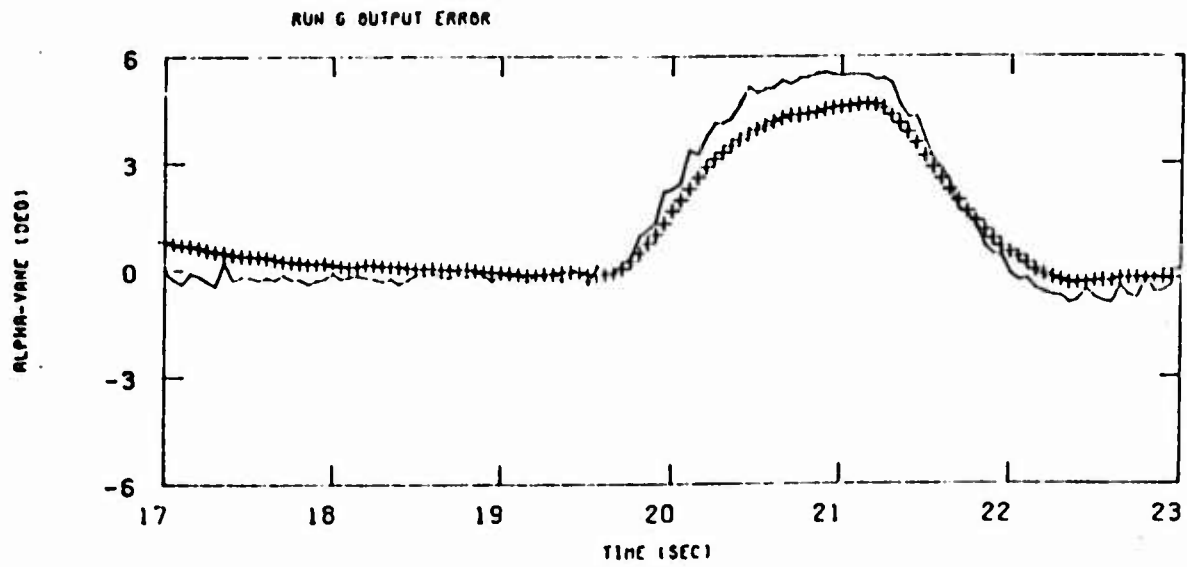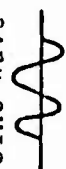
Figure 17 (Concluded)   Time History Plots for Pulse Input (Run 6)

Table 13

Summary of Stability and Control Derivatives for Flight Condition 1
Speed 236 ft sec^{-1}
Altitude Sea Level

Configuration - Gear Down, Flaps Deflected 16°

RUN	2	3	5	6	COMBINED	WIND TUNNEL VALUES
INPUT	2 Cycle Sine Wave	Low Amplitude Pulse	2 Cycle Sine Wave	High Amplitude Pulse		
PARAMETER						
Z_α	-0.903 (0.052)	-0.788 (0.1245)	-0.9928 (0.076)	-0.921 (0.0454)	-0.913	-0.974
Z_q	1.0	1.0	1.0	1.0	1.0	1.0
M_α	-4.323 (0.0588)	-4.594 (0.1838)	-4.706 (0.0559)	-4.81 (0.119)	-4.564	-4.59
M_q	-1.658 (0.103)	-1.649 (0.1758)	-1.565 (0.102)	-2.56 (0.112)	-1.865	-1.42
$Z_{\delta e}$	-0.5724 (0.0787)	0.308 (0.0197)	-0.354 (0.121)	0.183 (0.0616)	0.244	-0.102
$M_{\delta e}$	-7.445 (0.196)	-7.084 (0.330)	-7.976 (0.347)	-9.38 (0.239)	-8.01	-9.63
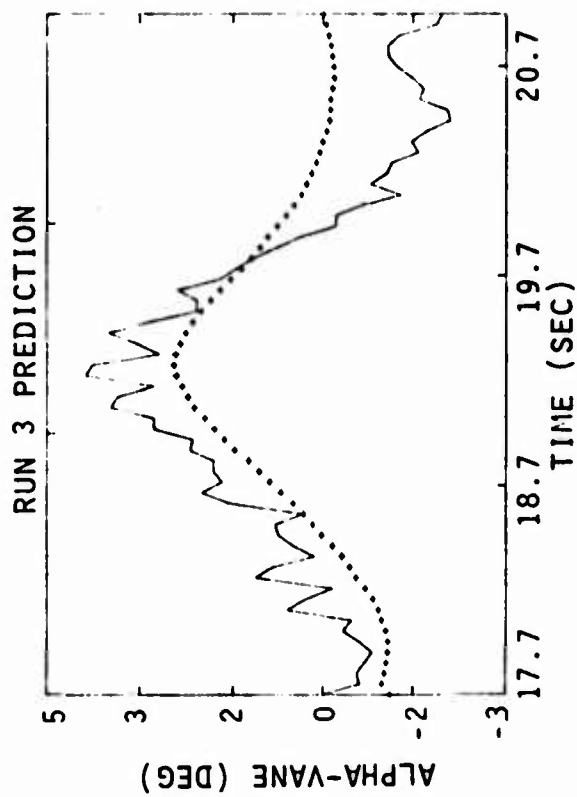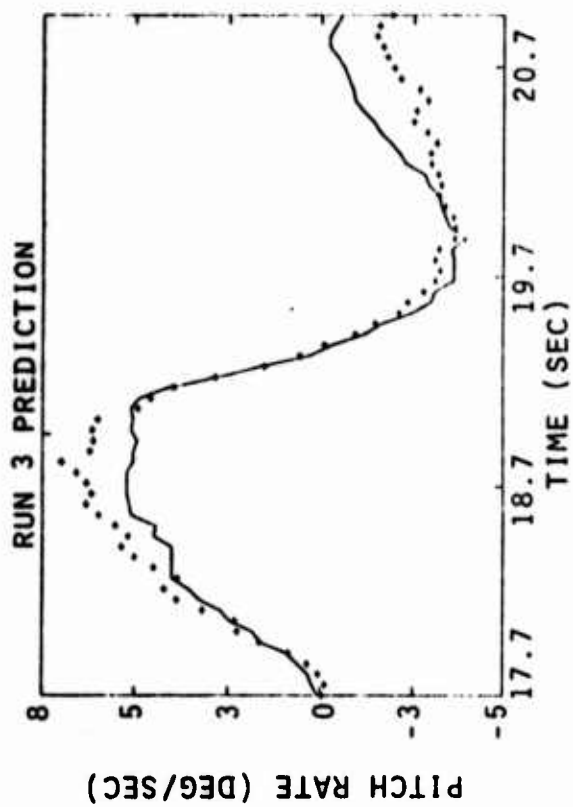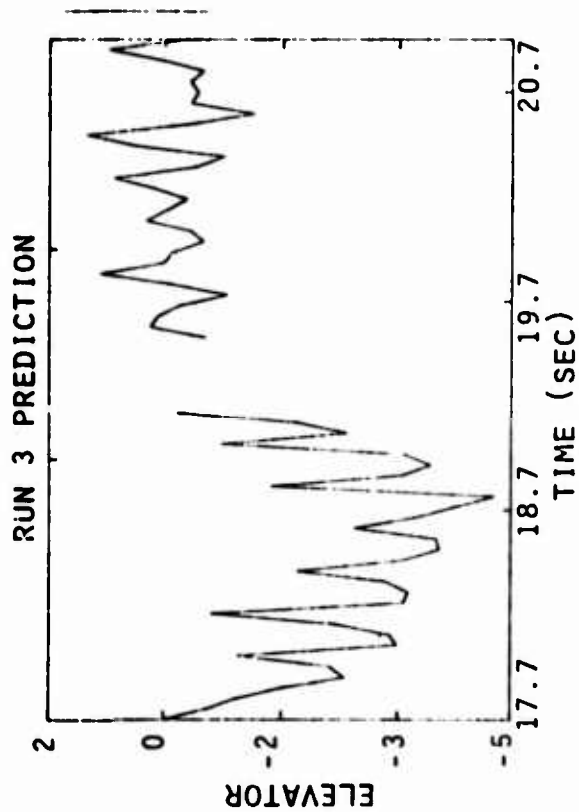
Figure 18   Time History Plots for Run 3 with Prediction
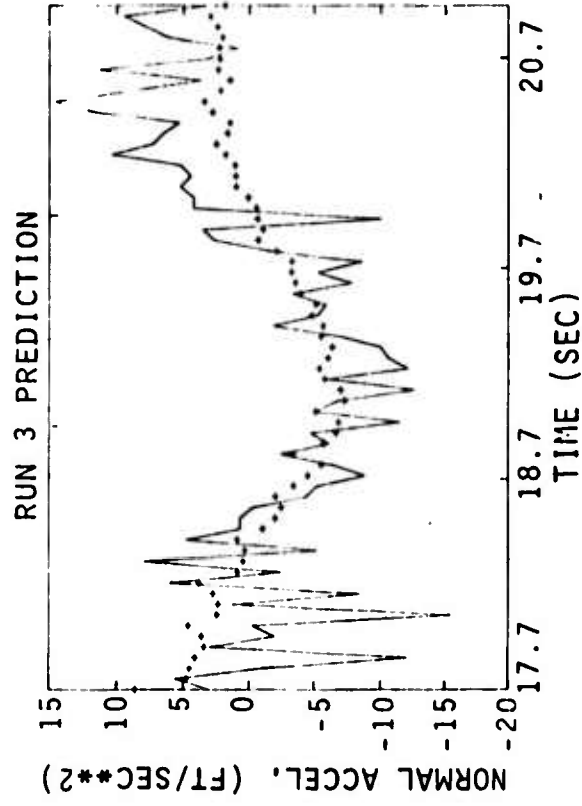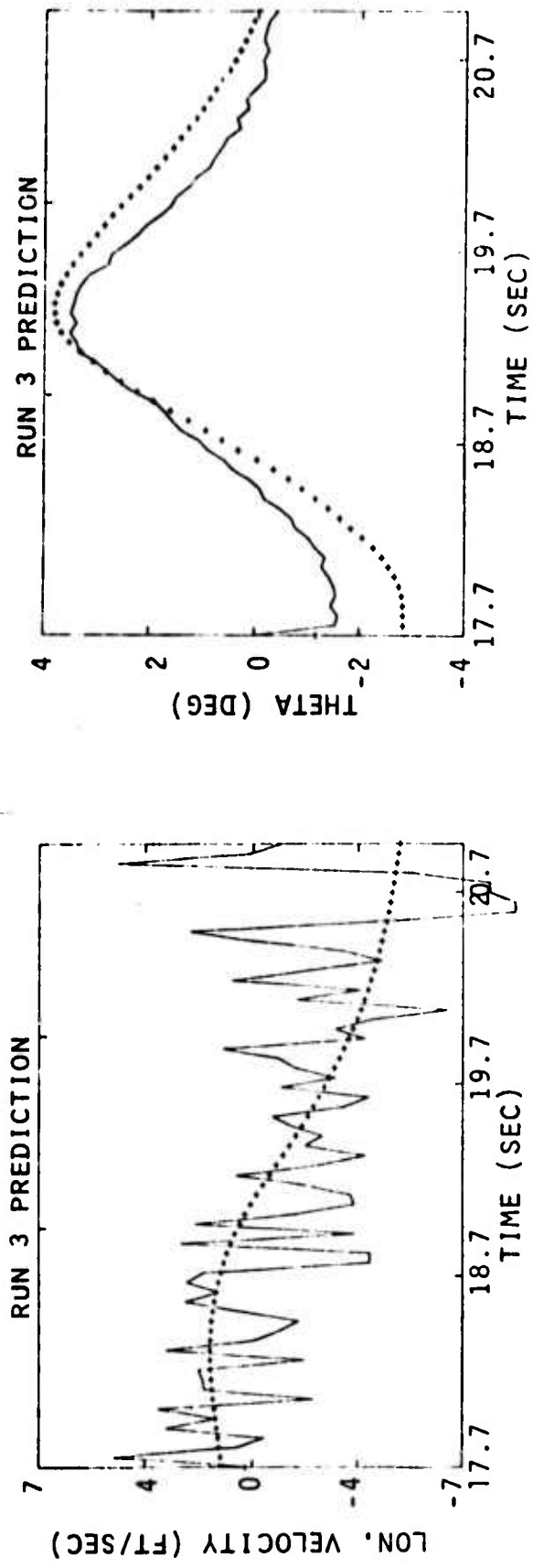
Figure 18 (Concluded)   Time History Plots for Run 3 with Prediction
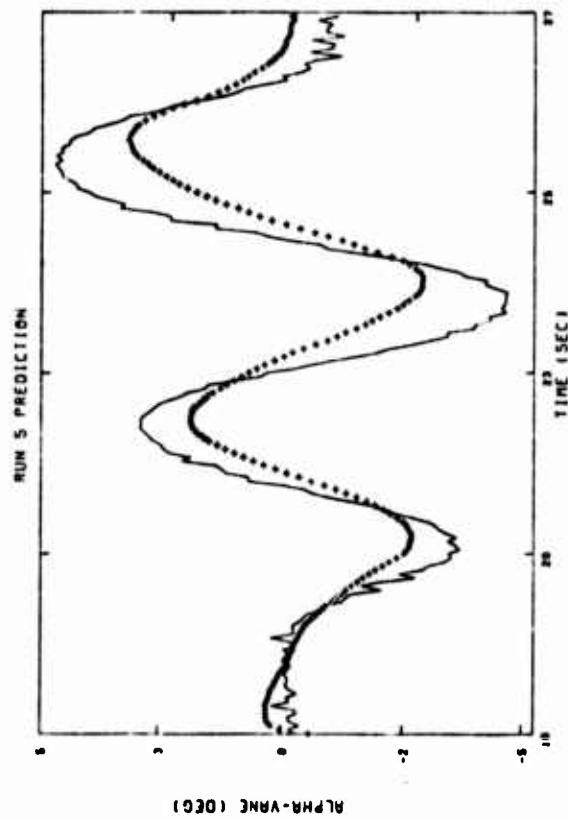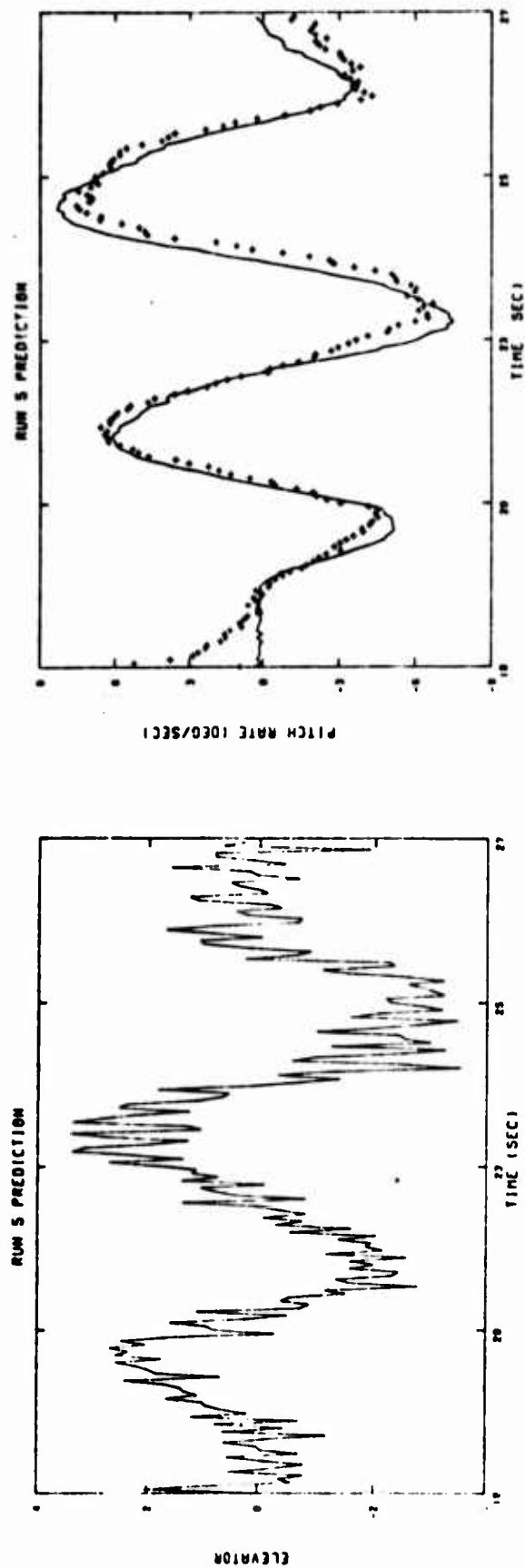
Figure 19   Prediction Time History Plots for Run 5
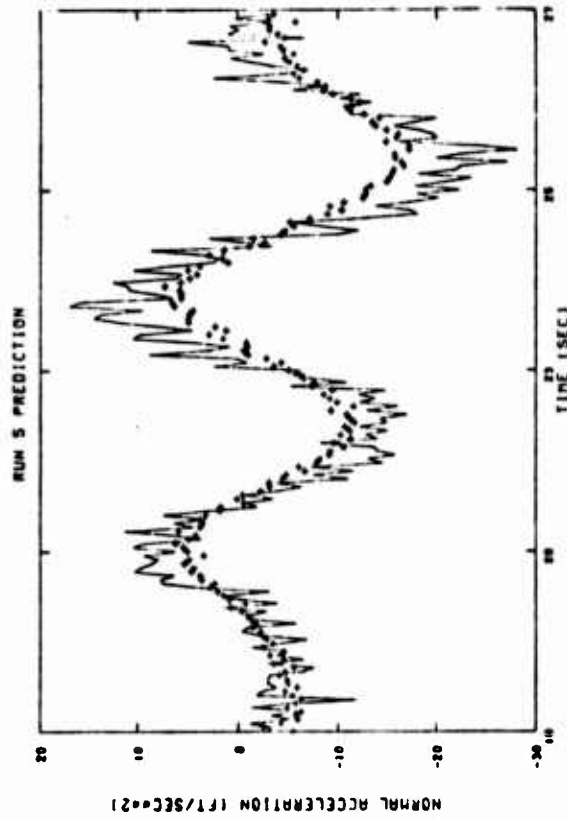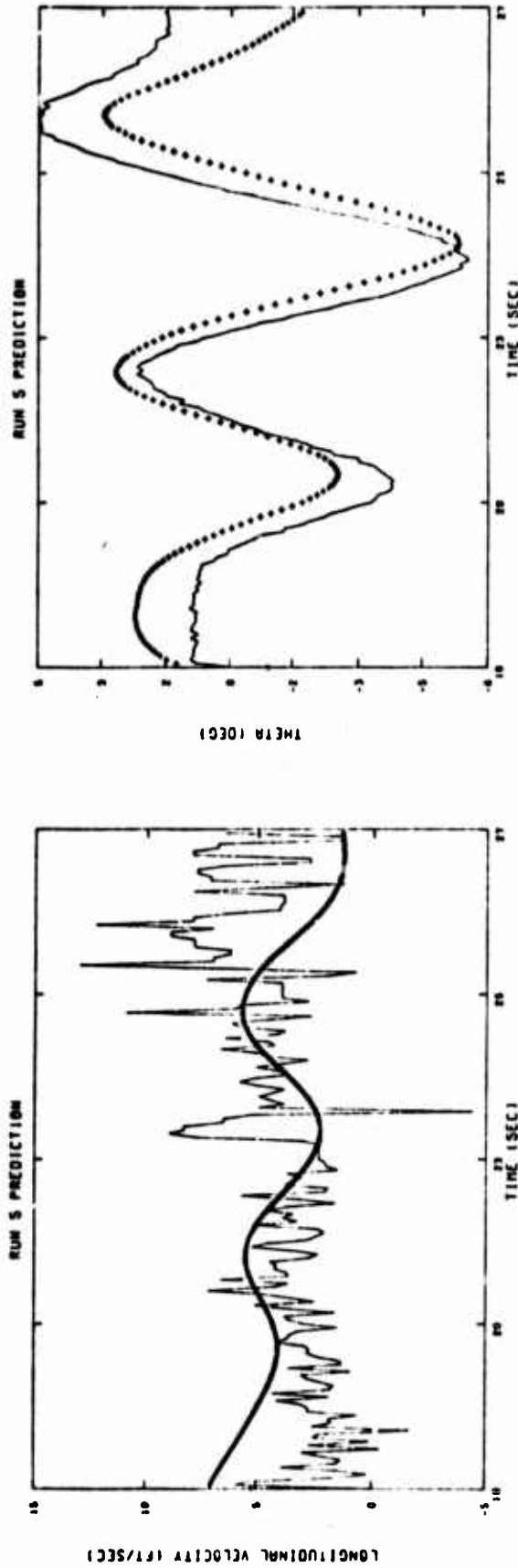
Figure 19 (Concluded) Prediction Time History Plots for Run 5

After the runs for flight condition 1 were processed, it was quite clear that it is important to include the possibility of out of trim condition at the beginning of the run. The effect of the out of trim condition is accounted for by including the initial conditions. An equivalent method is to consider bias terms in the equations of motion. In all runs at flight condition 2, these equation biases are identified. The measurement biases and mean square errors are also identified.

Table 14 shows the inputs used to excite the aircraft in each of the runs. Runs 10 and 11 use pulse inputs and run 12 is a step input. Runs 18 and 13 use specially designed input, of different amplitudes, supplied by SCI to NADC early in the program.* In Run 19, random input spanning 25 sec of data is applied.

Table 14 shows the identified stability and control derivatives, equation and measurement biases, and the standard deviation of the root-mean-square value of the random noise on the measurements. Also shown are the standard deviation on parameter estimation errors. The output error method is used in each case. Figures 20 to 25 show the comparison of the measured and estimated time history of the measurements of angle-of-attack, forward speed, pitch rate, pitch angle and vertical acceleration.

Note that the fit between the measured and the estimated time history in each case is good. The comparison of the standard deviations on parameter estimation error shows that inputs of runs 18 and 19 are the best and that of run 12 is the worst. The input of run 12 is so small that it cannot be distinguished from

----

*The input was designed using techniques developed over three years ago. Significantly better designs have been developed since then and are reported in References 6 and 7.

Table 14

Identified Derivatives from Different Runs at Flight Condition 2
Speed 679 ft/sec
Altitude 10,000 ft

RUN	10	11	12	13	18	19	COMBINED	WIND TUNNEL VALUES
INPUT			small amplitude	small amplitude	SCI optimum	random		
PARAMETER								
z_α	-2.397 (0.0542)	-2.481 (.151)	-3.7365 (0.243)	-3.161 (0.0905)	-2.618 (0.0536)	-2.621 (0.0255)	-2.641	-2.458
z_u	-0.00018	*	*	*	*	*	*	-0.00018
z_q	1.0	1.0	1.0	1.0	1.0	1.0	1.0	1.0
x_α	-36.91	*	*	*	*	*	*	-36.9
x_u	-0.016	*	*	*	*	*	*	-0.016
x_q	0.0	*	*	*	*	*	*	0.0
M_α	-24.37 (0.619)	-25.73 (1.47)	-26.85 (1.830)	-21.912 (0.839)	-32.29 (0.357)	-25.29 (2.28×10^{-9})	-25.29	-22.50
M_u	0.0017	0.0017	0.0017	0.0017	0.0017	0.0017	0.0017	0.0017
M_q	-4.317 (0.0258)	-6.551 (0.594)	-0.817 (0.495)	-6.72 (0.474)	-3.551 (0.140)	-4.656 (9.21×10^{-9})	-4.656	-4.96*
$z_{\delta e}$	0.2258 (0.0504)	0.298 (0.097)	0.0993 (0.0642)	0.0958 (0.0423)	0.1551 (0.0284)	0.1957 (0.0154)	0.166	-0.178
$x_{\delta e}$	0.0	*	*	*	*	*	*	0.0
$M_{\delta e}$	-28.57 (1.01)	-25.09 (1.57)	-16.06 (1.562)	-28.64 (1.56)	-22.05 (0.535)	-25.51 (0.114)	-25.36	-52.12

* $(M_q + M_\alpha)$

Table 14 (Concluded)

Identified Derivatives from Different Runs at Flight Condition 2
Speed 679 ft/sec
Altitude 10,000 ft

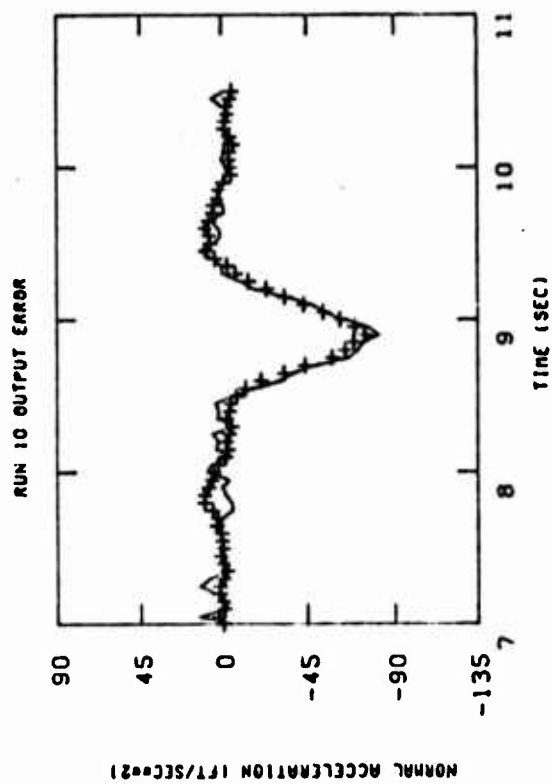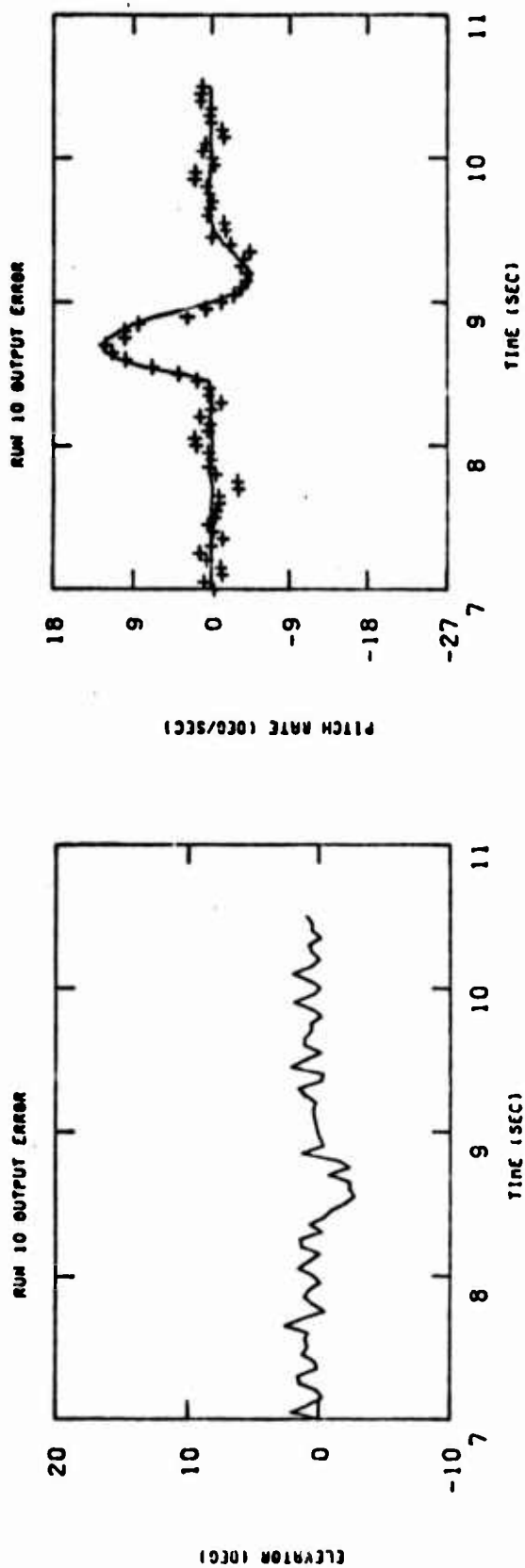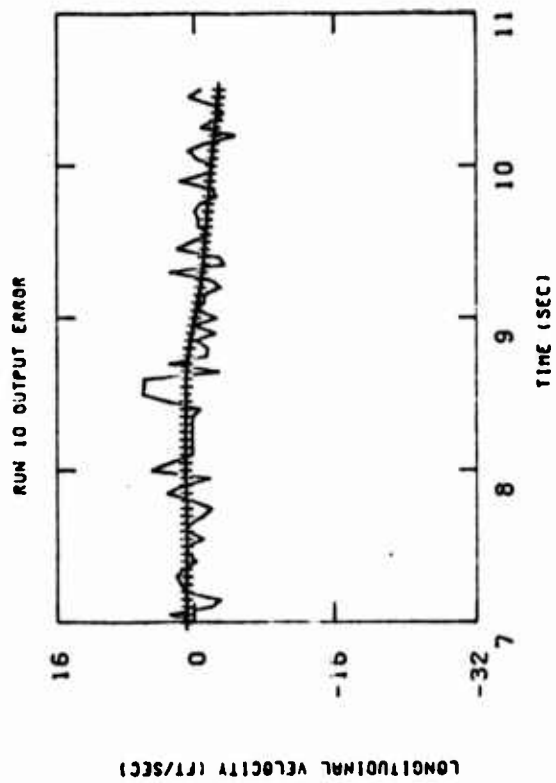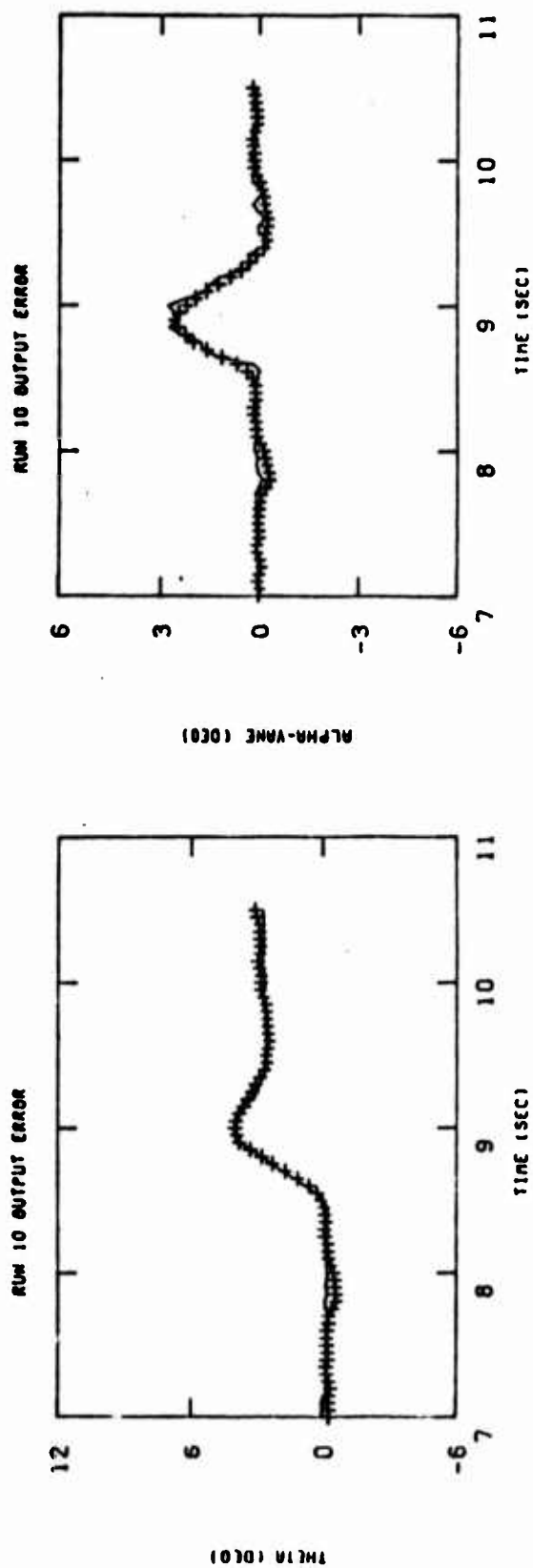| RUN	10 (7-10.5 sec)	11	12	13	18 (9.5-16 sec)	19 (2.5-25 sec)
INPUT			small amplitude	small amplitude	SCI optimum	random
EQUATION BIAS						
Z_0 rad	-0.00308	-0.00352	-0.00265	-0.00211	-0.00272	-0.00216
M_0	0.394	0.0862	-0.0892	-0.384	0.067	0.580
MEASUREMENT BIAS						
b_α rad	0.000059	0.00014	-0.000895	0.00152	0.000822	-0.00234
b_u ft sec^{-1}	0.982	0.893	1.66	-3.22	-0.0716	-3.3
b_q rad sec^{-1}	-0.00497	0.00323	0.00267	0.00241	-0.000115	-0.00113
b_θ rad	-0.00465	-0.00387	0.00577	0.00846	-0.0105	0.00146
b_{a_z} ft sec^{-2}	1.685	2.08	-0.00335	0.0582	0.901	-0.207
RANDOM NOISE STANDARD DEVIATIONS						
σ_α rad	0.00321	0.00271	0.00305	0.00267	0.00622	0.0054
σ_u ft sec^{-1}	2.16	1.52	1.61	2.08	3.17	3.17
σ_q rad sec^{-1}	0.0204	0.0195	0.0183	0.0201	0.0283	0.0287
σ_θ rad	0.00289	0.00312	0.00387	0.00488	0.00628	0.0198
σ_{a_z} ft sec^{-1}	5.40	5.35	6.55	7.86	9.67	9.35

Figure 20 Pulse Input (Run 10)
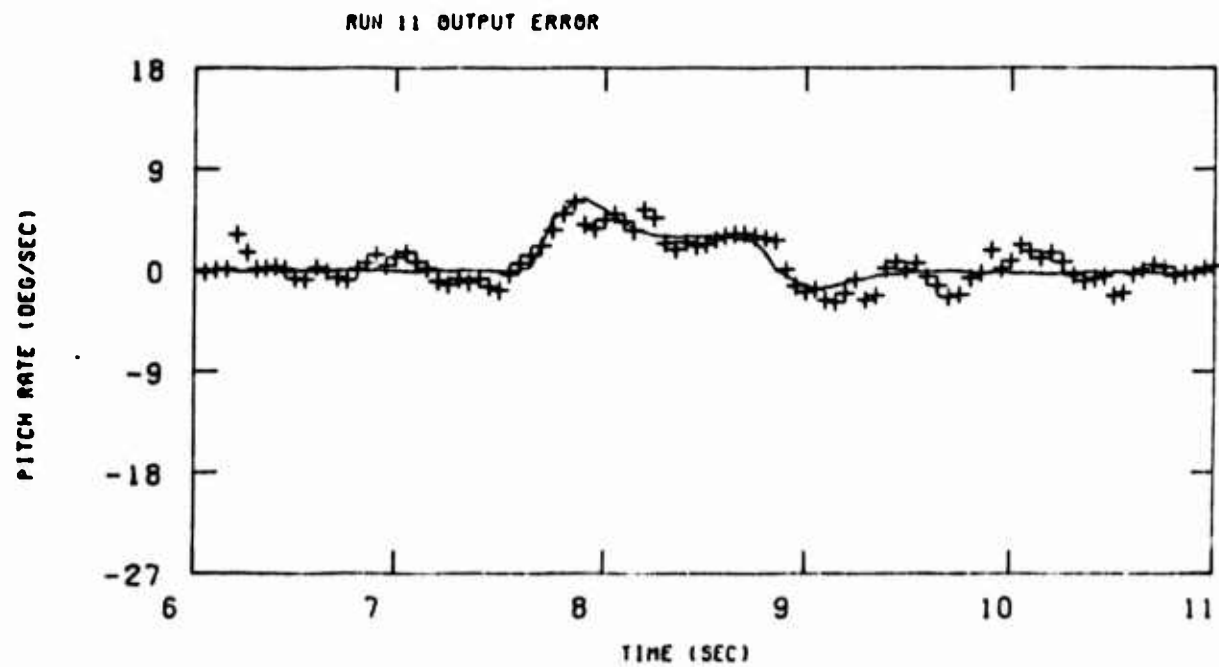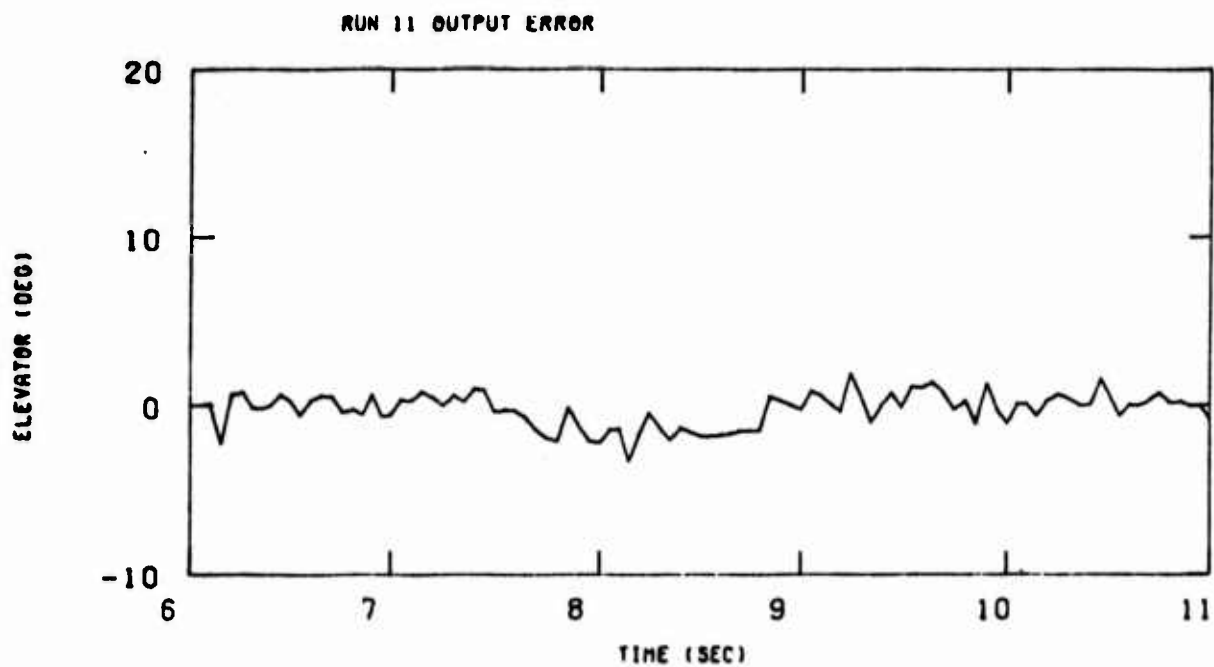
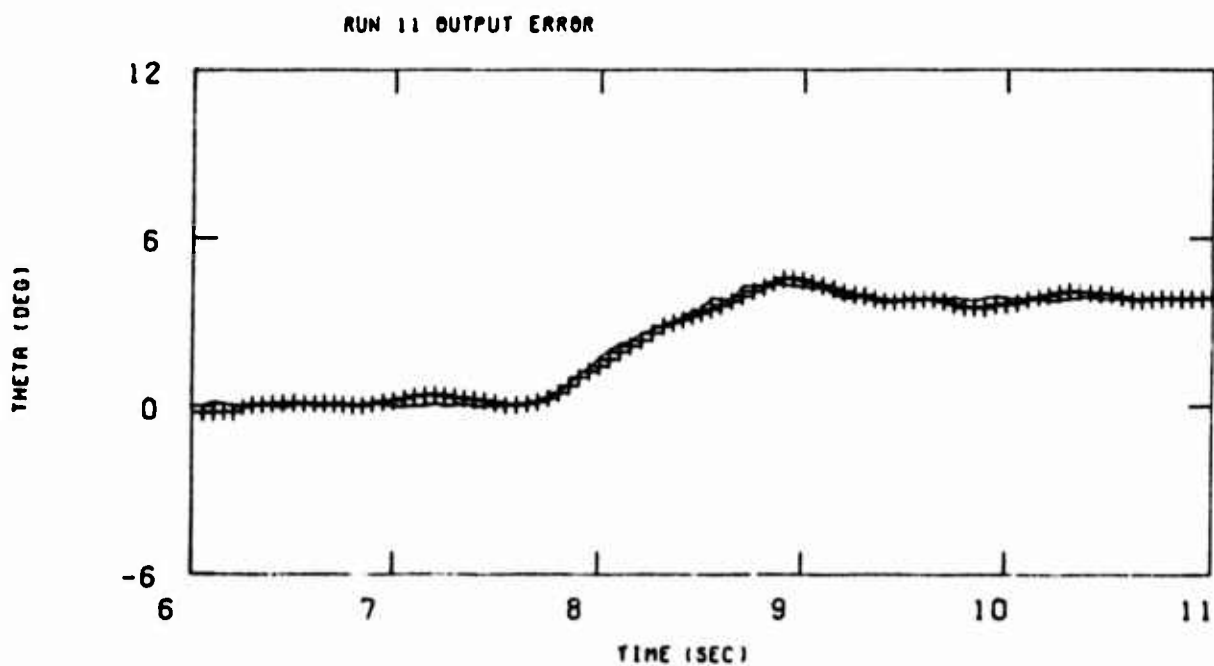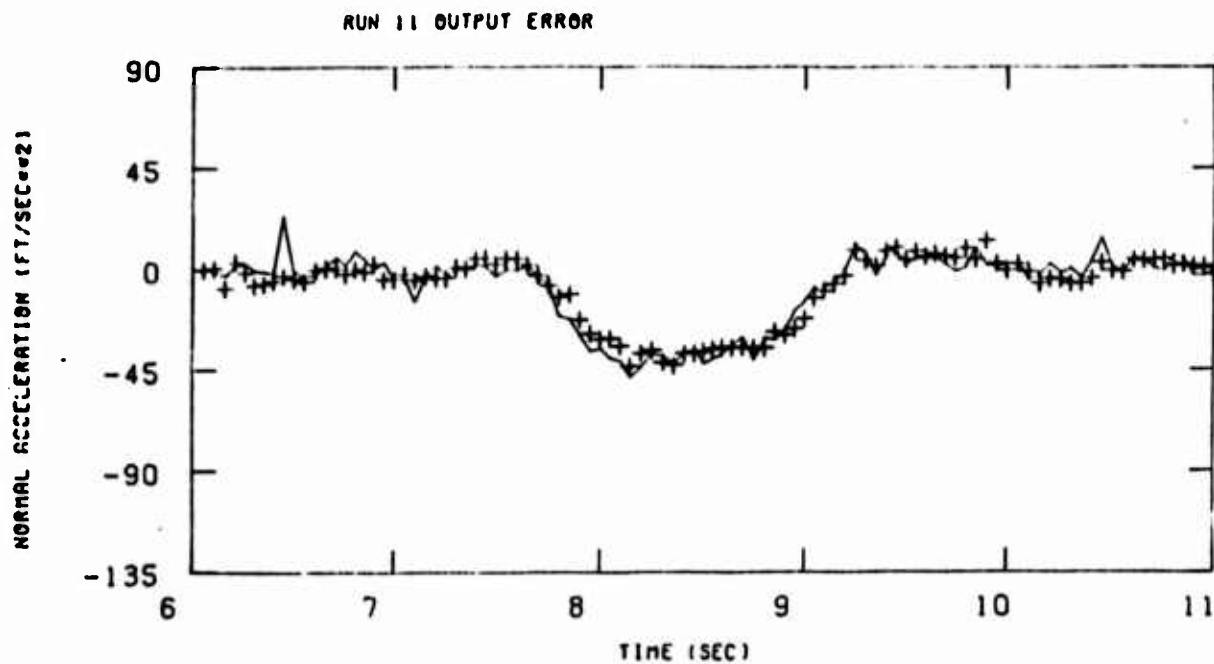Figure 20 (Concluded) Pulse Input (Run 10)

Figure 21 Pulse Input (Run 11)

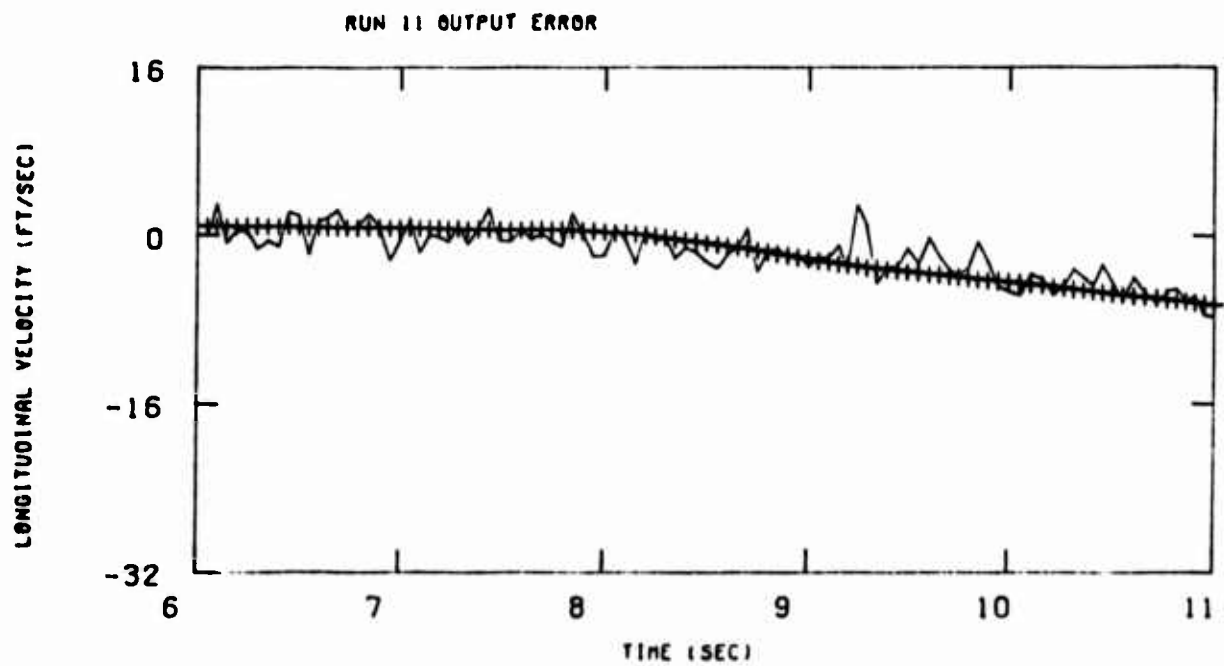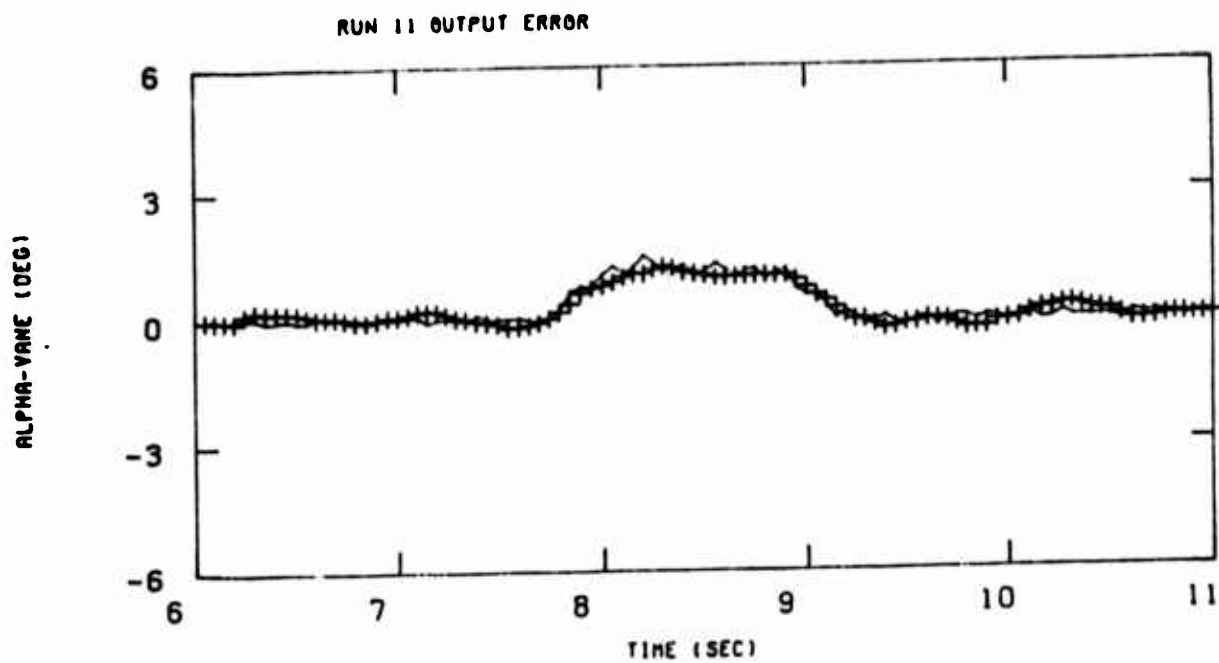Figure 21 (Continued)   Pulse Input (Run 11)

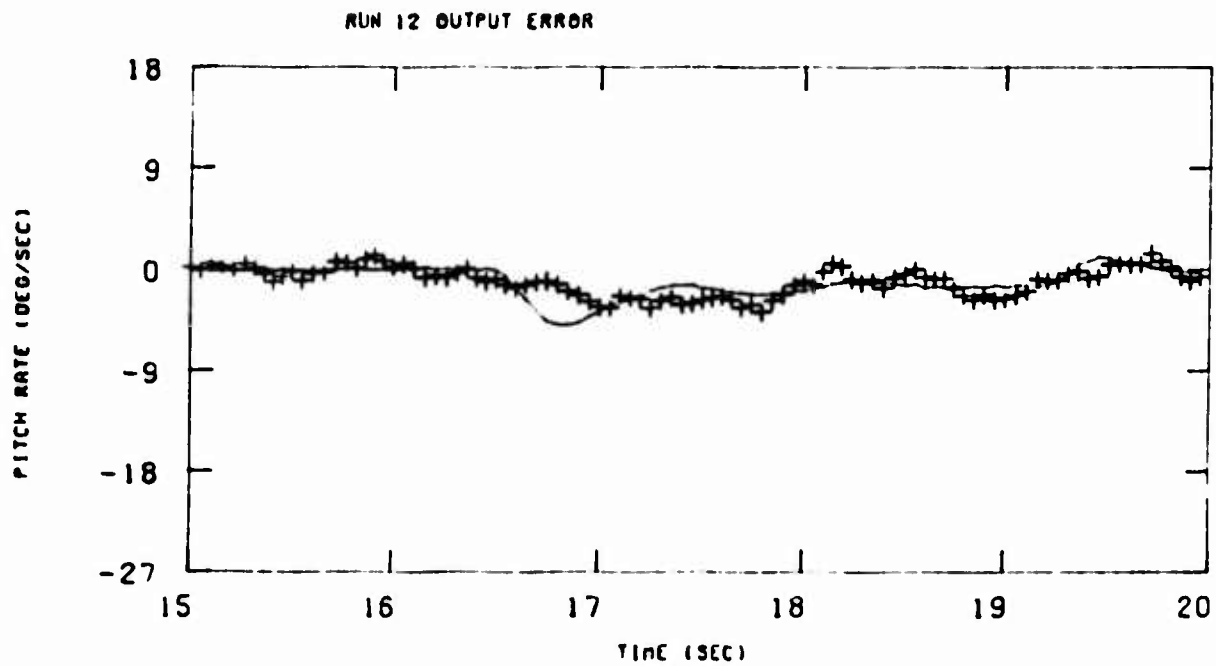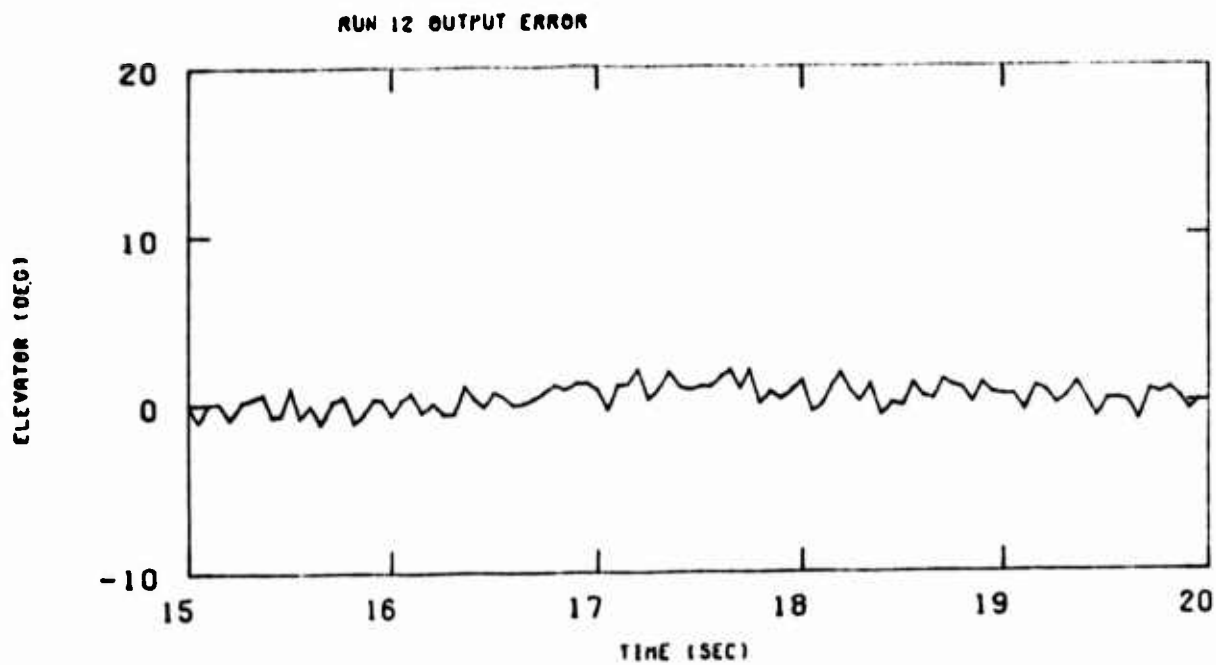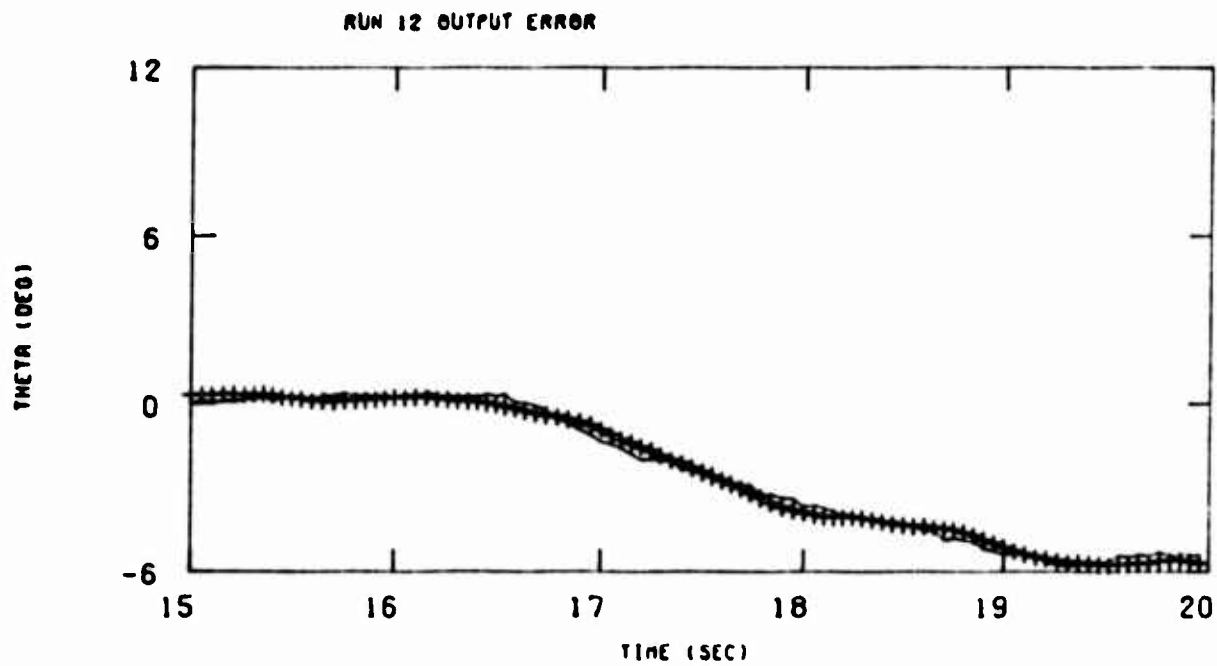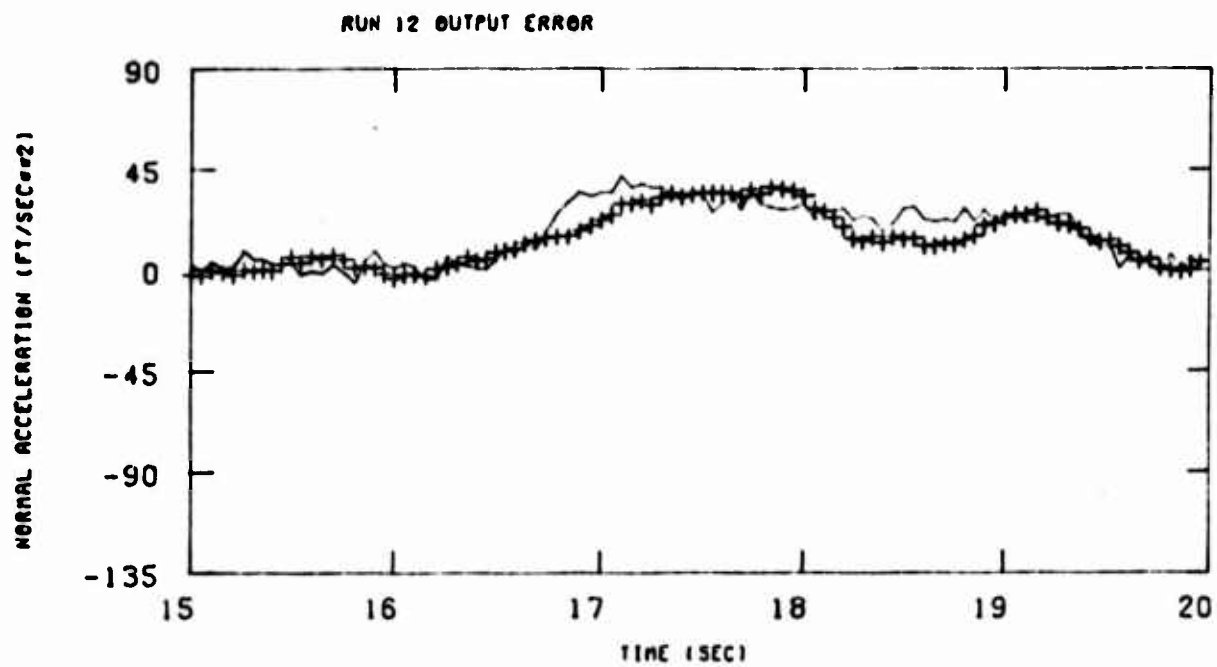Figure 21 (Concluded)   Pulse Input (Run 11)

Figure 22   Doublet Input (Run 12)

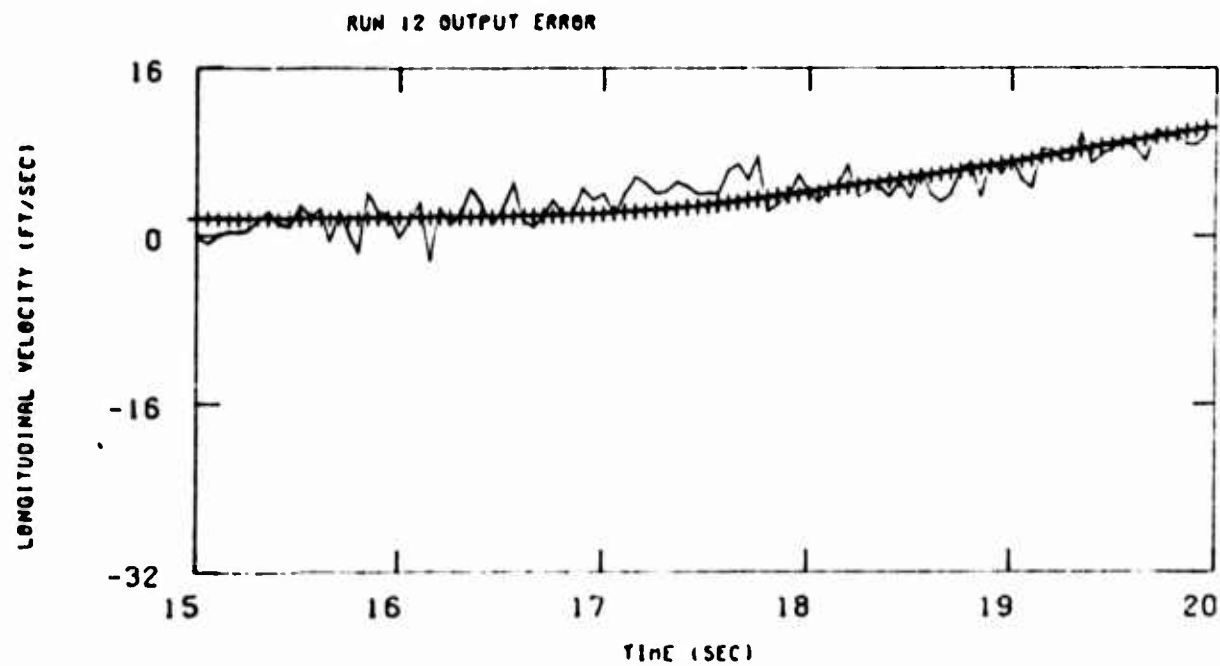Figure 22 (Continued) Doublet Input (Run 12)

Figure 22 (Concluded) Doublet Input (Run 12)
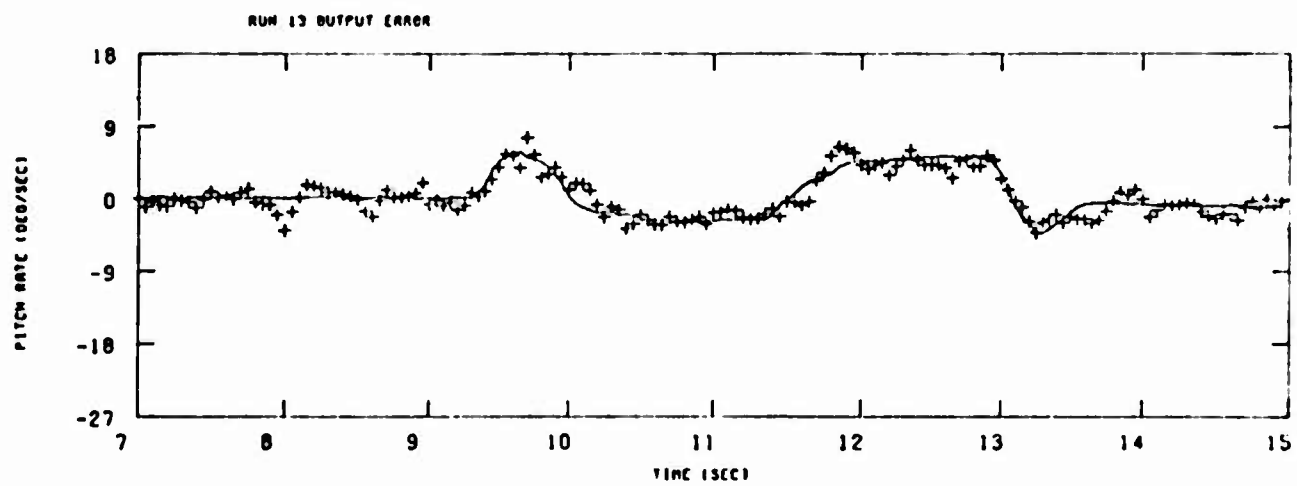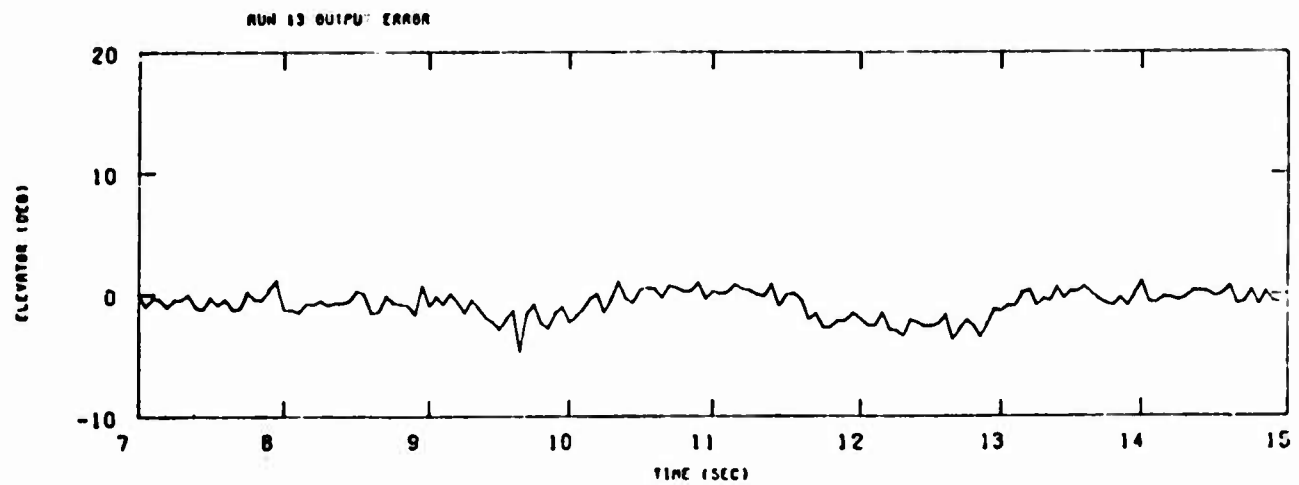
Figure 23 Doublet Input (Run 13)

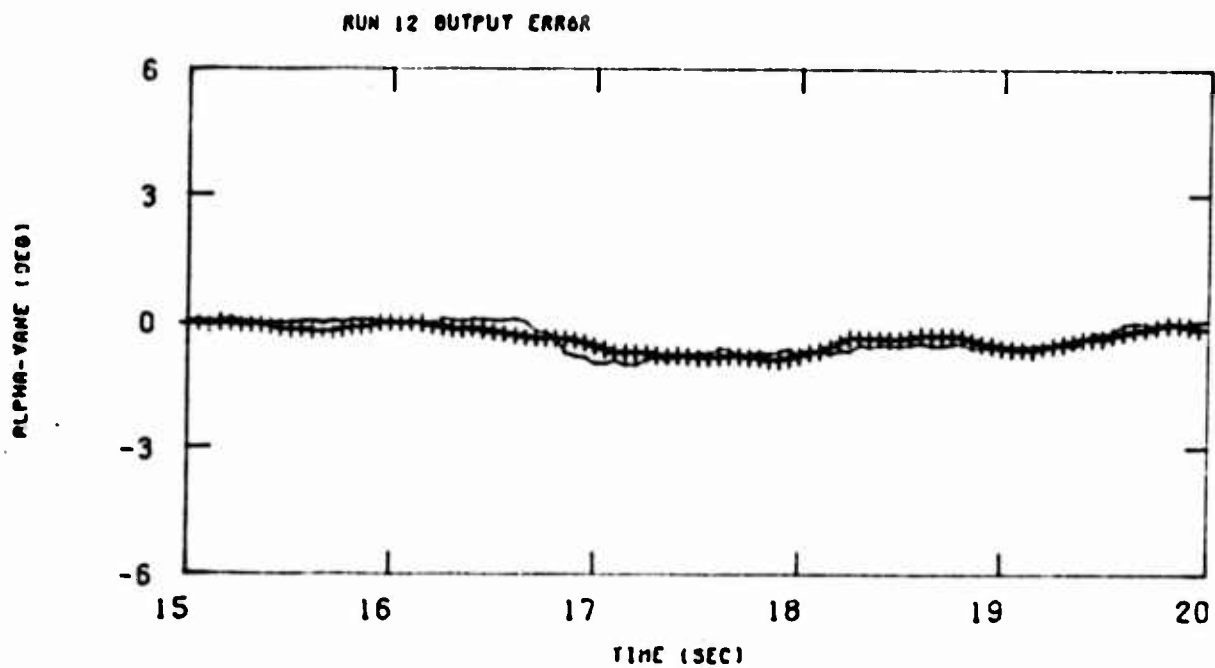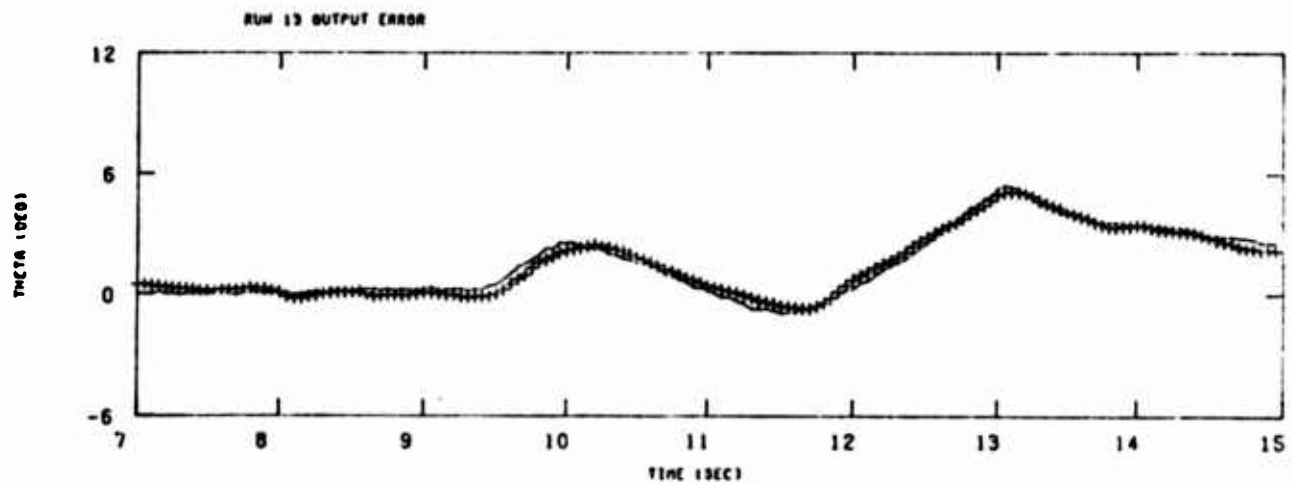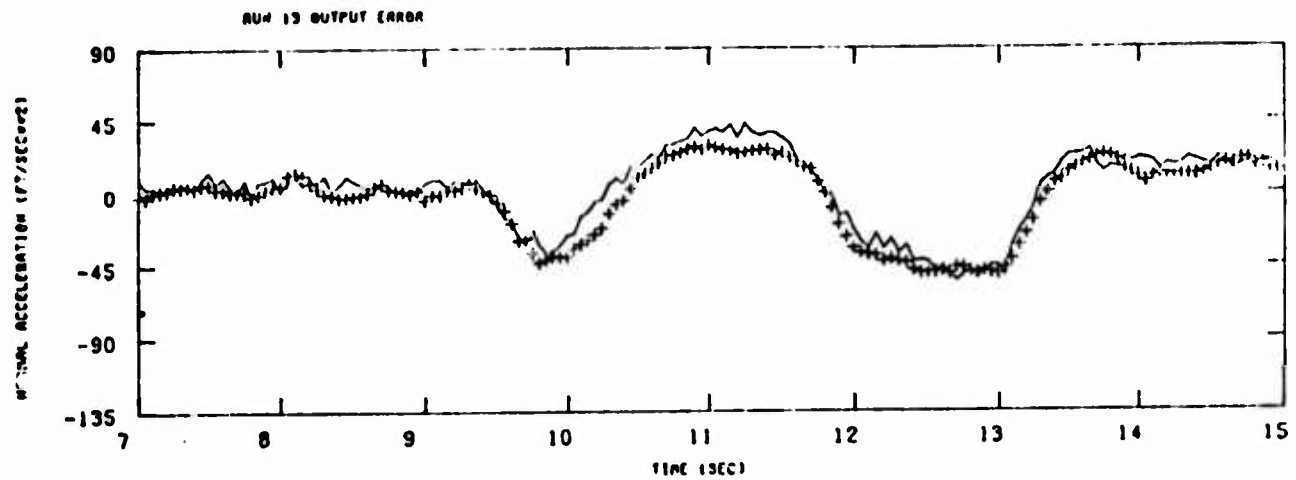Figure 23 (Continued) Doublet Input (Run 13)

Figure 23 (Concluded)   Doublet Input (Run 13)
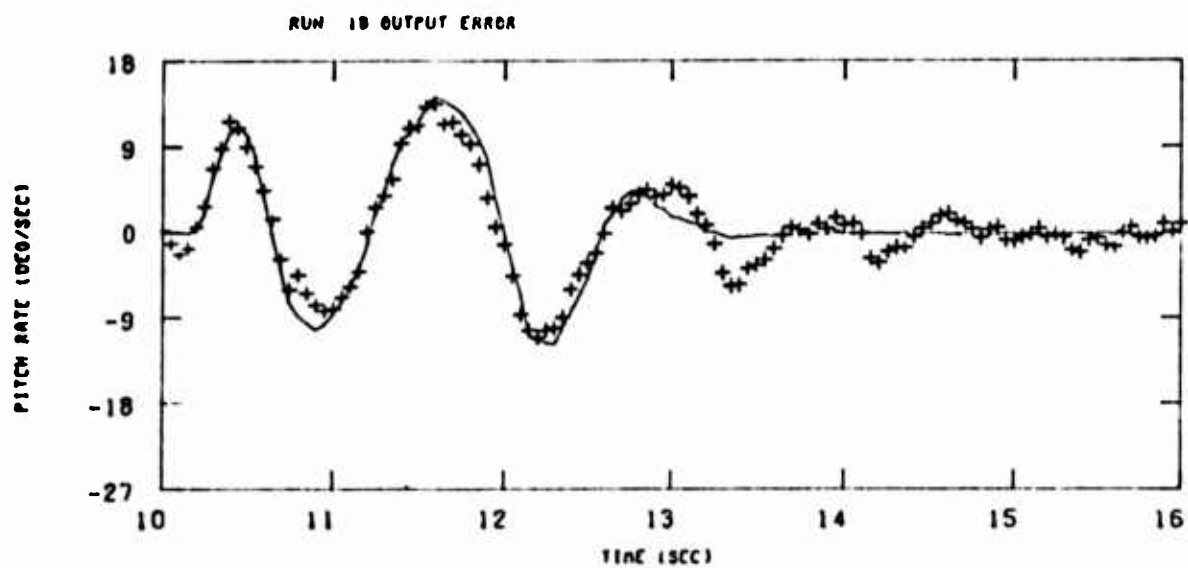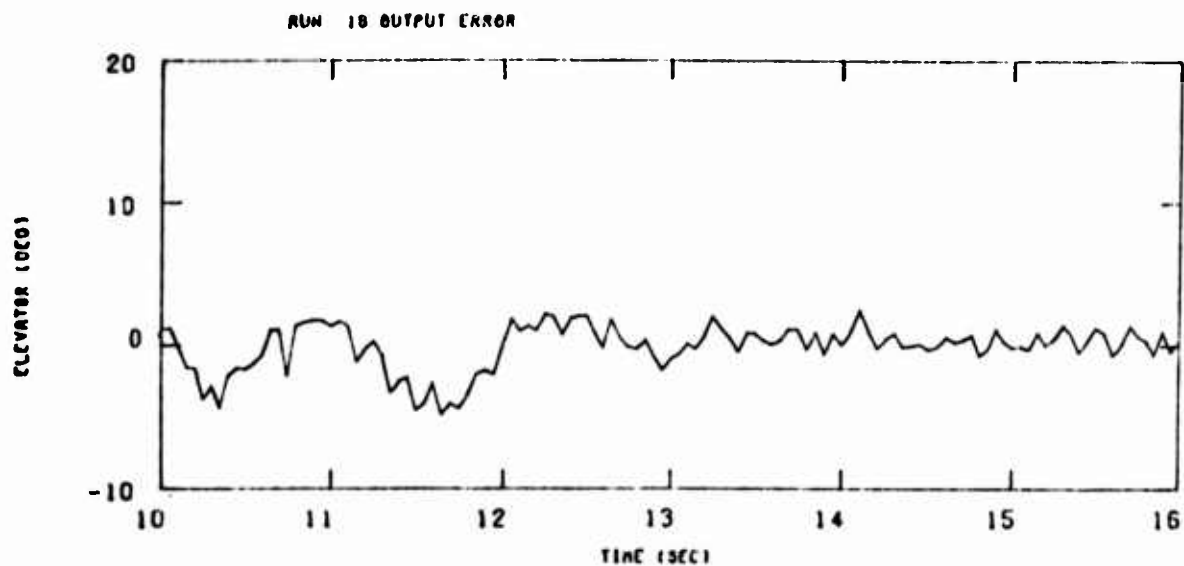
Figure 24   Special Input (Run 18)

RUN 18 OUTPUT ERROR

NORMAL ACCELERATION (FT/SEC²)

TIME (SEC)

RUN 18 OUTPUT ERROR

THETA (DEG)

TIME (SEC)
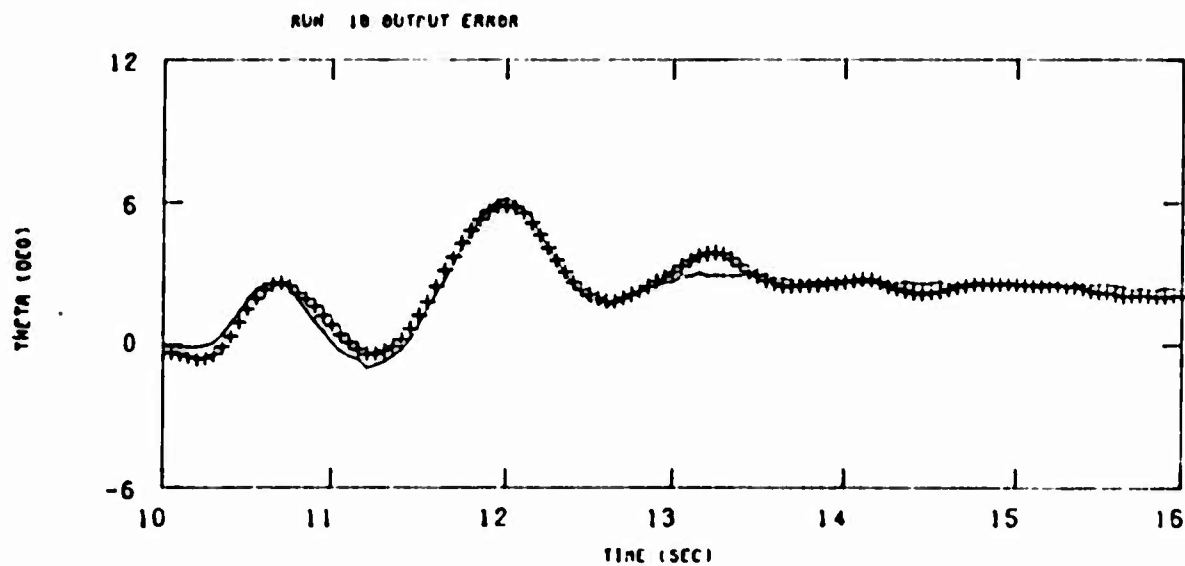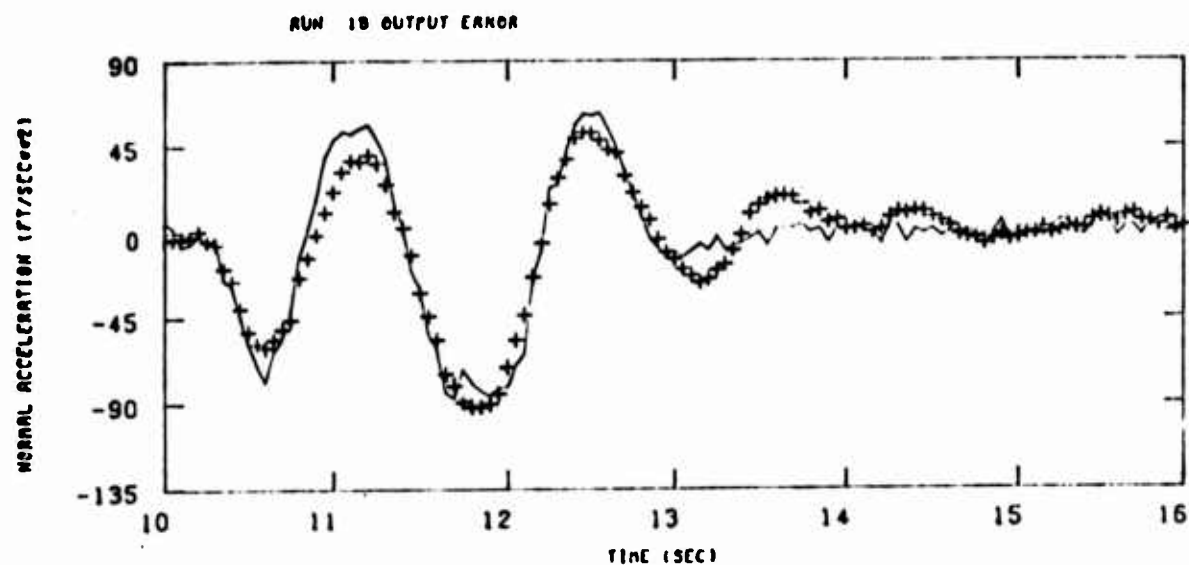
Figure 24 (Continued)   Special Input (Run 18)

17

RUN 18 OUTPUT ERROR

RUN 18 OUTPUT ERROR
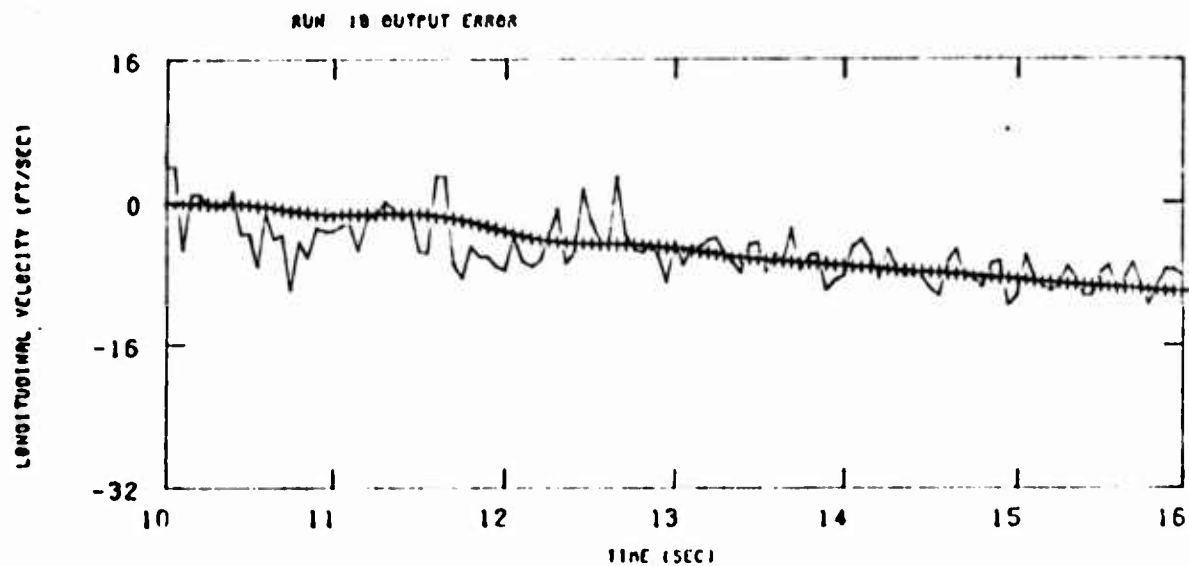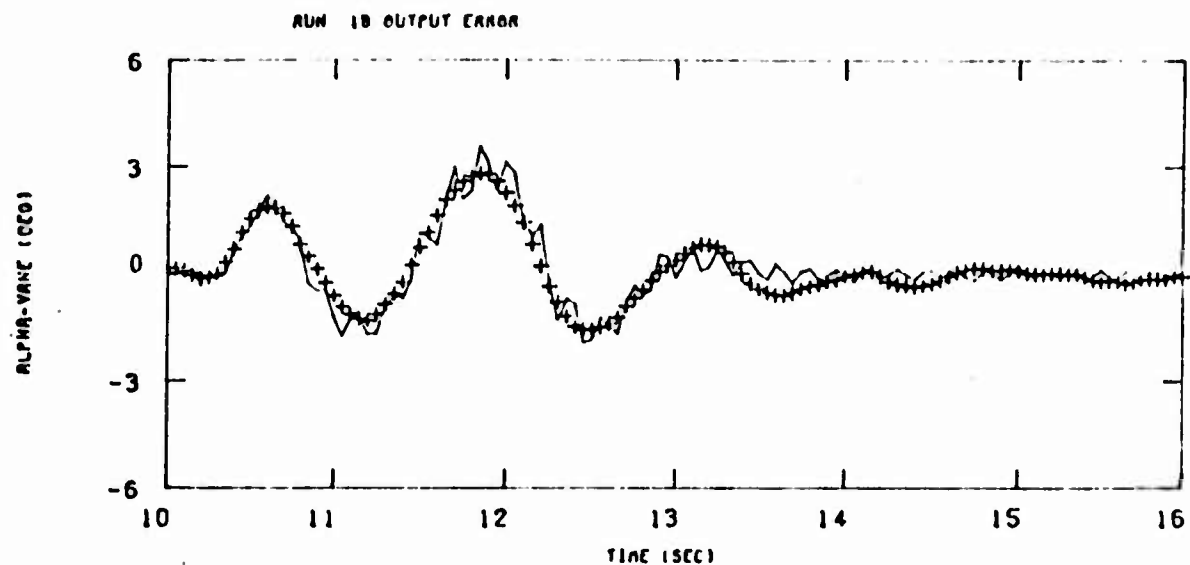
Figure 24 (Concluded) Special Input (Run 18)
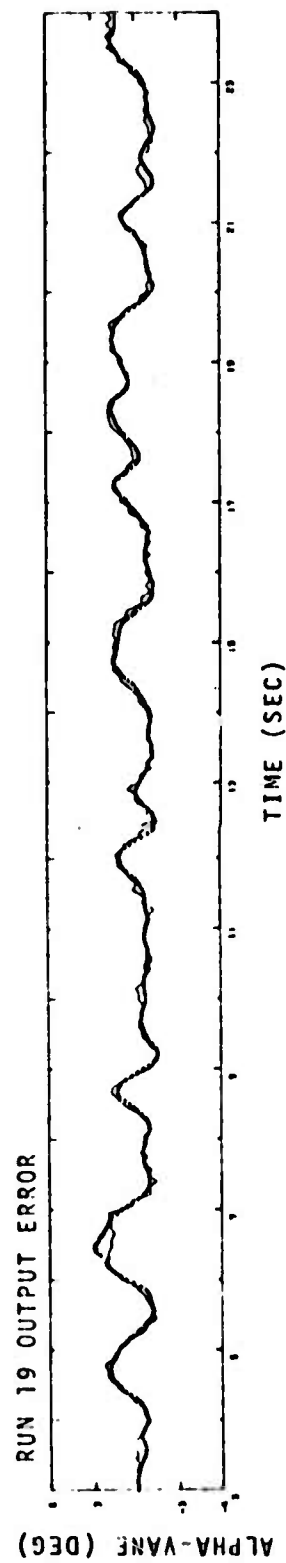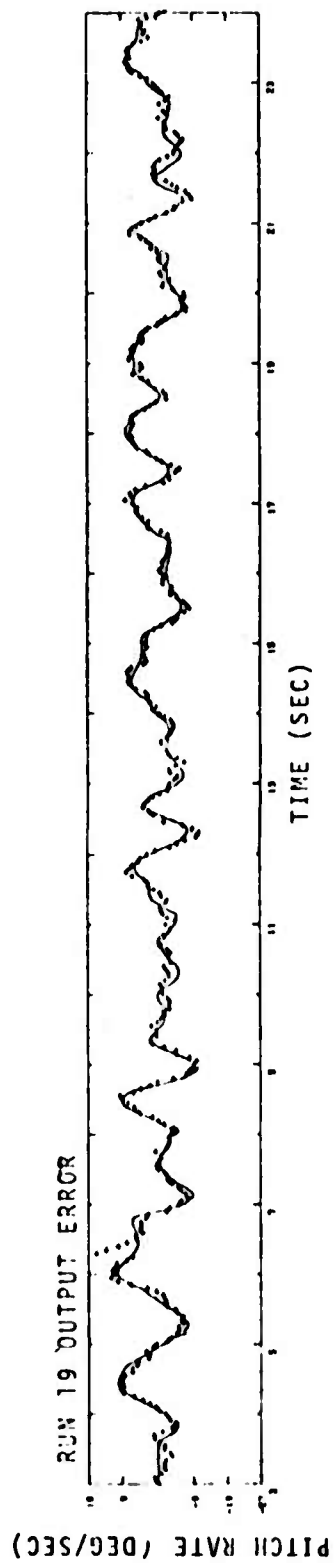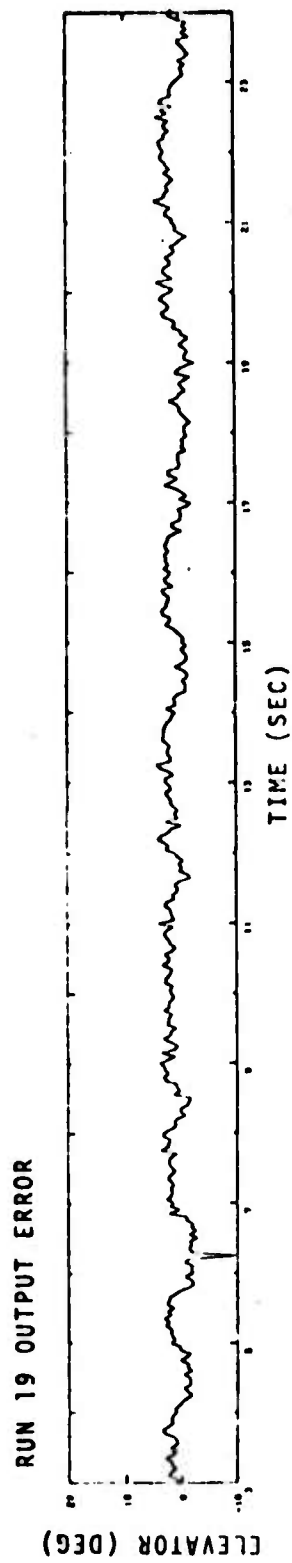
Figure 25 Random Input (Run 19)

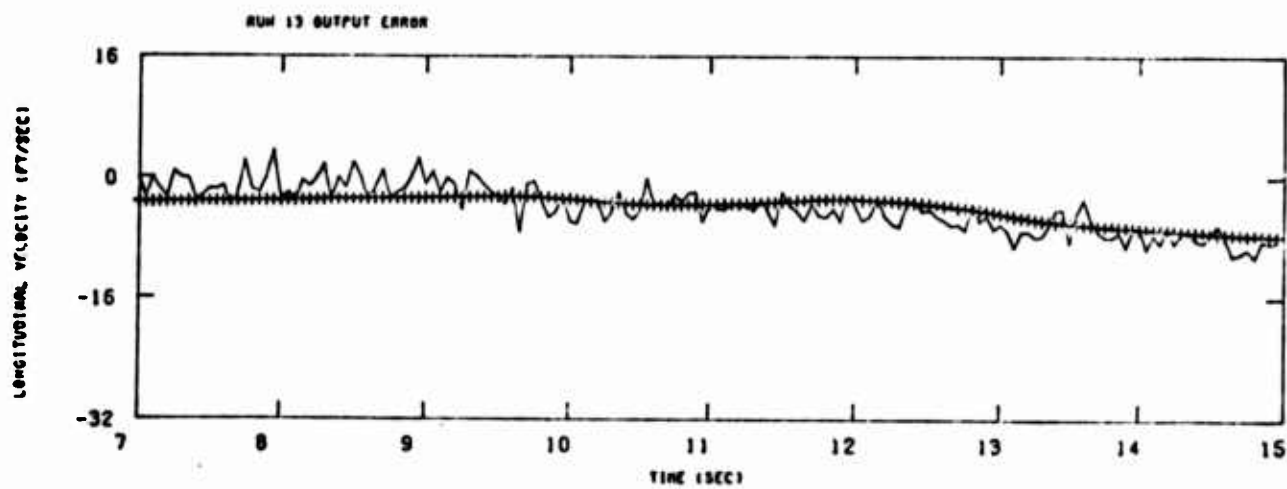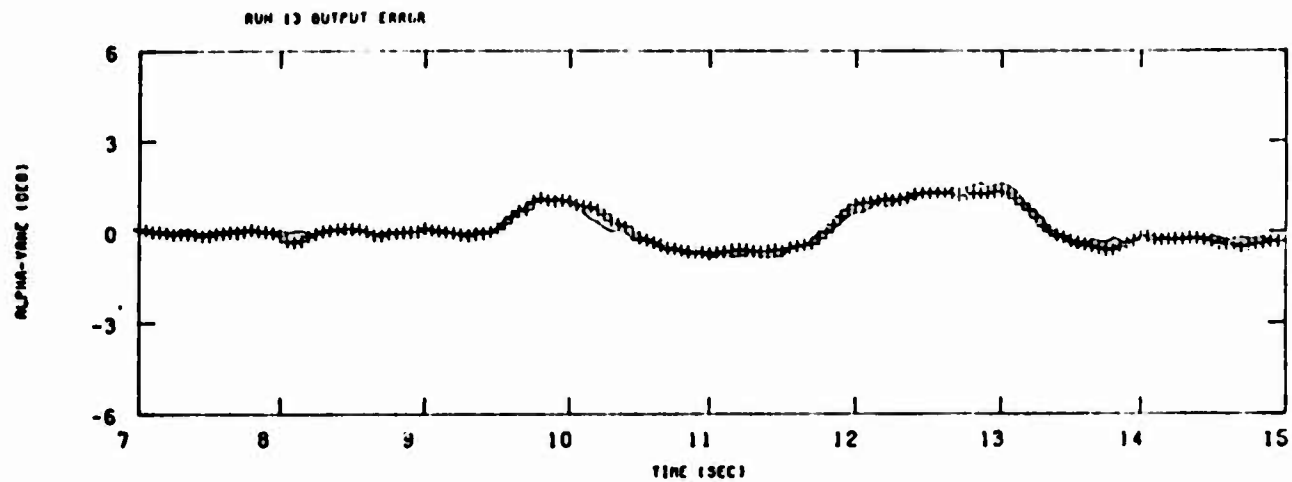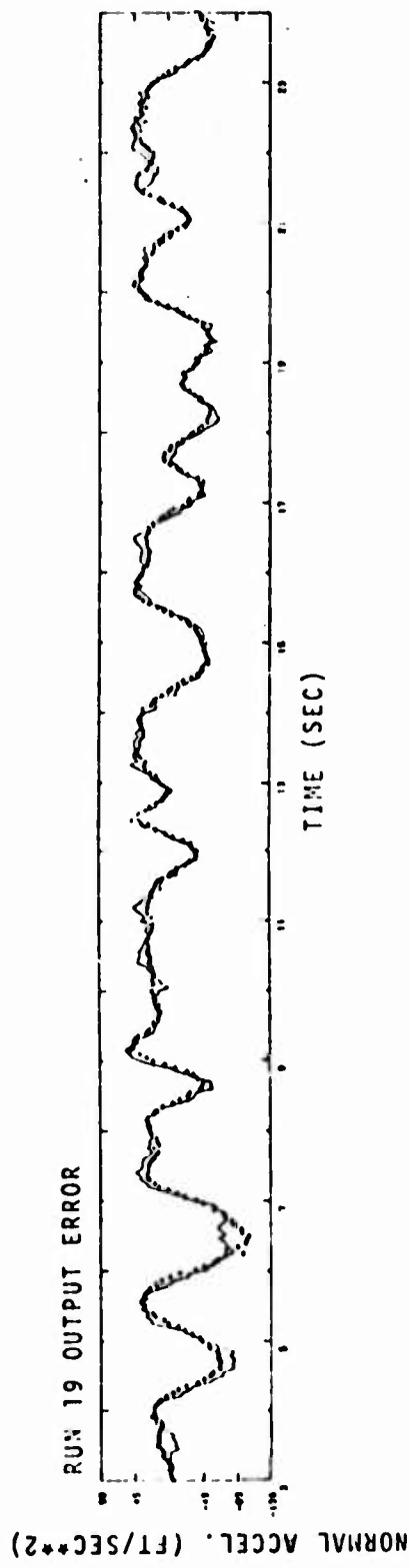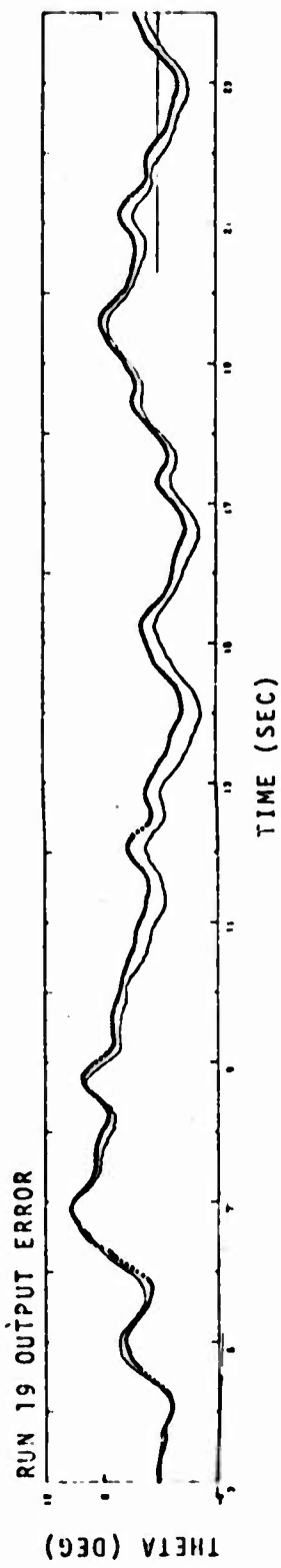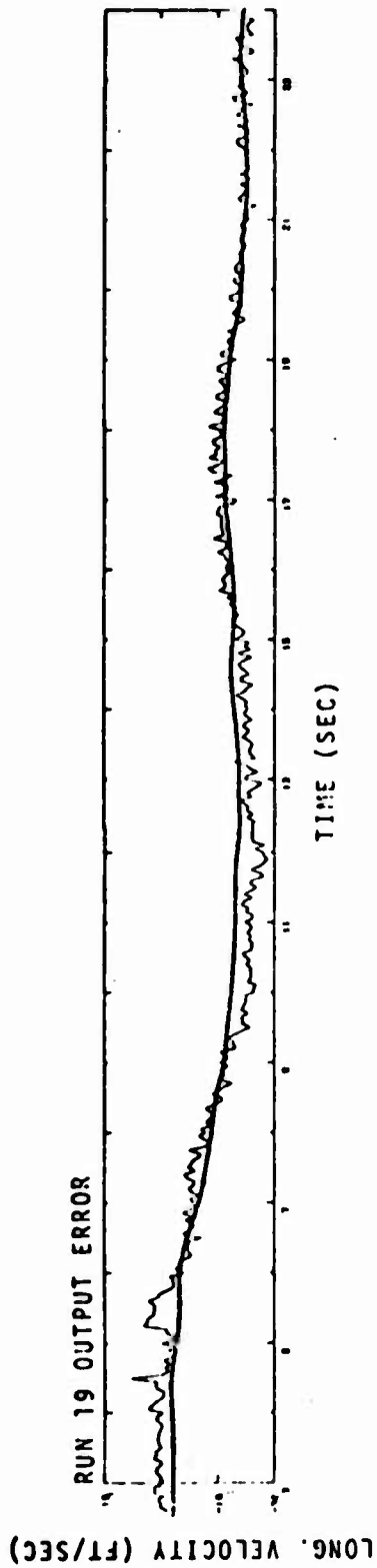Figure 25 (Concluded) Random Input (Run 19)

the measurement noise in the input. The identified parameters from runs 10, 18 and 19 are close to each other confirming that these inputs are "good". On the other hand, the parameter estimates from runs 11, 12 and 13 are scattered showing that the inputs produce insufficient excitation of the aircraft.

The equation bias terms, Z_o and M_o, are, in each case, almost equivalent (e.g., proportional) to the control inputs, $Z_{\delta_e}\delta e$ and $M_{\delta_e}\delta e$. This indicates that the control input is out of trim. In other words, the correct trim value of the elevator deflection is not subtracted from the time history to determine the input perturbation from trim. In run 19, this error is about $1°$. Such large error in trim value, if not accounted for, would result in a considerable error in estimated parameters.

Run 18 is processed again including the process noise but excluding the equation error terms. Table 15 shows the parameter values and Figure 26 shows the comparison of the measured and estimated responses. Since the excitation from the deterministic input is high, there does not seem to be an improvement in parameter estimates when the process noise is included.

4.4 IDENTIFICATION OF PHUGOID PARAMETERS

As mentioned earlier, several of the runs have excitation of the phugoid motion. The maximum likelihood computer program SCIDNT is used to estimate Z_u, X_u and M_u in run 10.

Table 15
Flight Condition 2 - Run 18 (See Table 1)
9-16 Sec. Data Length

PARAMETER	WIND TUNNEL	STARTING VALUES	PROCESS NOISE
Z_α	-2.46	-2.46	-2.682 ± 0.739
Z_u	-0.00018	-0.00018	*
Z_q	1.0	1.0	1.0
γ	0.0	0.0	*
X_α	-36.91	-36.91	*
X_u	-0.016	-0.016	*
X_q	0.0	0.0	*
M_α	-22.5	-22.5	-33.43 ± 1.06
M_u	0.0017	0.0017	*
M_q	-4.96	-4.96	-3.858 ± 0.343
ω_c	- - - -	0.5	0.5
$Z_{\delta e}$	-0.1786	-0.1786	0.194 ± 0.040
$X_{\delta e}$	0.0	0.0	*
$M_{\delta e}$	-52.12	-52.12	-23.72 ± 1.38
K_α	1.0	1.0	*
$K_\alpha \ell_\alpha / V$	0.0	0.0	*
Q	- - - -	0.0001	0.0000622 ± 0.0000106
σ_α	- - - -	0.007	0.0055
σ_q	- - - -	0.015	0.0252
σ_θ	- - - -	0.015	0.0160
σ_{a_z}	- - - -	0.9	7.65
b_α	- - - -	- - - -	0.00235
b_u	- - - -	- - - -	-1.23
b_q	- - - -	- - - -	0.00985
b_θ	- - - -	- - - -	0.0113
b_{a_z}	- - - -	- - - -	-3.28

(All values in units of ft, sec, rad)
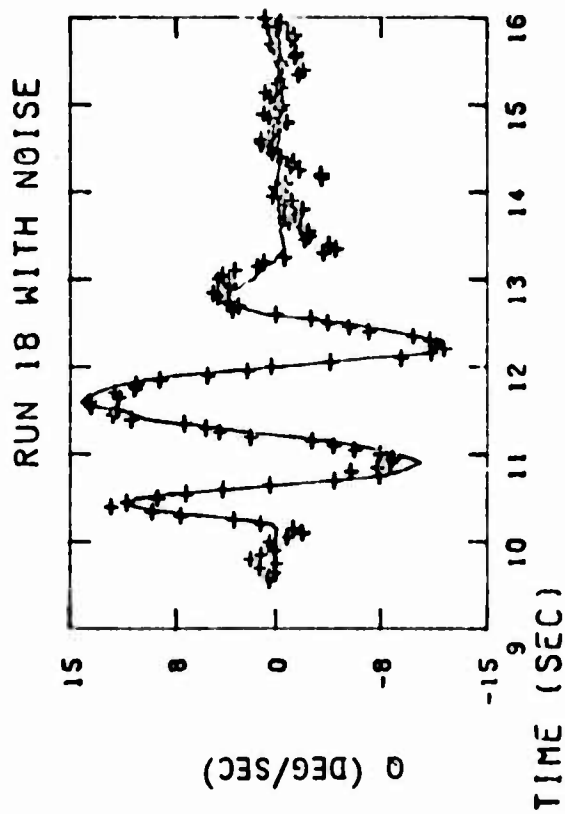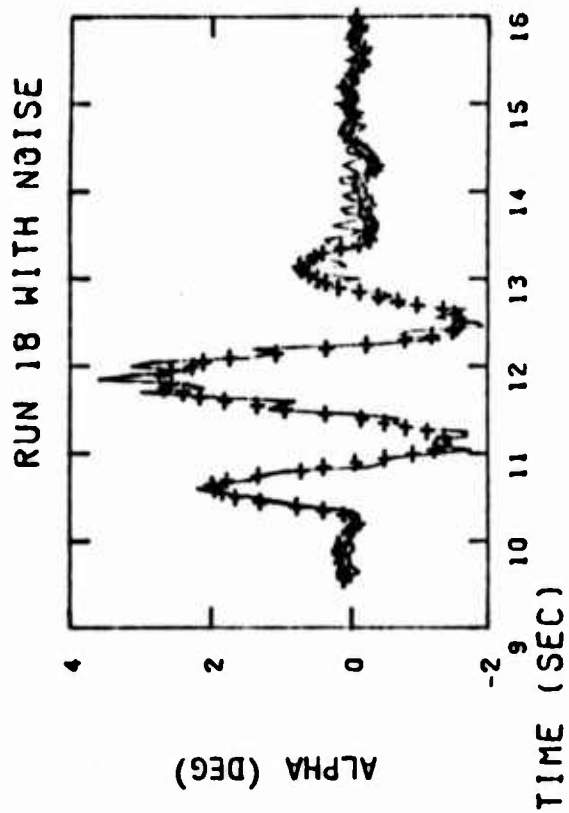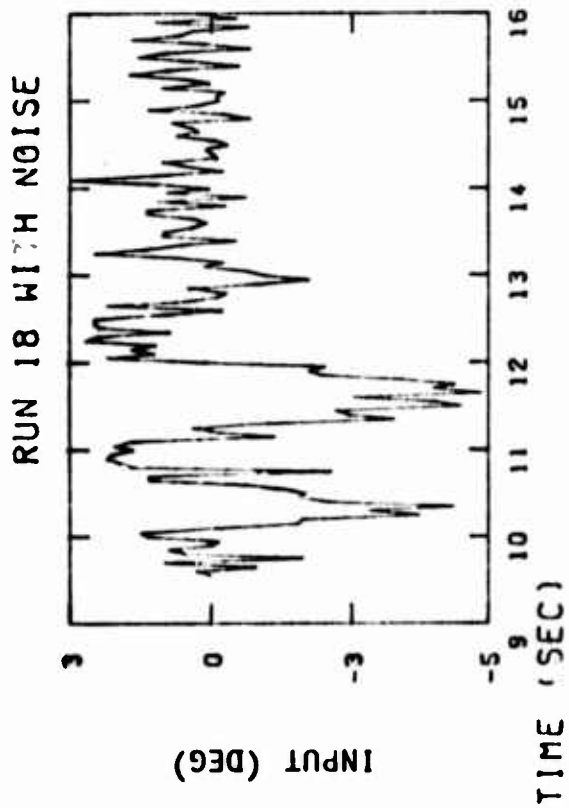
Figure 26 Time History Plots for Run 18 with Noise
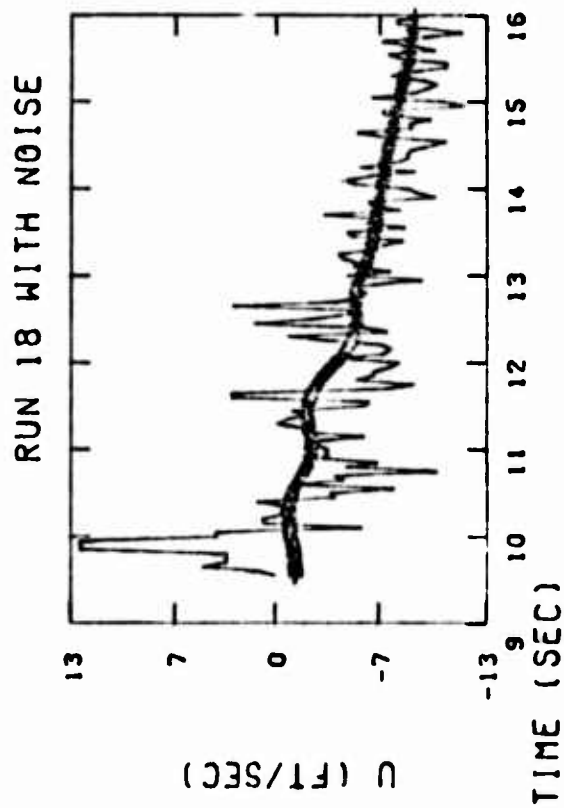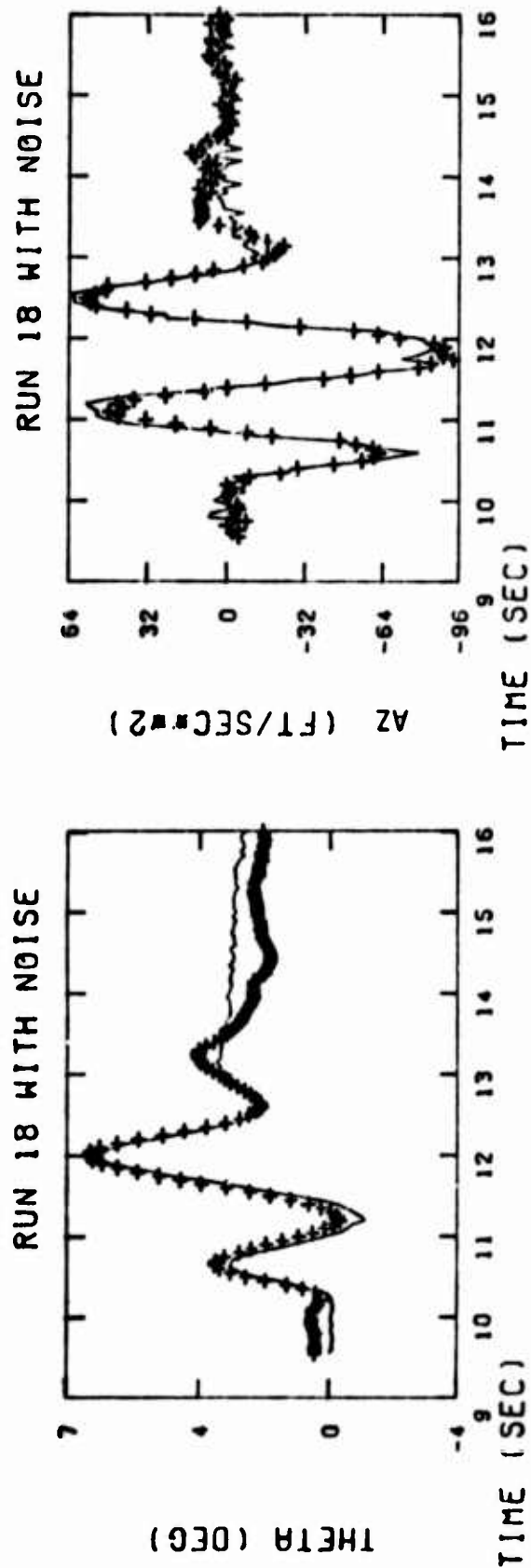
Figure 26 (Concluded) Time History Plots for Run 18 with Noise

The phugoid motion in run 10 is started by a pulse elevator input, which disturbs the airplane from trim conditions. The aircraft is, then, allowed to go through the phugoid oscillation without any further input. A direct identification of the parameters from the recorded data gave erroneous derivatives and poor time history fits because of excessive noise in the input. When the input is assumed zero for $t > 10$ sec, SCIDNT gave the time history fit of Figure 27 and the phugoid parameters as follows

$$Z_u = 0.0009289 \pm 0.0000394$$

$$X_u = -0.0175 \pm 0.001863$$

$$M_u = 0.01642 \pm 0.000424$$

The identified phugoid poles are at

$$\omega_{ph} = -0.0259 \pm 0.122j$$

It is necessary to have better measurements of the velocity, input and fore-aft acceleration to estimate phugoid parameters.
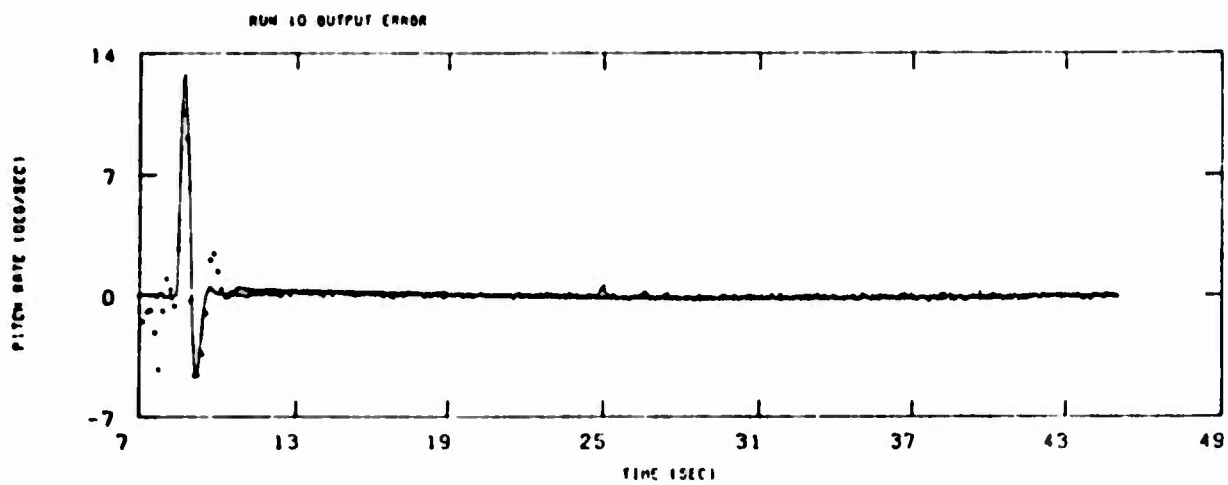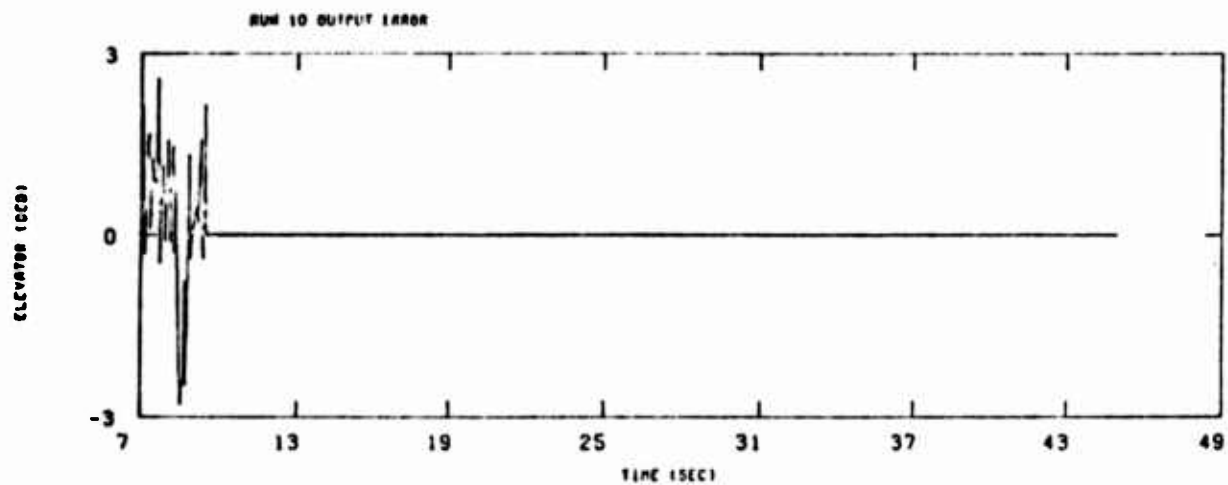
Figure 27   Identification of Phugoid Parameters (Run 10)
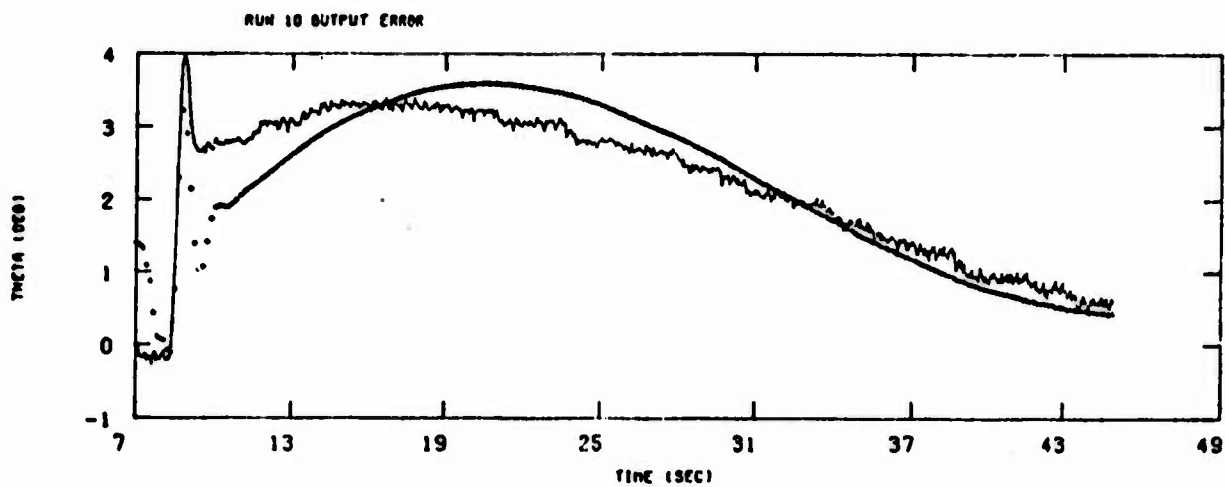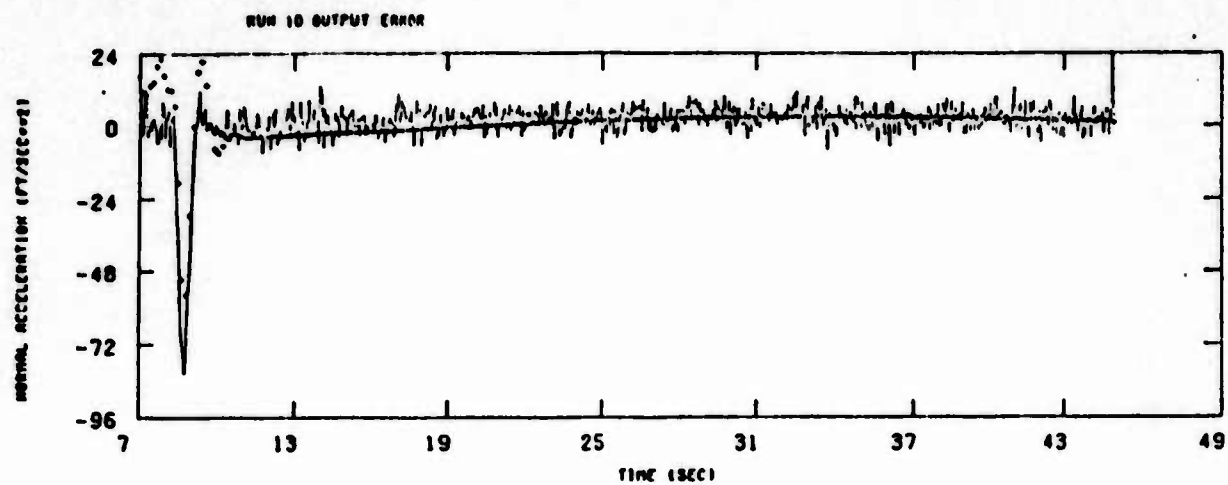
Figure 27 (Continued)   Identification of Phugoid Parameters (Run 10)

RUN 10 OUTPUT ERROR

RUN 10 OUTPUT ERROR
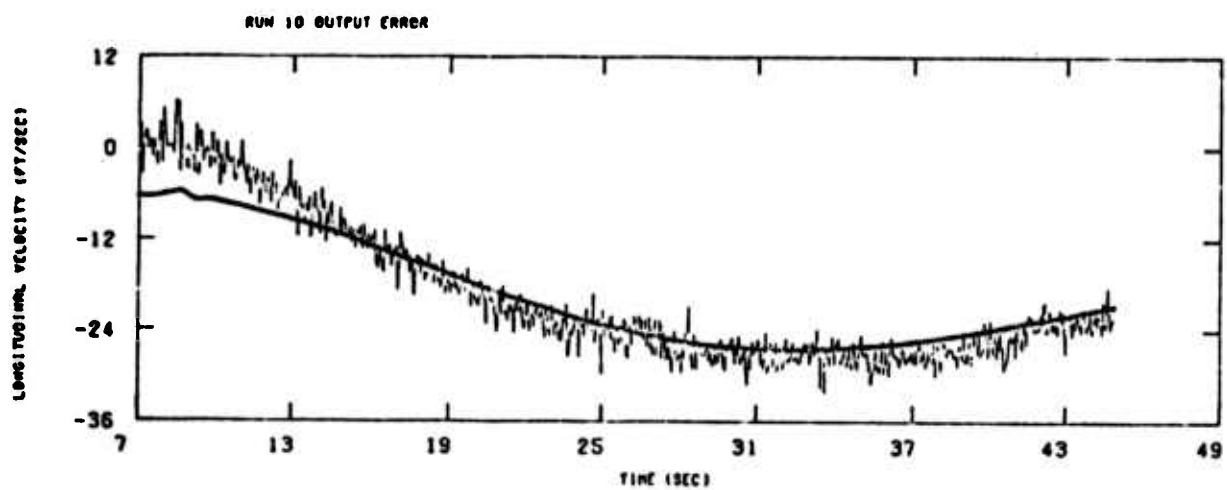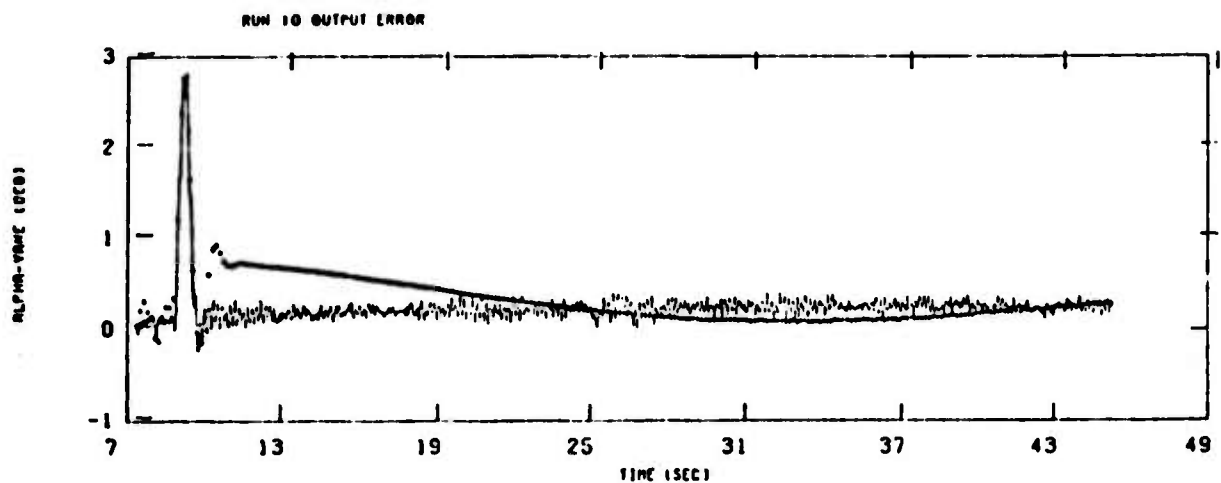
Figure 27 (Concluded)   Identification of Phugoid Parameters (Run 10)

88

V. SUMMARY AND CONCLUSIONS

5.1 SUMMARY

A total of ten separate T-2B maneuvers have been processed to
determine stability and control derivatives from data sets supplied
by the Naval Air Development Center. Of these ten, four are low-
speed approach configuration responses to sine waves, (two) and
pulses (two) elevator inputs. Six maneuvers are high-speed clean
configuration responses to small and high amplitude pulses and
step a specially designed input, and a random input.

Results for the low-speed maneuvers are summarized in Table 13
of Chapter IV and in Figure 28. Identified values of Z_α, M_α, M_q,
$Z_{\delta e}$ and $M_{\delta e}$ are shown in Figure 28 for the four runs 2, 3, 5 and
6 (ref. input schematics at bottom of figure). Also shown are the
1σ standard deviation estimates for each identified run (e.g., the
larger the deviation, the less confidence in the estimate. On the
basis of the identified values and their respective confidence
bounds, a χ^2 statistical average of the estimates is indicated as
the overall best estimate (<).

Classifying the inputs on the basis of the overall accuracy
and consistency of the estimates, the following ranking from best
to worst is concluded:

(1) Two Cycle Sine Wave (Run 2)

(2) Two Cycle Sine Wave (Run 5)

(3) Pulse (run 6)

(4) Pulse (run 3)
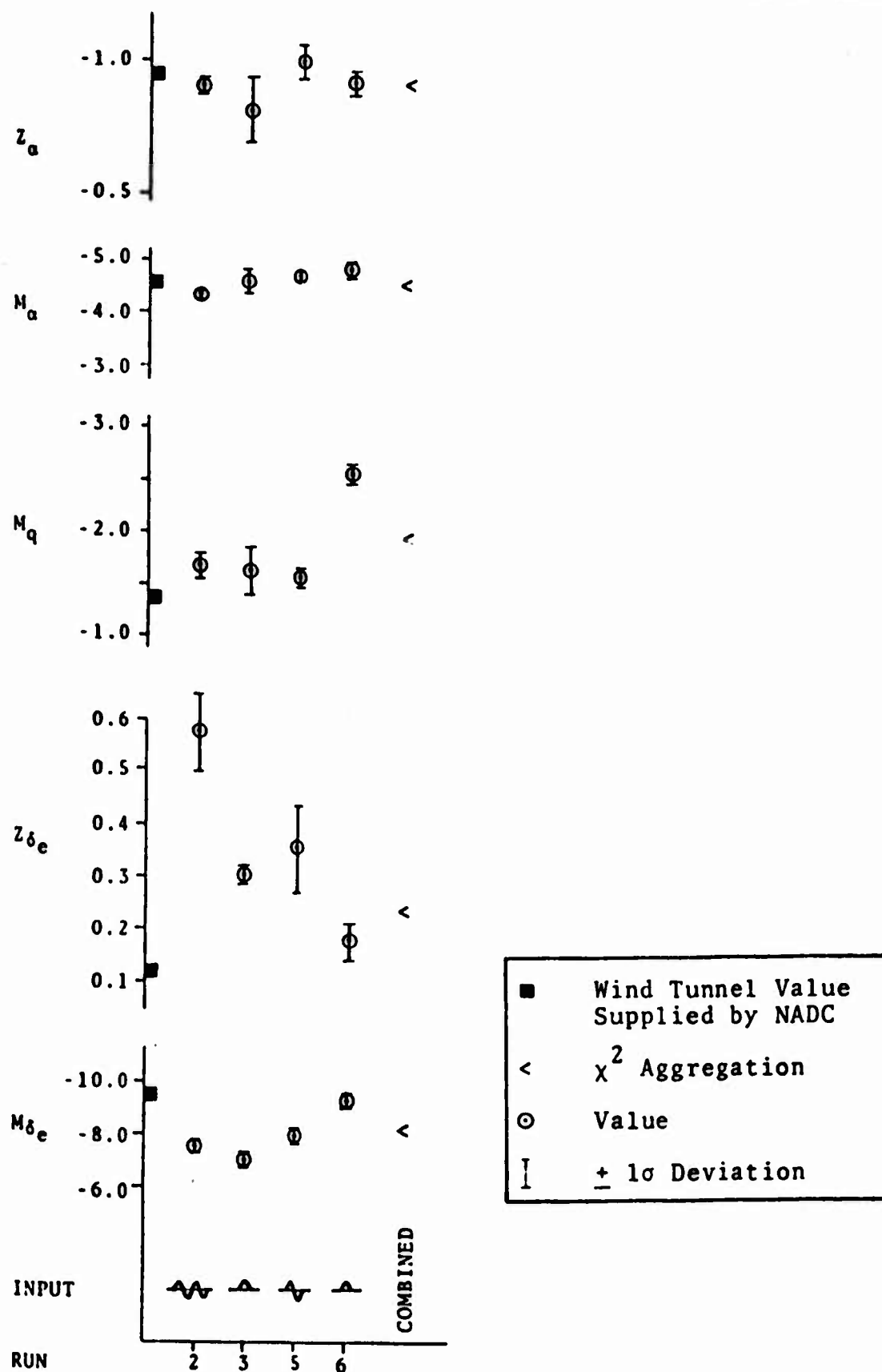
Figure 28 Comparison of Stability and Control Derivatives
at Low Speed Approach Configuration

The variation of $Z_{\delta e}$ is notable over the four runs, a result due to the difficulty of identifying this vertical lift from elevator deflection coefficient without a sudden (e.g., high frequency) elevator input.

Figure 29 summarizes the estimated values of stability and control derivatives for the six runs at high speed and clean configuration. The estimates for the high amplitude pulse (run 10), sepcially designed input (run 18) and random input (run 19) are the best. The small amplitude pulse (run 11) step (Run 12) and specially designed input (Run 13) are the poorest. Again, the estimates of $Z_{\delta e}$ are poor.

Most of the information regarding the true value of $Z_{\delta e}$ is contained in the input measurement and the vertical acceleration measurement. It is concluded that both of these measurements should have smaller instrument errors to improve the estimates of $Z_{\delta e}$ with the inputs which were tested. Improved estimation of $Z_{\delta e}$ is indicated by the use of specially designed inputs (e.g., a high frequency elevator component).

An attempt is made to identify the phugoid parameters (run 10). It was necessary to assume that the input is zero beyond the short period excitation. A good time history match was obtained but the parameter estimates are only fair. Again, the determination of the phugoid parameters requires a better measurement of the input and the aircraft velocity.

In summary, the flight test data provides reliable and useful stability and control derivatives (and instrumentation errors and calibration) if the inputs are properly designed and the errors in important instruments are not large.
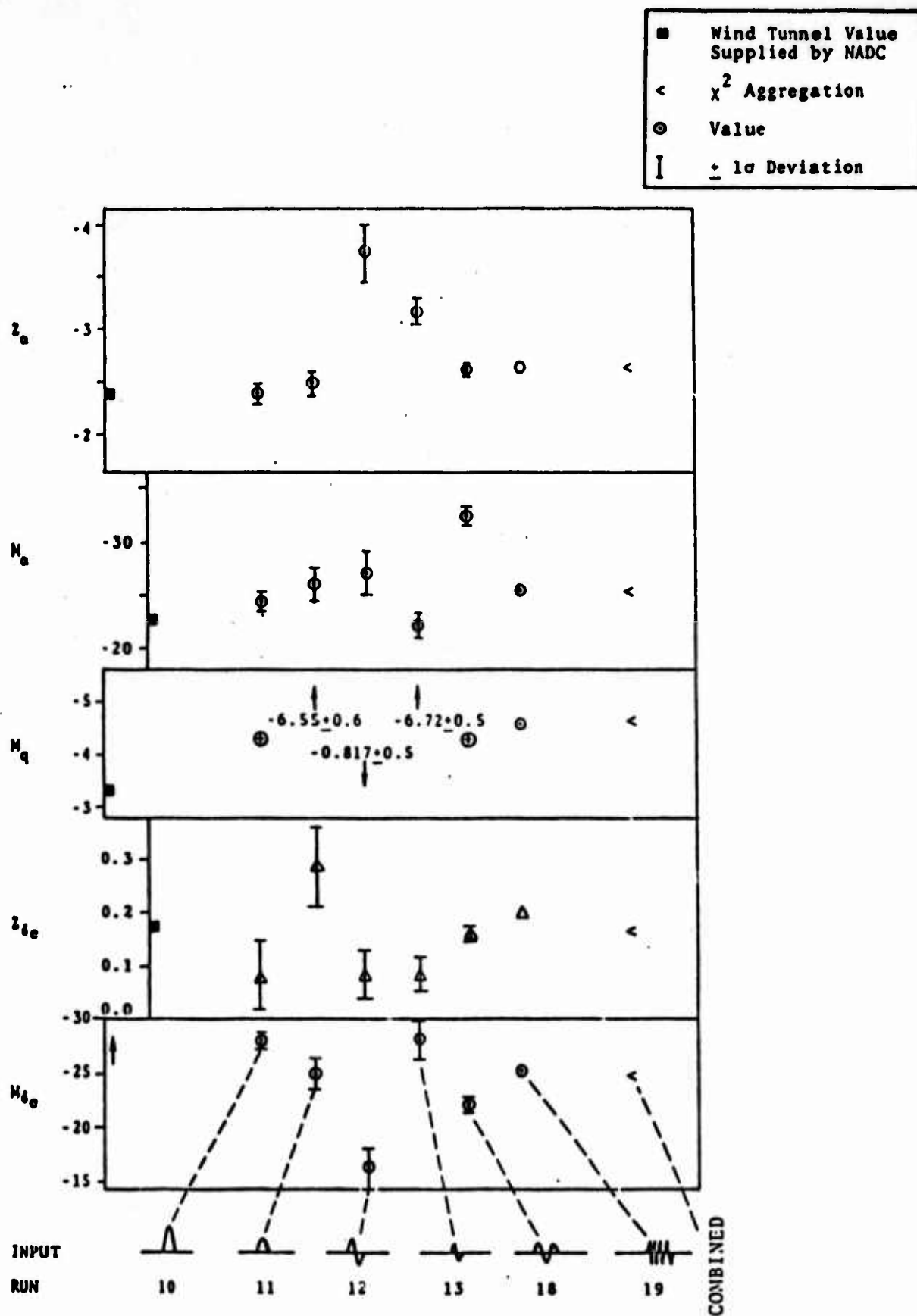
Figure 29   Comparison of Stability and Control Derivatives at High Speed Clean Configuration

5.2 CONCLUSIONS

On the basis of processing of the response data of highly instrumented aircraft, the following principal conclusions are made:

1. Identification Algorithm Requirements: In order to achieve the desired accuracy of parameter estimates, the following capabilities are desirable for the identification algorithm:

    (a) Trim state estimation: It is necessary to estimate steady state errors due to out-of-trim controls to reduce parameter estimate error.

    (b) State noise estimation: Significant reduction in parameter estimate errors is achievable by identifying the state noise (e.g., process noise) effects. In particular, it is necessary to identify the random error in measurement of the control inputs. (In these cases, identification of noise in input measurement leads to more consistent parameter estimates.)

    (c) Isolation of Identifiability Deficiencies: It is necessary to include a quantitative method of testing the amount of information in a given data record to ascertain if particular parameters can be identified. To not include such a method can lead to erroneous conclusions about the "true" values of nonidentifiable parameters.

2. Input Design and Measurement Requirements: Where parameters are not easily identified from pulses and doublets,

specially designed inputs (for desired short data lengths) or random inputs (where arbitrarily long data lengths are practical) offer significant improvements in parameter estimates. Particularly difficult to identify parameters, such as $Z_{\delta e}$, may require sudden step inputs to excite high levels of initial transient responses. In some cases, more accurate instrumentation may reduce but not eliminate requirements for such specialized inputs.

3.   <u>Verification of Identification Accuracy</u>: Evaluation of the accuracy of identified parameters should not be based on time history matches between actual and identified model responses alone. Estimated confidence bounds should also be used. Most importantly, the prediction test is a very strong test of estimate accuracy.

A central question which is raised by these results is the relationship between the wind tunnel and flight data identified estimates. The results seen in Figures 28 and 29 demonstrated that wind tunnel static stability derivatives (Z_α, M_α) are verified by the flight data (ref. statistical average of identified derivatives denoted by <). There is, however, less validation of wind tunnel results for the dynamic M_q and control derivatives $M_{\delta e}$, $Z_{\delta e}$.

It cannot be concluded that one or the other of the results is the more valid. It may be noted, however, that the wind tunnel values, placed in a simulation of the aircraft response, do not match the recorded aircraft response, while the identified estimates do (this is implicit in the identification algorithm cost function). A combined fight test/wind tunnel program, of larger scope than conducted here, is necessary to isolate the causes of the apparent discrepancy.

Finally, it is concluded that flight testing of well-instrumented aircraft, such as the T-2, offers an effective procedure for better definition of aircraft aerodynamics and instrumentation evaluation. This procedure is significantly enhanced by use of advanced parameter identification algorithms, and careful attention to control inputs. Such efforts yield the base for even more effective research into particular critical flight regimes such as those at high angle-of-attack.

REFERENCES

1. Blakelock, J.H., Automatic Control of Aircraft and Missiles, John Wiley and Sons, New York, 1965.

2. Gupta, N.K., "Instrumental Variables Approach for On-Line Identification of Aircraft Parameters," Systems Control, Inc., Internal Report, July 1974.

3. Gupta, N.K. and Mehra, R.K., "Computation Aspects of Maximum Likelihood Estimation and Reduction in Sensitivity Functions Computations," IEEE T-AC, pp. 774-783, Dec. 1974.

4. Akaike, H. "Stochastic Theory of Minimal Realization," IEEE T-AC, pp. 667-673, Dec. 1974.

5. Taylor, L., "A New Criterion for System Modeling," AGARD Specialist Meeting on State and Parameter Estimation, NASA Langley Research Center, Nov. 1974.

6. Gupta, N.K. and Hall, W.E., "Input Design for Identification of Aircraft Stability and Control Derivatives," NASA CR-2493, February 1975.

7. Mehra, R.K. and Gupta, N.K., "Status of Input Design for Aircraft Parameter Identification," AGARD Specialist Meeting on Aircraft State and Parameter Estimation, NASA Langley Research Center, Nov. 1974.

APPENDIX A
AIRCRAFT PARAMETER IDENTIFICATION USING THE
MAXIMUM LIKELIHOOD METHOD

Consider the aircraft equations of motion in discrete form

$$x(t+1) = \phi x(t) + Gu(t) + \Gamma w(t) \tag{1}$$

$$y(t) = Hx(t) + v(t) \tag{2}$$

where $x(t)$ is $n \times 1$ state vector, $u(t)$ is $p \times 1$ input vector, $w(t)$ is $q \times 1$ vector of random forcing functions, $y(t)$ is $r \times 1$ output vector, $v(t)$ is $r \times 1$ vector of output errors and

$$E\{w(t)\} = 0, \quad E\{w(t)\, w^T(\tau)\} = Q\delta_{t,\tau} \tag{3}$$

$$E\{w(t)\, v^T(\tau)\} = 0 \tag{4}$$

$$E\{v(t)\} = 0, \quad E\{v(t)\, v^T(\tau)\} = R\delta_{t,\tau} \tag{5}$$

where δ is the Kronecker Delta function.

It is assumed that the structure of the model is known. The vector of unknown parameters from $x(0)$, ϕ, G, Γ, H, Q, and R is denoted by Θ. The problem is to identify θ using the maximum likelihood method.

For an aircraft in steady flight, and if the wind gust statistics remain constant, the negative log-likelihood function is given by

$$J = \frac{1}{2} \sum_{i=1}^{N} \left[\nu^T(i) \, B^{-1}\nu(i) + \log |B| \right] \tag{6}$$

where $\nu(i)$ are the innovations from a Kalman filter and B is the innovations covariance and are given by the following equations

$$\hat{x}(k+1) = \phi\hat{x}(k) + Gu(k) + \phi K\nu(k) \tag{7}$$

$$\nu(k) = y(k) - H\hat{x}(k) \tag{8}$$

$$K = PH^T B^{-1}$$

$$B = HPH^T + R \tag{9}$$

$$P = \phi(P-KBK^T)\phi^T + \Gamma Q\Gamma^T$$

In the computer implementation, the negative log-likelihood function is minimized using a Gauss-Newton gradient procedure. Minimization of (6) with respect to elements in matrix B gives (unknowns in R can be mapped into unknowns in B)

$$\hat{B} = \frac{1}{N} \sum_{i=1}^{N} \nu(i) \, \nu^T(i) \tag{10}$$

For other parameters θ, the first and second gradients of J are, approximately,

$$\frac{\partial J}{\partial \theta} = \sum_{i=1}^{N} \nu^T(i) \, \hat{B}^{-1} \frac{\partial \nu(i)}{\partial \theta} \tag{11}$$

$$\frac{\partial^2 J}{\partial \theta^2} = \sum_{i=1}^{N} \frac{\partial \nu^T(i)}{\partial \theta} \, B^{-1} \, \frac{\partial \nu(i)}{\partial \vartheta} \tag{12}$$

The gradients of ν are obtained using Equations (7) and (8)

$$\frac{\partial \nu(k)}{\partial \theta_i} = - \frac{\partial H}{\partial \theta_i} \, \hat{x}(k) - H \, \frac{\partial \hat{x}(k)}{\partial \theta_i} \tag{13}$$

and

$$\frac{\partial \hat{x}(k+1)}{\partial \theta_i} = \frac{\partial \phi}{\partial \theta_i} \, \hat{x}(k) + \phi \, \frac{\partial \hat{x}(k)}{\partial \theta_i} + \frac{\partial G}{\partial \theta_i} \, u(k) + \frac{\partial \phi}{\partial \theta_i} \, K\nu(k)$$

$$+ \phi \, \frac{\partial K}{\partial \theta_i} \, \nu(k) + \phi K \, \frac{\partial \nu(k)}{\partial \theta_i} \tag{14}$$

where θ_i is the ith parameter. The steady state value of $\frac{\partial K}{\partial \theta_i}$ is used in Equation (14). This can be computed using Equations (9) for each parameter. In the present computer implementation, a continuous system representation is used to compute steady state filter and its gradient.

In the absence of process noise (wind gust effects), the Kalman filter gains and its covariance are zero. Therefore, Equation (14) simplifies to,

$$\frac{\partial \hat{x}(k+1)}{\partial \theta_i} = \frac{\partial \phi}{\partial \theta_i} \, \hat{x}(k) + \phi \, \frac{\partial \hat{x}(k)}{\partial \theta_i} + \frac{\partial G}{\partial \theta_i} \, u(k) \tag{15}$$

The second gradient matrix $\frac{\partial^2 J}{\partial \theta^2}$ is called the information matrix, which has a special significance in parameter identification. If

$$\Sigma = \left(\frac{\partial^2 J}{\partial \theta^2}\right)^{-1} \tag{16}$$

then

$$\text{Standard deviation } (\theta_i - \hat{\theta}_i) = \sqrt{\Sigma_{ii}} \tag{17}$$

i.e., the standard deviation of estimation error of the ith parameter is the square root of the ith term of the diagonal of Σ.

APPENDIX B
MAXIMUM LIKELIHOOD ESTIMATION WITH BIAS
AND RANDOM NOISE IN INPUT MEASUREMENT

The measurement of input signal is usually contaminated by bias, random noise and other errors. These errors can be accounted for in the likelihood approach. In what is to follow, we assume that there is no random excitation from gusts and the input has errors due to bias and random noise only. Extension to other cases is straightforward.

Consider the discrete time representation of a system in which the state x follows the equation

$$x(k+1) = \phi x(k) + Gu(k) \tag{1}$$

There are noisy measurements of linear combinations of states and of inputs

$$y(k) = Hx(k) + v(k) \tag{2}$$

$$u'(k) = u(k) + b + v_u(k) \tag{3}$$

where b is a constant bias and $v_u(k)$ is white random noise. Substituting (3) in (1), we have

$$x(k+1) = \phi x(k) + Gu'(k) - Gb - Gv_u(k) \tag{4}$$

Equation (4) can be used with measurements of Equation (2) for identification. Gb is the equation bias since both G and b are not time functions. The last term in Equation (4) is a random excitation term corresponding to process noise. Therefore, even though the system does not have gust effects, the process noise formulation is required

$$\hat{x}(k+1) = \phi\hat{x}(k) + Gu'(k) - Gb + \phi K\nu(k) \qquad (5)$$

$$\nu(k) = y(k) - H\hat{x}(k) \qquad (6)$$

When the Newton-Raphson technique is used, the gradients are computed as before except for the bias in measurement of the input

$$\frac{\partial\hat{x}(k+1)}{\partial b} = \phi(I - KH)\frac{\partial\hat{x}(k)}{\partial b} - G \qquad (7)$$

If there were no random noise in the measurement of input

$$\frac{\partial x(k+1)}{\partial b} = \phi\frac{\partial x(k)}{\partial b} - G \qquad (8)$$